

Intranasal MSCs:
**Boosting regeneration of the
neonatal injured brain**

Vanessa Donega

This publication has been kindly supported by the division of Perinatology, University Medical Center Utrecht, AbbVie Nederland and Stichting Gilles Hondius Foundation.

The research described in this thesis was financially supported by by Zon-MW Project (no 116002003) and EU-7 Neurobid (HEALTH-F2-2009-241778) from the European Union.

Copyright:

Chapter 2: Journal of Cerebral Blood Flow and Metabolism, Nature Publishing Group, 2013

Chapter 3: PLoS ONE, Public Library of Science publisher, 2013

Chapter 4: Experimental Neurology, Elsevier B.V., 2014

© Vanessa Donega, Utrecht, The Netherlands, 2014. All rights reserved. No part of this publication may be reproduced or transmitted in any form or by any means, either electronic or mechanical, including photocopy, recording, or any information storage and retrieval system without permission from the copyright owner.



Author	Vanessa Donega
Front cover illustration	By author
About the image	Hippocampal structure of a MSC-treated mouse. Top layer: Green= neurons; Blue=cell nuclei; Bottom Layer: Green=astrocytes; Red=microglia; Blue=cell nuclei
Lay-out & Print	Gildeprint Drukkerijen
ISBN	9789039361719

Intranasal MSCs:
**Boosting regeneration of the
neonatal injured brain**

Intranasaal MSCs:
**Boosting regeneratie van het neonataal
beschadigd brein**
(met samenvatting in het Nederlands)

Proefschrift

ter verkrijging van de graad van doctor aan de Universiteit Utrecht
op gezag van de rector magnificus, prof. dr. G.J. van der Zwaan,
ingevolge het besluit van het college voor promoties
in het openbaar te verdedigen op
dinsdag 2 september 2014 des middags te 2.30 uur

door

Vanessa Marques Donegá
geboren op 6 september 1985 te Sao Paulo, Brazilië

Promotoren:

Prof. dr. C.J. Heijnen
Prof. dr. F. van Bel
Prof. dr. A. Kavelaars

Copromotor:

Dr. C.H. Nijboer

“The only real voyage of discovery consists not in seeking new landscapes but in having new eyes.”

Marcel Proust

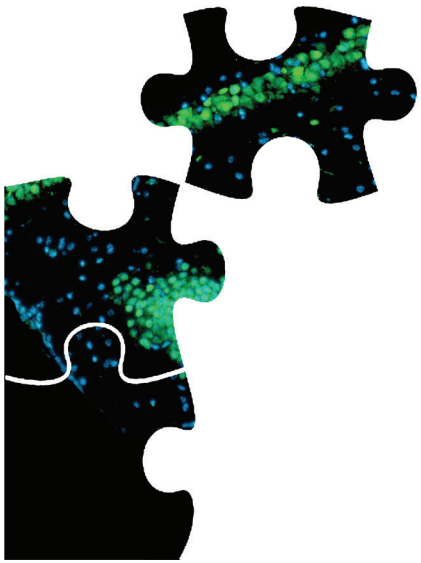
“To know the brain.... is equivalent to ascertaining the material course of thought and will, to discovering the intimate history of life in its perpetual duel with external forces.”

Ramon y Cajal (from Recollections of my life, 1937)

Voor mijn ouders

Contents

Chapter 1	General Introduction	9
Chapter 2	The endogenous regenerative capacity of the damaged newborn brain: Boosting neurogenesis with mesenchymal stem cell treatment. <i>JCBFM</i> (2013) 33: 625-634	19
Chapter 3	Intranasal mesenchymal stem cell treatment for neonatal brain damage: Long-term cognitive and sensorimotor improvement. <i>Plos One</i> (2013) 8: e51253	49
Chapter 4	Intranasally administered mesenchymal stem cells promote a regenerative niche for repair of neonatal ischemic brain injury. <i>Experimental Neurology</i> (2014), in press	67
Chapter 5	Intranasal administration of human MSC for ischemic brain injury in the mouse: In vitro and in vivo neuroregenerative functions.	95
Chapter 6	Assessment of long-term safety and efficacy of intranasal Mesenchymal Stem Cell treatment for neonatal brain injury.	123
Chapter 7	Summary and General Discussion	145
Chapter 8	Nederlandse Samenvatting (Summary in Dutch)	155
Dankwoord (Acknowledgements)		I
List of Publications and Presentations		V
Curriculum Vitae		VII



Chapter 1

General Introduction

General Introduction

This chapter gives a general introduction to the topic of this thesis, *i.e.* mesenchymal stem cells (MSCs) as a treatment strategy for neonatal hypoxic-ischemic (HI) brain damage. First, a concise overview will be given of the causes and mechanisms underlying HI brain damage. Finally, we will briefly review the current state of therapeutic strategies and discuss the potential of MSC administration as a treatment option for neonatal HI by boosting endogenous regenerative processes.

Definition and pathophysiology of HI brain damage in neonates

Neonatal encephalopathy due to perinatal HI leads to extensive neuronal loss and glial scar formation in the brain resulting in long-term neurological deficits such as cerebral palsy and mental retardation. Moreover, HI remains a major cause of perinatal death in newborn babies. HI has an incidence of 1 to 6 per 1000 live-born neonates worldwide and may occur during pregnancy, intrapartum or postpartum due to *e.g.* severe respiratory distress and cardiac failure of the newborn baby. There are several known risk factors for HI such as maternal diabetes, pregnancy induced hypertension or placental insufficiency. The extent of the brain lesion depends not only on the duration of the HI insult, but also on the maturity of the brain, as most cases of severe white matter injuries occur in preterm babies, while in term neonates the gray matter is mostly affected¹⁻⁵.

HI results from reduced blood perfusion and oxygenation of the neonatal brain for a certain period of time. The decrease in oxygen and glucose results in low intracellular ATP levels, which increases membrane depolarization and impairs ATP-dependent glutamate reuptake from the synaptic cleft. These events lead to glutamate excitotoxicity, which plays a major role in neuronal and oligodendroglial cell death. The increase in intracellular Ca^{2+} activates several enzymes such as phospholipases, proteases and nucleases resulting in *e.g.* membrane and DNA degradation, and free radical production. Free radicals (*e.g.* superoxide and nitric oxide (NO)) are very reactive molecules that damage the cellular membranes, proteins and DNA, resulting in cell death. This cascade of detrimental events will also trigger an inflammatory response, which culminates in more cell death and may ultimately lead to tissue loss and cyst formation.

Glial cells and their role in HI brain injury

The degree of neuroinflammation after HI depends on the severity of the insult. A few hours following HI, increased levels of *e.g.* CXCL10, ATP and glutamate released by injured neurons activate microglial cells (resident macrophages of the brain)⁹, which are the first cells that migrate to the injury site followed by immune cells from the periphery (*e.g.* neutrophils and macrophages). Microglia migrate with a speed of 1.5µm/min, which makes them the fastest moving cells in the brain¹⁰. Microglia make up a heterogeneous cell population that can either be pro-inflammatory (M1) or anti-inflammatory and pro-repair (M2a/b)^{11,12}. They express several receptors to sense changes in the brain environment. Once activated, microglia lose their ramified star shape by retracting their processes and developing an amoeboid phenotype. Subsequently, they produce pro-inflammatory cytokines such as TNF- α , IL-1 β and free radicals, and phagocytize cell debris and dying cells, thereby further exacerbating neural damage and promoting astrogliosis^{9,11-13}.

Astrocytes, like microglia, are a very heterogeneous glial cell population that respond to a plethora of signaling molecules from the environment by expressing a vast array of receptors. Following HI, astrocytes proliferate and migrate to the lesion border in response to chemokines (*e.g.* CXCL10 and CCL2)¹⁴⁻¹⁶ secreted by microglia and immune cells. Pro-inflammatory proteins (*e.g.* IFN- γ , TNF- α and IL-1 β) and factors such as damage signaling molecules, also known as danger-associated molecular patterns (DAMPs), activate the astrocytes¹⁵. Upon activation, astrocytes become hypertrophic and show increased expression of the intermediate filament proteins glial fibrillary acid protein (GFAP) and vimentin¹⁵⁻¹⁷. This process, known as astrogliosis, results in a scar that demarcates the lesion area. The scar consists mainly of reactive astrocytes, activated microglia and proteoglycans^{15,16}. In the uninjured brain, processes of individual astrocytes do not overlap. However, following HI the processes of reactive astrocytes interdigitate in a heterogeneous fashion that depends on the injury extent. In the most severe cases, the processes from reactive astrocytes substantially intertwine and intermingle at the lesion border¹⁸.

In the early phase after injury, the resulting scar tissue acts as a dense physical barrier to prevent inflammatory molecules from spreading through healthy brain tissue and further aggravating the lesion. However, in the long-term, astrogliosis is extremely detrimental to neurogenesis and axon regeneration, due to the production of factors such as chondroitin sulphate proteoglycan (CSPG) and keratin

sulphate proteoglycan (KSPG), which induce growth cone arrest and collapse¹⁸. This is aggravated by the fact that the glial scar does not resolve even after the pro-inflammatory cues have decreased, thereby leading to impaired axon regeneration and neurogenesis¹⁵.

Therapeutic strategies

Currently, hypothermia (cooling of the head or whole body by 2-4 °C) is the only clinically available therapeutic option, which must be applied within the first 6 hours following the insult. Moreover, it is only effective in babies born at term¹⁹⁻²¹. Hence, there is a growing number of studies investigating new treatment options. One line of research focusses on developing neuroprotective strategies to *prevent* neuronal cell death by for instance inhibiting apoptosis or inflammation²²⁻²⁵. However, these strategies have a short therapeutic window and have to be applied within a few hours after the insult. Previous studies of our group showed that inhibition of NF-KB activity by the compound TAT-NBD reduces the brain lesion by more than 80%. We showed that NF-KB inhibition prevented caspase 3 activation and thereby also apoptosis²². A different approach, with a longer therapeutic window, is geared at *repairing* the damaged brain tissue. Indeed, a few studies on intracranial or intravenous transplantation of neural stem cell (NSCs) following neonatal HI, show that NSCs decrease lesion size and improve motor behavior²⁶⁻²⁹. NSCs differentiate into neuronal cells and there is increased axonal sprouting towards the damaged cortex²⁹. Besides NSCs administration, work by our group and others has demonstrated the positive effects of intracranial and intracarotid transplantation of MSCs on lesion volume and motor behavior after HI³⁰⁻³⁴. Furthermore, MSCs enhanced axonal sprouting towards the damaged hemisphere and induced gene expression of several anti-inflammatory proteins and neurotrophic factors^{32,33}. Previous work from our group also demonstrated that intranasal MSC application, a non-invasive administration route, can be as effective as intracranial transplantation after neonatal HI³⁵. Thus, intranasal MSC application may hold the potential to become an effective treatment option.

MSCs: Definition

MSCs are multipotent stem cells found in different tissues such as, bone marrow, adipose tissue, Wharton's Jelly and umbilical cord blood. These cells can differentiate into adipocytes, chondrocytes and osteoblasts and express the stem cell markers

CD73, CD90 and CD105^{36,37}. They are known to secrete several proteins ranging from immunomodulatory (*e.g.* IL-10, IFN- γ and TGF β) to neurotrophic factors (*e.g.* VEGF, FGF-2, BDNF and NGF). Furthermore, MSCs are hardly immunogenic as they do not express MHC class II or co-stimulatory proteins (*e.g.* CD86, CD80 and CD40)³⁶⁻³⁹. Hence, over 300 clinical trials worldwide (www.clinicaltrials.gov) are currently investigating the efficacy and safety of MSCs as a therapeutic option for several diseases ranging from graft-versus-host disease to cardiovascular disease⁴⁰.

Conclusion

There is an urgent need for additional therapeutic options for neonatal HI injury that have a long therapeutic window. In this thesis, the therapeutic potential of non-invasive intranasal MSC administration is addressed. To this end, HI was induced in 9 days old (P9) C57BL/6 mouse pups, which is an animal model that reflects perinatal events in the near-term human baby (32-34 weeks of gestation). We have studied not only clinically relevant aspects, such as dosage and long-term effects, but also fundamental questions such as how MSCs mediate the significant improvement on lesion volume and functional outcome.

Thesis outline

In **chapter 2**, the concept of neurogenesis will be introduced and we discuss the capacity of the neonatal brain to regenerate following a HI insult.

Chapter 3 focuses on the fine-tuning of intranasal MSC treatment after HI by investigating the optimal MSC dose, the therapeutic window and whether repeated MSC administration further improves the outcome on HI brain injury. Furthermore, we determine whether intranasal MSC treatment improves cognitive behavior, as this may have important implications for the clinic.

In **chapter 4**, the kinetics of MSC migration to the HI lesion site are determined by both fluorescence microscopy and MRI. We go further into the mechanisms underlying the remarkable effect that intranasal MSC administration has on neonatal HI brain injury.

Chapter 5 focuses on the effect of *human* MSCs on motor behavior, lesion volume and scar formation following HI brain damage in neonatal mice. Two *in vitro* methods for assessing quality of human MSCs before *in vivo* administration are investigated.

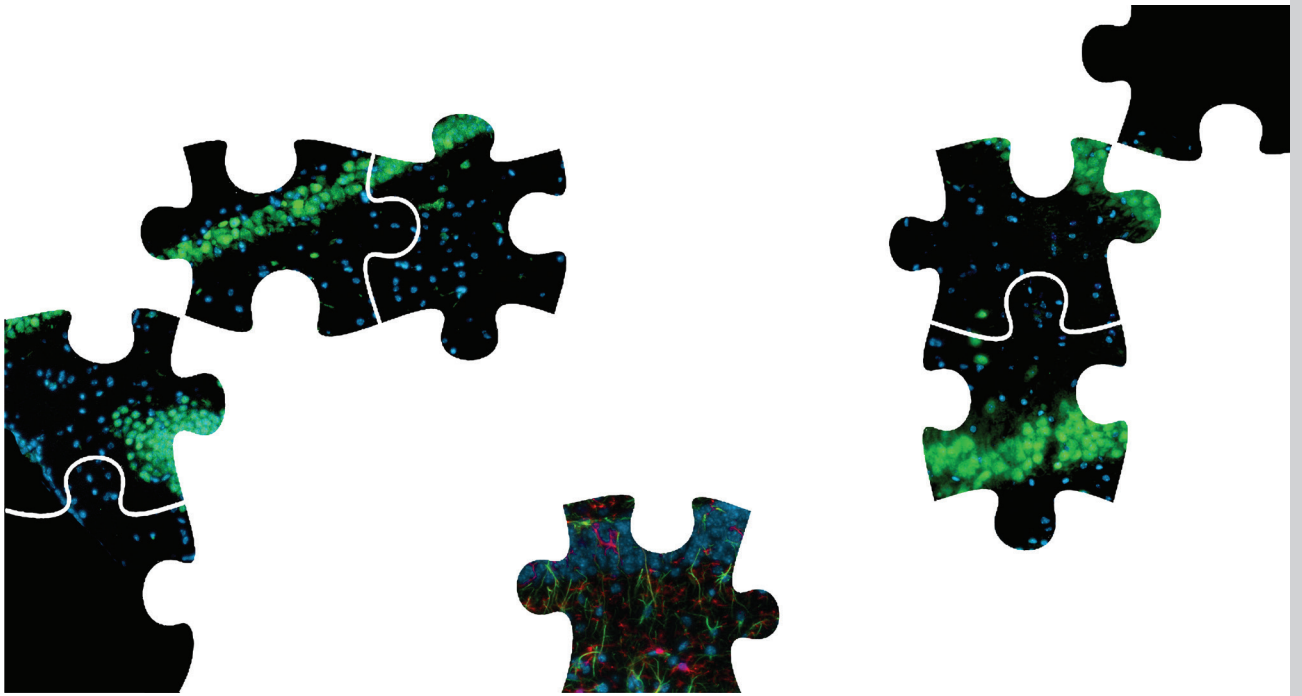
In **chapter 6**, we investigate whether intranasal MSC treatment has any side effects on the mouse brain in the long-term. Furthermore, the long-term effects of intranasal MSC administration on motor and cognitive behavior and lesion volume are described.

References

1. Dammann O, Ferriero D, Gressens P. Neonatal encephalopathy or hypoxic ischemic encephalopathy? Appropriate terminology matters. *Pediatr Res* 2011; 70: 1-2.
2. De Haan M, Wyatt JS, Roth S, et al. Brain and cognitive-behavioural development after asphyxia at term birth. *Dev Sci* 2006; 9: 350-358.
3. Ferriero DM. Neonatal brain injury. *N Engl J Med* 2004; 351: 1985-1995.
4. Graham EM, Ruis KA, Hartman AL, et al. A systematic review of the role of intrapartum hypoxia-ischemia in the causation of neonatal encephalopathy. *Am J Obstet Gynecol* 2008; 199: 587-595.
5. van Handel M, Swaab H, de Vries LS, et al. Long-term cognitive and behavioural consequences of neonatal encephalopathy following perinatal asphyxia: a review. *Eur J Pediatr* 2007; 166: 645-654.
6. Groenendaal F, van Bel F. Neuroprotection after perinatal asphyxia: Recent advances and future perspectives. Mechanisms of hypoxic brain injury in the newborn and potential strategies for neuroprotection. Chapter 5: 77-97, Kerala India, Transworld Research Network.
7. Vexler ZS, Ferriero DM. Molecular and biochemical mechanisms of perinatal brain injury. *Semin Neonatol* 6:99-108.
8. Vannucci SJ, Hagberg H. Hypoxia-ischemia in the immature brain. *J Exp Biol* 2004; 207: 3149-3154.
9. Hagberg H, Gressens P, Mallard C, et al. Inflammation during fetal and neonatal life: Implications for neurologic and neuropsychiatric disease in children and adults. *Ann Neurol* 2012; 71: 444-457.
10. Kettenmann H, Kirchhoff F, Verkhratsky A. Microglia: new roles for the synaptic stripper. *Neuron* 2013; 77: 10-18.
11. Czeh M, Gressens P, Kaindl AM. The Yin and Yang of microglia. *Dev Neurosci* 2011; 33: 199-209.
12. Neumann J, Gunzer M, Gutzeit HO, et al. Microglia provide neuroprotection after ischemia. *FASEB J* 2006; 20: 714-720.
13. Wake H, Moorhouse AJ, Miyamoto A, et al. Microglia: actively surveying and shaping neuronal circuit structure and function. *Trends Neurosci* 2013; 36: 209-217.
14. Rusnakova V, Honsa P, Dzamba D, et al. Heterogeneity of Astrocytes: from development to injury-single cell gene expression. *PLOS One* 2013; 8: e69734.
15. Sofroniew MV. Multiple Roles for astrocytes as effectors of cytokines and inflammatory mediators. *Neuroscientist* 2014; 20: 160-172.
16. Robel S, Berninger B, Gotz M. The stem cell potential of glia: lessons from reactive gliosis. *Nat Rev* 2011; 12: 88-104.
17. Silver J, Miller JH. Regeneration beyond the glial scar. *Nat Rev* 2004; 5: 146-156.
18. Azzopardi DV, Strohm B, Edwards AD, et al. Moderate hypothermia to treat perinatal asphyxia encephalopathy. *N Engl J Med* 2009; 361: 1349-1358.
19. Gluckman PD, Wyatt JS, Azzopardi D, et al. Selective head cooling with mild systemic hypothermia after neonatal encephalopathy: multicentre randomised trial. *Lancet* 2005; 365: 663-670.

20. Perlman JM. Intervention strategies for neonatal hypoxic-ischemic cerebral injury. *Clin Ther* 2006; 28: 1353-1365.
21. Compagnoni G, Pogliani L, Lista G, et al. Hypothermia reduces neurological damage in asphyxiated newborn infants. *Biol Neonate* 2002; 82: 222-227.
22. Nijboer CH, Heijnen CJ, Groenendaal F, et al. Strong neuroprotection by inhibition of NF{ κ }B after neonatal hypoxia-ischemia involves apoptotic mechanisms but is independent of cytokines. *Stroke* 2008; 39: 2129-2137.
23. Nijboer CH, Heijnen CJ, van der Kooij MA, et al. Targeting the p53 pathway to protect the neonatal ischemic brain. *Ann Neurol* 2011; 70: 255-264.
24. Han BH, Xu D, Choi J, et al. Selective, reversible caspase-3 inhibitor is neuroprotective and reveals distinct pathways of cell death after neonatal hypoxic-ischemic brain injury. *J Biol Chem* 2002; 277: 30128-30136.
25. Leonardo CC, Eakin AK, Ajmo JM, et al. Delayed administration of a matrix metalloproteinase inhibitor limits progressive brain injury after hypoxia-ischemia in the neonatal rat. *J Neuroinfl* 2008; 5: 34-44.
26. Daadi MM, Davis AS, Arac A, et al. Human neural stem cell grafts modify microglial response and enhance axonal sprouting in neonatal hypoxic-ischemic brain injury. *Stroke* 2010; 41: 516-523.
27. Bacigaluppi M, Pluchino S, Jametti LP, et al. Delayed post-ischaemic neuroprotection following systemic neural stem cell transplantation involves multiple mechanisms. *Brain* 2009; 132: 2239-2251.
28. Shinoyama M, Ideguchi M, Kida H, et al. Cortical region-specific engraftment of embryonic stem cell-derived neural progenitor cells restores axonal sprouting to a subcortical target and achieves motor functional recovery in a mouse model of neonatal hypoxic-ischemic brain injury. *Front Cell Neurosci* 2013; doi: 10.3389/fncel.2013.00128
29. Daadi MM, Davis AS, Arac A, et al. Human neural stem cell grafts modify microglial response and enhance axonal sprouting in neonatal hypoxic-ischemic brain injury. *Stroke* 2010; 41: 516-523.
30. Shen LH, Li Y, Chen J, et al. Intracarotid transplantation of bone marrow stromal cells increases axon-myelin remodelling after stroke. *Neuroscience* 2006; 137: 393-399.
31. Pimentel-Coelho PM, Magalhaes ES, Lopes LM, et al. Human cord blood transplantation in a neonatal rat model of hypoxic-ischemic brain damage: functional outcome related to neuroprotection in the striatum. *Stem Cells Dev* 2010; 19: 351-358.
32. Van Velthoven CTJ, Kavelaars A, van Bel F, et al. Repeated mesenchymal stem cell treatment after neonatal hypoxia-ischemia has distinct effects on formation and maturation of new neurons and oligodendrocytes leading to restoration of damage, corticospinal motor tract activity, and sensorimotor function. *J Neurosci* 2010; 30: 9603-9611.
33. Van Velthoven CT, Kavelaars A, van Bel F, et al. Mesenchymal stem cell transplantation changes the gene expression profile of the neonatal ischemic brain. *Brain Behav Immun* 2011; 25: 1342-1350.
34. Van Velthoven CT, Braccioli L, Willems HL, et al. Therapeutic potential of genetically modified mesenchymal stem cells after neonatal hypoxic-ischemic brain damage. *Mol Ther* 2014; 22: 645-654.

35. van Velthoven CT, Kavelaars A, van Bel F, et al. Nasal administration of stem cells: a promising novel route to treat neonatal ischemic brain damage. *Pediatr Res* 2010; 68: 419-422.
36. Deans RJ, Moseley AB. Mesenchymal stem cells: Biology and potential clinical uses. *Exp Hematol* 2000; 28: 875-884.
37. Salem HK, Thiemermann C. Mesenchymal stromal cells: Current understanding and clinical status. *Stem Cells* 2010; 28: 585-596.
38. Zhang R, Liu Y, Yan K, et al. Anti-inflammatory and immunomodulatory mechanisms of mesenchymal stem cell transplantation in experimental traumatic brain injury. *J Neuroinflammation* 2013; 10: 106-118.
39. Crigler L, Robey RC, Asawachaicharn A, et al. Human mesenchymal stem cell subpopulations express a variety of neuro-regulatory molecules and promote neuronal cell survival and neuritogenesis. *Experimental Neurology* 2006; 198: 54-64.
40. Trounson A, Thakar RG, Lomax G, et al. Clinical trials for stem cells therapies. *BMC Med* 2011; 9: 52.



Chapter 2

The endogenous regenerative capacity of the damaged newborn brain: Boosting neurogenesis with mesenchymal stem cell treatment

Vanessa Donega¹, Cindy T. J. van Velthoven¹, Cora H. Nijboer¹, Annemieke Kavelaars² and Cobi J. Heijnen^{1,2}

¹Lab. of Neuroimmunology and Developmental Origins of Disease (NIDOD), University Medical Centre Utrecht, The Netherlands. ² Department of Symptom Research, MD Anderson Cancer Center, TX, USA.

Journal of Cerebral Blood Flow and Metabolism (2013) 33: 625-634

Abstract

Neurogenesis continues to proliferate throughout adulthood. The neurogenic capacity of the brain increases following injury by *e.g.* hypoxia-ischemia. However, it is well-known that in many cases brain damage does not resolve spontaneously, indicating that the endogenous regenerative capacity of the brain is insufficient. Neonatal encephalopathy leads to high mortality rates and long-term neurological deficits in babies worldwide. Therefore, there is an urgent need to develop more efficient therapeutic strategies. The latest findings indicate that stem cells represent a novel therapeutic possibility to improve outcome in models of neonatal encephalopathy. Transplanted stem cells secrete factors that stimulate and maintain neurogenesis, thereby increasing cell proliferation, neuronal differentiation and functional integration.

Understanding the molecular and cellular mechanisms underlying neurogenesis after an insult is crucial for developing tools to enhance the neurogenic capacity of the brain. The aim of this review is to discuss the endogenous capacity of the neonatal brain to regenerate following a cerebral ischemic insult. We present an overview of the molecular and cellular mechanisms underlying endogenous regenerative processes during development as well as after a cerebral ischemic insult. Furthermore, we will consider the potential to employ stem cell transplantation as a mean to boost endogenous neurogenesis and restore brain function.

1. Introduction

The intriguing discovery of proliferating cells in the mature rat brain by Altman and Das in the mid-60s was met with great scepticism by the scientific community^{1,2}. However, the development of proliferation markers such as, [³H]-thymidine or 5-bromo-2'-deoxy-uridine (BrdU) during the last decades confirmed the discovery of the existence of proliferating cells in the mature mammalian brain. These studies have indisputably established that neural stem cells (NSCs) from the subgranular zone (SGZ) of the dentate gyrus of the hippocampus and the subventricular zone (SVZ) of the lateral ventricles continue to proliferate under normal conditions throughout mammalian adulthood³⁻⁵ (see review by Gould E *et al.*, 2007). Evidence from studies in rodents suggests that every month around 6% of proliferating cells in the dentate gyrus is functionally integrated into the hippocampus⁷. However, aging decreases neurogenesis in the mammalian brain due to an increase in negative regulators of neurogenesis⁸⁻¹¹. For instance, Wnt production was shown to decline with aging, which in turn decreases neural stem cell proliferation¹¹.

One might suppose that cerebral damage would lead to a molecular and cellular imbalance in the neurovascular niche favouring negative regulators and thus impair endogenous neurogenesis. However, studies in rodents provide accumulating evidence that the neurogenic capacity is preserved or even increases after injurious events such as seizures¹², stroke¹³ or hypoxia-ischemia (HI)¹⁴. This intriguing discovery prompted a wave of studies addressing not only the more fundamental aspects of neurogenesis, but also its possible role in the development and treatment of several neurological disorders, such as epilepsy¹², Parkinson's¹⁵ and Alzheimer's disease¹⁶. In this review, we will focus on the endogenous capacity of the *neonatal* brain to regenerate following a cerebral ischemic insult.

Currently, a growing number of studies focus on the development of strategies to protect and regenerate the ischemic injured neonatal brain. Neonatal encephalopathy due to perinatal cerebral ischemia remains a significant cause of neonatal mortality and leads to neurological deficits, such as cerebral palsy, mental retardation and seizures¹⁷⁻²⁰. At present, the only available therapy is hypothermia, which is only effective in babies born at term with mild to moderate brain damage²¹⁻²². Moreover, hypothermia has a short therapeutic window as it has to be applied within 6 hours after the ischemic event²³. Hence, there is an urgent need to unravel the mechanisms

underlying neurogenesis in the immature brain to assist development of alternative therapeutic interventions that induce and/or support endogenous neurogenesis.

Several studies by our group and others have shown that pharmacological intervention aimed at preventing neuronal cell death or neuroinflammation can provide efficient neuroprotection when administered within the first 24h after hypoxic-ischemic neonatal brain damage in experimental animal models²⁴⁻³¹. Additionally, there are a number of compounds that have a longer therapeutic window presumably because they promote neuronal migration, neurogenesis and oligodendrogenesis^{32,33}. We propose that an additional strategy with a potentially longer therapeutic time window is represented by stem cell therapy, to regenerate the damaged brain areas. Recent work by our group and others support the concept that stem cell transplantation may have therapeutic potential with a relatively long time window and can help repair the damaged brain³⁴⁻³⁹.

In this review, we will first give an overview of developmental events taking place in the normal postnatal mammalian brain with emphasis on neuronal migration, spine/axon pruning, synapse formation and myelin formation. Subsequently, we will discuss recent findings demonstrating the endogenous capacity of the neonatal brain to regenerate following a hypoxic-ischemic insult and the molecular mechanisms underlying endogenous regenerative processes after brain damage. Finally, the potential to employ stem cell transplantation as a mean to promote endogenous repair and restore brain function will be discussed.

2. The developing mammalian brain

2.1. Neural stem cells in the postnatal brain

Neural stem cells from the SVZ and SGZ are self-renewing and are capable of differentiating into neurons, astrocytes and oligodendrocytes⁴⁰. In this review, the term lineage-specific progenitors or precursors refers to cells with restriction to one specific lineage (*e.g.* neuronal, astroglial and oligodendroglial). There are three types of stem cells in the SVZ (*viz.*, Type B, C and A cells). Type B cells give rise to actively proliferating C cells⁴¹, which in turn give rise to type A cells. Type A cells are immature neuroblasts that migrate in chains to the olfactory bulb^{42,43}. Evidence suggests that type B cells have an astrocytic nature as they show morphological characteristics

of astrocytes and express astroglial markers, such as glial fibrillary acidic protein (GFAP). The adult SGZ contains two types of stem cells (*viz.*, Type I and Type II)^{44,45}. Type I progenitors are radial astrocytes that, in contrast to other astrocytes in the SGZ, express both GFAP and nestin⁴⁶. The lineage-specific Type II progenitors (also called type D cells) are derived from Type-I cells^{44,45}. Immature type II progenitors cells divide and will later show properties of neurons, *e.g.* express doublecortin (DCX), poly-sialylated neural adhesion molecule (PSA-NCAM) or NeuN^{7,45,47}.

Until recently, neural stem cells (NSCs) had only been observed in the SVZ and SGZ of the healthy mammalian brain. However, an intriguing study identified neural progenitor cells in the neocortical layer 1 of adult rats subjected to mild ischemia⁴⁸. These cells were shown to migrate radially into cortical layers 2-6 and differentiate into a subtype of GABAergic interneurons. The authors showed that proliferating cells in layer 1 are not derived from SVZ neural stem cells or progenitors, but rather from local progenitors that do not differentiate under normal conditions. However, the question remains whether these cortical progenitor cells are functionally integrated into cortical networks (see Fishell G. and Goldman JE. 2010).

Thus, although some impressive experimental data suggest that neurogenesis can also take place in neocortical layer 1, indisputable proof is still lacking due to discrepancies between studies. Hence, the general theory is that under normal conditions, neurogenesis is restricted to the SVZ and SGZ in the adult brain, although progenitors may be present in other areas of the brain. This suggests that specific factors have to be present in the environment surrounding the NSCs allowing the formation of new neurons. This concept is clearly demonstrated in a study where progenitor cells from the spinal cord, a known non-neurogenic region, differentiate into neurons when transplanted into the SGZ, illustrating that the SGZ and SVZ provide an environment that supports neurogenesis⁵⁰. This environment is known as the neurovascular niche, which comprises progenitor cells, different types of neurons (*e.g.* granule cells), astrocytes, and oligodendrocytes in close proximity to blood vessels (Fig 1). These cells not only express membrane-associated factors, but also secrete factors, including mitogenic factors, growth factors and neurotrophic factors that play a role in promoting cell proliferation, fate determination, neuronal survival and maturation⁵¹. Therefore, we would like to propose that progenitors may be present outside the known stem cell niches in the brain, but that the environment

of the progenitors will dictate differentiation and proliferation. The neurovascular niche will be described in more detail in section 4.

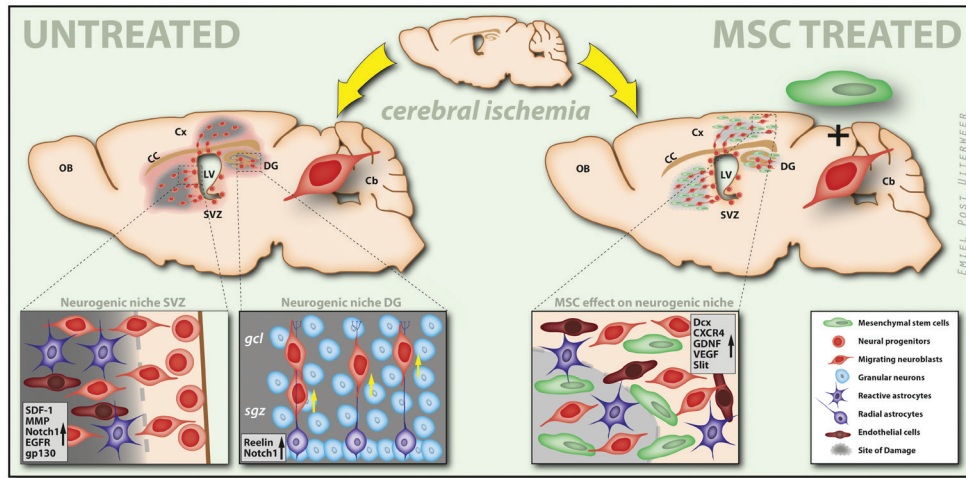


Figure 1: Neurogenesis and migration in the SVZ and SGZ following HI and MSC treatment. Schematic overview of the neurogenic niche in the SVZ and SGZ. Neural progenitors in the SVZ differentiate into neuroblasts (DCX⁺), which not only migrate towards the damaged striatum, but also through radial migration along the corpus callosum towards cortical regions. Neuroblasts in the SGZ migrate along radial astrocytes towards the GCL in the DG. HI induces the production of several factors that promote neurogenesis and migration. Regenerative processes following intranasal MSC treatment in the HI damaged brain. MSC increases the production of several factors that are involved in cell proliferation, differentiation and migration. OB = olfactory bulb; CC = corpus callosum; LV = Lateral Ventricle; Cx = cortex; Cb = cerebellum; DG = dentate gyrus; sgz = subgranular zone; gcl = granular cell layer

2.2. Postnatal development of the brain

The mammalian brain is not yet fully developed at the time of birth and thus several developmental processes are still taking place postnatally. It is during this period that neurons will form synapses, which in turn develop into neural networks. Hence, an injurious event at this period will hinder maturational processes which may lead to life-long detrimental effects on, *e.g.* cognitive and motor modalities.

During the first postnatal weeks, a substantial amount of migrating cells can be found in the SGZ and SVZ of the rodent brain. The majority of these cells are glial progenitors, as gliogenesis persists in the SVZ for several weeks. These progenitors migrate in two distinct ways depending upon their target area in the brain. While some progenitors migrate radially towards the dorsal cortex, others first migrate

tangentially along the white matter and then radially towards the lateral cortex. The mechanisms that regulate neuronal migration from the neurogenic regions, SVZ and SGZ in the postnatal brain, are comparable to those in the adult SVZ. In both cases progenitors from the SGZ migrate towards the hippocampal granule cell layer and those from the SVZ migrate tangentially towards the olfactory bulb (OB) through the rostral migratory stream (RMS). The progenitors migrating through the RMS, which consists of astrocyte tubes, form chains of cells that, when reaching the OB, migrate radially into the granule cell layer and glomerular layer of the OB⁵² (see review by Cayre M. *et al.* 2009). One major difference between migration from the postnatal and adult SVZ is that the astrocyte tubes only appear two to three weeks after birth⁵³. Therefore, migration to other brain regions, such as the striatum, may be facilitated in the first three postnatal weeks, as glial tubes may restrict the migration of progenitors within the RMS.

Neuronal network formation involves substantial reorganization of existing neuronal circuits, which is mediated by events such as spine/axon pruning and cell death. Spine/axon pruning and cell death are important opposing mechanisms establishing the patterning of the neural networks within the mammalian brain, and are essential for normal development and functioning of neural circuits. Indeed, abnormalities of spine structure and dynamics have been correlated to several diseases including Fragile-X syndrome^{54,55}, Alzheimer⁵⁶ and ischemia⁵⁷⁻⁵⁹. Spine and axon pruning is characterized by the removal of inappropriate connections in different regions of the mammalian brain. Axon pruning can either involve the elimination of certain axon terminals within the same target area by competition or the removal of collateral branches targeting functionally inappropriate areas^{60,61}. This event is tightly regulated by intrinsic factors, such as transcription factors⁶², the ubiquitin-proteasome system⁶³ and the fragile-X mental retardation protein (FMRP)⁶⁴ which are triggered in response to differentiation or maturation of the neuron. Pruning can also be triggered by extrinsic factors such as axon repulsion molecules⁶⁵⁻⁶⁷, hormones^{68,69} and trophic factors⁷⁰ (see review by P. Vanderhaeghen and H.J. Cheng 2009).

Synapse formation takes place in the developing brain, a process that shares several similarities with axon guidance. Dendritic filopodia, like growth cones, search the proximal environment for a potential site to form a synapse. Furthermore, axon guidance cues also play a role in synaptogenesis as they promote or inhibit the formation of presynaptic terminals⁶⁰. After the formation of axon-dendritic complexes, some

contacts will become stabilized. At present, the molecular mechanisms underlying the stabilization of synapses remain poorly understood. This process may be mediated by interactions between proteins found on the cell surfaces of axon-dendritic complexes, such as cadherins, neurexin and neuroligin⁷¹. Synaptic maturation is characterized by recruitment of post- and presynaptic proteins such as ion channels, scaffolding proteins and presynaptic vesicles^{72,73}.

Axon myelination is essential for neurons to function. The majority of myelin production by mature oligodendrocytes takes place early in life and continues until adolescence. Myelination depends upon differentiation of oligodendrocytes and factors secreted by axons (see review by Emery B. 2010). Mature oligodendrocytes will wrap their own cell membrane around axons forming sheaths of compact multilayered membranes that function as an isolating membrane due to their rich lipid content. Axon myelination is a crucial step in the development of the central nervous system as it reduces energy consumption during the restoration of ion gradients by Na⁺/K⁺-ATPases. The restriction of action potential and ion currents combined with the isolating properties of myelin increase the conduction velocity, enabling 'saltatory' signal propagation in the nervous system^{75,76}. Thus, axon myelination is of critical importance for normal brain function. This is clearly illustrated in debilitating disorders such as leukodystrophies, in which oligodendrocytes fail to assemble or to maintain myelin, leading to impaired motor-sensory and cognitive development⁷⁵.

3. Neurogenesis following a hypoxic-ischemic insult

3.1. Hypoxic-ischemic induction of neurogenesis in the SGZ and SVZ region

A hypoxic-ischemic insult, which can occur during or after delivery, will lead to cerebral injury despite the endogenous neurogenic capacity of the brain. Accumulating evidence suggests that hypoxic-ischemic (HI) injury promotes extensive cell proliferation in the SVZ of the rodent brain^{14,77-83}. Several studies in which P6 and P7 rats and P10 mice were subjected to moderate HI, showed that the SVZ expands in size, illustrated by increased cresyl-violet staining and nestin-positive cells in the ipsilateral SVZ^{78,79,83}. Furthermore, an increase in BrdU⁺ cells was observed in the affected SVZ from one week to three weeks following HI, implying that cell proliferation is stimulated in this region^{14,77-79,81,83,84}. Interestingly, BrdU⁺ cells were also shown in the striatum^{14,77,78,81,83}

and cortical regions^{14,77,82} from one to four weeks after the insult. This finding suggests that proliferating cells in the SVZ migrate to these regions or that local progenitors proliferate due to molecular changes in the environment of the cells. Overall, these results indicate that the SVZ maintains the capacity to promote cell proliferation, that the progenitor cells are capable to migrate to damaged brain regions and that the striatal and cortical environments support proliferating cells after HI injury.

Accumulating knowledge has been gained on the capacity of the hippocampus of the adult brain to regenerate following an injurious event. Yet, only a few studies have investigated the proliferative capacity of the SGZ in the injured *neonatal* brain. Qui *et al.* 2007 compared neurogenesis after HI injury in immature (P9) and juvenile (P21) C57BL/6 mice by injecting BrdU during the first seven days after the insult. Four weeks later, BrdU⁺ cells were quantified in the dentate gyrus (DG) and the cornu ammonis (CA) region individually, thus making it possible to determine whether these regions differ in proliferative capacity⁸⁵. Interestingly, HI injury did not affect cell proliferation in the DG, while in the CA region a significant increase in proliferation rate was detected in the immature (P9) brain⁸⁵. However, HI injury in juvenile (P21) mice induces a substantial increase in the proliferation rate in both the DG and the CA region showing the potential capacity of cells in the DG to increase proliferation in response to an insult. The apparent lack of cell proliferation in the immature (P9) DG may be explained by normal developmental processes, *i.e.* under baseline conditions, proliferation is substantially higher in P9 mice compared to P21 mice and may already have a maximal rate in the immature P9 mice⁸⁵.

In contrast to the results discussed above, recent work by Kadam *et al.* 2008 showed decreased cell proliferation in the DG region of CD-1 mice subjected to ischemia alone at P12. This discrepancy may be explained by the fact that different strains were used in the two studies or differences in the severity of the insult. CD-1 mice are more sensitive to HI injury than other mice strains like C57BL/6⁸⁶. Even though only unilateral carotid artery ligation was performed in the model used by Kadam *et al.* 2008, histological data shows that the brain damage observed in their study was more severe than that experienced by the more resilient C57BL/6 strain. Nevertheless, one should keep in mind that hypoxia might function as an additional trigger for cell proliferation. Another explanation could be the different BrdU injection protocols that were used. Qui *et al.* 2007 administered BrdU from P10 to P17 once every day, while in the study by Kadam *et al.* 2008 BrdU was given every 9 hours from P18 to

P20. Therefore, the study by Qui *et al.* 2007 detected cells that were proliferating just after the insult, *i.e.*, during a period when the DG is still developing in the P9 mouse, while the study by Kadam *et al.* injected the BrdU during a phase in which DG was almost fully developed. Thus, the study paradigm may account for the lower levels of proliferating cells detected in the DG region by Kadam *et al.* 2008 and emphasizes the importance of standardizing experimental set-ups. One of the major challenges encountered when comparing literature results is to correctly identify and account for differences in the selection of ischemia paradigms and experimental protocols.

3.2. Cell fate commitment of proliferating cells in the SGZ and SVZ

The next question to be addressed is the cell fate commitment of BrdU⁺ cells found in the SGZ and SVZ. At present, studies suggest that glial cell fate increases after HI in the dentate gyrus, while neuronal fate (commitment) remains surprisingly unchanged^{87,88}. This shows that although progenitor cells are able to proliferate after a HI insult, the damaged dentate gyrus is incapable of increasing neurogenesis and compensating for lost neurons and instead there is a trend towards astrocytic cell fate commitment. Studies in adult rodents also suggest a limited regenerative capacity as only a few or no new neurons have been detected following HI injury^{87,88}. Furthermore, studies by Miles *et al.*, 2008 and Nakatomi *et al.*, 2002 show that HI leads to extensive loss of neurons and that only a few newly formed neurons survive up to 6 months after HI^{87,89}. It is also unclear whether the newborn neuronal cells integrate into the local circuitry and become functional in the immature brain, and whether this effect is long-term. It has been described in studies using adult rodents that newborn neuronal cells show attenuated electrophysiological properties, such as field excitatory postsynaptic potentials (fEPSPs), which means that stimulation of a presynaptic terminal, *e.g.*, the Schaffer collaterals, evokes a decreased postsynaptic response in the regenerated hippocampus⁷. These data indicate that the hippocampal environment no longer supports neuronal cell fate commitment and functionality after HI. More systematic studies are necessary to clarify the mechanisms underlying impaired neuronal cell fate commitment in the HI injured brain.

A growing number of studies address cell fate commitment in the SVZ, striatum and cortex following HI. Several studies observed a significant increase in DCX/BrdU double-positive cells in the SVZ, striatum and cortex from one to four weeks after injury^{77,79,81-83}. These double-positive cells were clustered in chains in the striatum

and cortex and displayed the morphology of migrating neuroblasts⁸²⁻⁸⁴. Studies investigating the differentiation rate of proliferating cells into neurons and their survival show contradicting results. Current data show a decrease^{14,78}, increase^{83,84} or no change (cortical area)¹⁴ in NeuN/BrdU double-labeled cells compared to healthy brains. This discrepancy is possibly due to the use of different strains in the studies, which may affect the extent of brain damage after HI. It is striking that only the studies that used a neonatal HI model in Wistar rats observed increased neurogenesis in the striatum and cortex. This suggests that Wistar rats are more resilient to HI-induced cerebral damage than other rat or mice strains (*e.g.*, Sprague-Dawley rats or CD-1 mice). For instance, in CD-1 mouse pups, a decrease in neuronal committed cells in the striatum and cortex was detected although substantial cell proliferation takes place in the HI-affected SVZ⁷⁹. On the other hand, a substantial increase in GFAP/BrdU double labeled cells was observed at P24 and P31, suggesting that proliferating cells tend to differentiate towards an astrocytic cell fate⁷⁹. This finding is supported by all studies in rodents, independent of the strain used, since in all cases a substantial increase in glial cell fate commitment takes place in the striatum and cortex, implying that the environment after injury shows a predisposition towards gliogenesis. An alternative conclusion would be that this predisposition towards glial cell fate could be expected, as astrocytes form the largest glial cell population in the brain; they outnumber neurons by 5 times and comprise ~50% of human brain volume^{90,91}.

Investigations on the differentiation of neuron-committed cells in the striatum has surprisingly shown that most proliferating cells were calretinin (CR) positive, a marker for an interneuron subtype that encompasses only a small percentage of striatal neurons^{80,82}. Furthermore, no BrdU⁺ cells were shown to differentiate into striatal medium-sized spiny projection neurons, cholinergic neurons or parvalbumin (PV), calbindin (CB) or somatostatin (SOM) interneuron subtypes. Also in the cortex BrdU⁺ cells seem to differentiate into CR-expressing interneurons, which is unexpected since the majority of the cortical interneurons are of the PV subtype. These findings suggest that the progenitors from the SVZ are predisposed to differentiate into CR-expressing interneurons.

Survival of newborn neurons has been shown to be impaired following a HI insult. Several TUNEL⁺/BrdU⁺ cells were found at P31 in the striatum, showing that proliferating cells undergo cell death⁷⁹. Furthermore, only 15% of newly generated neurons in the cortex survived five weeks after HI⁸². The authors proposed that

newborn neurons mature slowly⁸³, raising the possibility that the failure to detect NeuN /BrdU positive cells in previous studies^{78,79} may be due to the relatively short period of time elapsed (2-3 weeks) after BrdU injection. Yet, prolonging the interval after BrdU administration may also lead to negative results, as the low number of newborn neurons could be the consequence of both slow maturation and impaired survival of neuroblasts.

Little is known about the functionality of newborn neurons in the brain following HI injury. A recent study by our group has demonstrated for the first time that a HI insult induces changes in neuronal connectivity in the corticospinal tract⁹². To visualize the axonal projections from the damaged (ipsilateral) motor cortex to the lateral corticospinal tract (contralateral side), biotinylated dextran amine (BDA) was injected into the damaged (ipsilateral) motor cortex. BDA is actively taken up by neurons and transported anterogradely towards the axon terminals, thus allowing the detection of neuronal connectivity. Our data showed that axons from the damaged (ipsilateral) motor cortex rewire towards the contralateral (undamaged) motor cortex by crossing the corpus callosum instead of projecting to the spinal cord through the corticospinal tract. Furthermore, injection of the retrograde transsynaptic tracer PRV into the left forelimb muscles (labeled with mRFP) and right forepaw muscles (labeled with eGFP) showed a significant decrease in mRFP positive neurons indicating a loss of neurons projecting from the impaired cortex along the corticospinal tract. Interestingly, mRFP positive neurons were detected in the contralateral (undamaged) cortex providing evidence of adaptive functional processes taking place in the neonatal brain following HI.

Although the postnatal brain has the capacity to initiate regenerative processes following an insult, cell proliferation, neuronal differentiation, and possibly functionality of these newborn neurons are impaired. For this reason it seems that the complex network of molecular and cellular processes that orchestrate neurogenesis and long-term survival of newborn cells are disrupted by HI injury. It would be interesting to establish which factors determine postnatal cell fate commitment and to which degree the molecular mechanisms overlap with early developmental programs. The mechanisms underlying this impairment are yet to be clarified and will be shortly addressed in the next section.

4. Molecular and cellular processes in the neurovascular niche following HI brain damage

4.1. Factors involved in regulating neurogenesis in the healthy brain

As mentioned before, the neurovascular niche plays a crucial role in regulating proliferation, differentiation and survival of newborn neurons. Astrocytes provide structural support for proliferating cells besides producing several factors that are required to sustain neurogenic processes. Astrocytes comprise almost half of the cells in the dentate gyrus and are in direct contact with proliferating cells and in proximity to blood vessels^{93,94}. Endothelial cells play an important role in neurogenesis as they produce several factors (*e.g.* FGF-2) that are essential for promoting cell proliferation, neuronal fate commitment and supporting both projection neuron and interneuron cell fate⁹⁵.

The precise role of proteins involved in neurogenesis in the healthy adult brain has still to be unravelled, but during the last decade several studies using different approaches, including *in vivo* loss and gain of gene function, have shed some light on the role of some of these factors. Cell proliferation is mostly regulated by growth factors and neurotrophins, *e.g.*, BDNF and VEGF, but also by morphogens, such as Wnt3 and Shh. The latter class of proteins is also involved in neuronal cell fate commitment. Most factors regulate more than one process, *e.g.*, the morphogen Noggin that plays a role in neuronal cell differentiation and survival, and BDNF, which is amongst others involved in cell proliferation and survival (see review by Zhao, Deng, and Gage, 2008)⁵¹.

Besides growth and neurotrophic factors, the local neuronal network in the neurovascular niche is of pivotal importance in regulating neurogenesis in the adult brain. Dopaminergic signalling was shown to promote proliferation, GABAergic innervations are important for synapse formation and glutamatergic innervations play a role in neuroblasts survival, dendritic development and synaptogenesis (see review by Pathania *et al.* 2010)⁹⁶. More studies are necessary to determine the role that neurotransmitters play in regulating neuronal commitment, dendritic development, synaptic integration and survival of newborn neurons in the postnatal brain following HI injury.

4.2. Factors involved in the modulation and maintenance of neurogenesis following HI

Until now, only a few proteins that play a role in neurogenesis have been correlated to neurogenic processes following HI. However, growing evidence shows that a HI insult alters the cellular and molecular composition of the neurovascular niche⁹⁶⁻⁹⁹. Therefore, although cell proliferation is maintained in the SVZ and SGZ, detrimental changes in protein expression in the brain can lead to impairments in neuronal fate commitment, survival and functionality.

Results from microarray studies in the neonatal HI model show up- and down-regulation of several genes *e.g.* growth factors and inflammatory proteins^{84,97}. Recent studies are starting to unveil some of the proteins that may play a role in mediating neurogenesis after HI cerebral damage. Here, we will discuss some genes that were up-regulated in studies investigating neurogenesis following HI in the neonatal brain.

Increased mRNA levels of membrane receptors Notch1, EGFR and gp130 were observed in the ipsilateral SVZ at 48h after HI injury. These changes in mRNA levels coincide with increased cell proliferation in the ipsilateral SVZ, suggesting a possible role for these membrane receptors in regulating neurogenesis after HI brain damage⁸⁴. Notch1 was shown to be enriched in the SVZ and SGZ areas^{84,100}. Interestingly, recent data show that ablation of Notch1 expression in GFAP-expressing stem cells in postnatal mice results in a substantial decrease in proliferating cells and an increased preference for neural cell fate in the SGZ¹⁰⁰. Alternatively, over-expression of the intracellular portion of Notch1 (called NICD), which initiates transcription of target genes¹⁰¹⁻¹⁰³, increases proliferation and maintains GFAP-expressing stem cells. Notch1 ablation also leads to less complex arborisation and branching of newly generated neurons, which is modulated in a dosage-dependent way. Together these findings suggest that Notch1 may promote cell proliferation after HI injury and that its function may change during the different stages of neurogenesis.

Notch1 expression is increased by activation of Glycoprotein130 (gp130), which is a membrane receptor important for neural stem cell survival and proliferation¹⁰⁴. Importantly, Felling *et al.* 2006 showed that gp130 is upregulated in the SVZ where neurogenesis takes place following HI. Hence, it seems likely that gp130 may play a role in ensuring an environment that supports neurogenesis. Additionally, epidermal growth factor receptor (EGFR) is a receptor for several ligands, including Egf1 and TGF α , that acts on a plethora of signalling pathways including MAPK and Rac

pathways and therefore, plays a crucial role in promoting proliferation, migration, differentiation and survival¹⁰⁵.

Another protein that appears to play a role in neurogenic processes following HI is the fibroblast growth factor receptor 1 (Fgfr1), which promotes progenitor proliferation¹⁰⁶ and neuronal fate commitment in proliferating cells^{107,108}. A recent study demonstrated that ablation of the *Fgfr1* gene from GFAP-expressing cells in mice leads to attenuated cell proliferation in the SVZ and decreased cortical pyramidal neuron production following HI¹⁰⁹. Interestingly, *Fgfr1* knock-out does not increase apoptosis when compared to wild-type hypoxic mice, suggesting that Fgfr1 may be involved in mediating neurogenesis rather than neuroprotection following hypoxic injury. These results can therefore be interpreted as evidence that 48h after the insult, the SVZ environment supports proliferation, migration and cell survival⁸⁴.

Besides an increase in neurogenic factors, some pro-inflammatory cytokines have also been shown to be up-regulated after HI injury. Indeed, the expression level of the cytokines Interleukin-1 β (Il1 β) and Transforming Growth factor β -1 (Tgf β 1) increase following HI⁹⁷. Il1- β is expressed by activated microglia and promotes a pro-apoptotic and inflammatory environment¹¹⁰. Tgf1 β is not only expressed by activated microglia, but also by astrocytes. Conversely, Tgf1 β is a pro-neurogenic factor, as down-regulation of this factor reduces neurogenesis and impairs cognitive behaviour¹¹¹. Interestingly, the growth factor, Colony stimulation factor 1 (Csf1) was also up-regulated at 24h following HI⁹⁷. Csf1, which is expressed in astrocytes, promotes microglial development and survival, which in turn play an important role in promoting neurogenesis following HI injury¹¹². Microglia are involved in the uptake of cell debris and dying cells following an injury, which is essential for neuronal cell survival. Thereby, microglia can either be harmful or neuroprotective after HI (see Fig 1).

Future studies need to assess the level of neurogenic factors at later stages during neurogenesis, in order to understand how changes in the expression patterns of these proteins relate to neurogenic processes and cell survival.

4.3. Migration of immature neurons in the neonatal HI-injured brain

A recent study showed that the migration of neural stem cells in the SVZ can be followed in healthy and HI injured brains by *in situ* labeling the cells with MPIO and measuring with MRI, clearly showed that these cells no longer migrate towards the

olfactory bulb through the RMS, but instead migrate towards the damaged cortical areas¹¹³.

The mechanisms regulating neuroblast migration towards the striatum in the neonatal HI brain are still unclear (see review by Cayre *et al.*, 2009). However, there is evidence that in the rodent adult brain SDF-1/CXCR-4 signalling mediates migration of neuroblasts from the SVZ to the striatum. Results show that reactive astrocytes produce SDF-1, while immature neurons express the receptor CXCR-4¹¹⁴. Furthermore, migration of immature neurons could be inhibited by the specific CXCR-4 inhibitor AMD-3100, proposing that these molecules are important regulators of migration of immature neurons in this brain region. Another study showed that DCX/BrdU positive neuroblasts co-localize with matrix metalloproteinases (MMPs), a family of zinc endopeptidases that modulate all components of extracellular matrix in the brain, thus allowing the neuroblasts to migrate through axonal extension^{115,116}. Interestingly, inhibiting MMPs significantly suppressed migration of neuroblasts from the SVZ to striatum¹¹⁶. Furthermore, several studies have shown that MMPs are upregulated following ischemia¹¹⁷⁻¹¹⁹.

Evidence suggests that migrating neuroblasts in the hippocampus use radial glial fibers as a scaffold, since these cells extend their axons from the subgranular zone and traverse the granule layer perpendicularly (see Fig 1). Another cell type that regulates migration in the SGZ are the Cajal-Retzius cells that secrete reelin, which is an extracellular matrix (ECM) serine protease that seems to function as a stop- or detachment-signal for migrating neurons. The pivotal role of this protein is illustrated in so-called *reeler* mice, as lack of reelin results in an inverted cortex due to aberrant migration of neurons to the superficial plate¹²⁰. It remains unclear exactly how reelin regulates neuronal migration. So far, it seems to be mediated by very low-density lipoprotein receptor (VLDLR) and apolipoprotein E type 2 receptor (ApoER2), which leads to tyrosine phosphorylation of the adaptor protein Disabled-1 (Dab-1)¹²¹.

Hypoxia is a known trigger of angiogenesis. Several studies have shown that blood vessels play a role in progenitor cell migration in the adult brain. Thored *et al.* 2006 established that HI triggers angiogenesis in the SVZ and striatum and that DCX⁺ cells and blood vessels are closely associated. However, different numbers of progenitor cells were observed in areas with similar vascular density, suggesting that vessels are not sufficient to regulate migration efficiently.

In conclusion, it appears that the neurovascular niche in neonatal mice does not support full repair following HI damage and thus does not provide the structural and humoral support necessary for inducing and maintaining long-term neurogenesis (see Fig 1). The precise balance and gradient of proteins may be tightly regulated through the different stages of neurogenesis. Furthermore, cell migration and network formation is still taking place in the neonatal brain. It is therefore crucial to assist the neonatal brain in the process of regeneration after cerebral ischemia, allowing it to repair the cellular and structural damage and to keep up with the developmental phase.

5. Stem-cell based therapy: Enhancing the neurogenic potential of neural stem cells

Until now, no definitive proof has been obtained that the primary goal of neurogenesis is regeneration of the brain following an injurious event. Enriched odor exposure increases the survival of newborn neurons in the rodent olfactory bulb, thereby correlating neurogenesis to olfactory experience and learning in rodents^{47,122}. Methyl-CpG binding proteins (*Mbd1*) are highly expressed in progenitor cells and neurons, and are possibly involved in regulating DNA methylation in the adult rodent brain¹²³. Studies show that *mbd1* knockout mice have decreased SGZ neurogenesis and impaired learning and memory^{123,124}, suggesting a functional significance for neurogenesis in the SGZ of the rodent brain. Nevertheless, the fact that neurogenesis is restricted to specific brain regions implies that it plays a role in regulating the function of the hippocampus and olfactory system. Thus, current data raise the interesting possibility that neurogenesis may be important for the rodent brain to function normally. Nevertheless, evidence suggests that neurogenesis decreases following an injurious event, thereby proposing that regeneration may not be the primary goal of neurogenesis.

A growing number of studies suggest that MSC transplantation may be a promising tool to boost endogenous neurogenesis. Recent data show that administration of MSC following a HI insult significantly reduces lesion volume, improves behavioral performance and promotes neurogenesis^{35,125-127}. Furthermore, studies show that MSCs migrate to the ischemic boundary zone where they induce changes in brain

environment that promote and support neurogenesis¹²⁸⁻¹³⁰. A study from our group showed that intracranial MSC treatment at 3 and 10 days after HI-induced injury changes the expression of genes involved in regenerative processes. Some key functions associated with an increased gene expression are cell growth, cell proliferation, nervous system development and cell migration. Our findings are further supported by studies in which human neural stem cells were transplanted intracranially at 24h after HI inducing an increase in the expression of genes involved in neurogenesis (*e.g.* doublecortin), migration (*e.g.* CXCR4) and survival (*e.g.* glial derived neurotrophic factor)³⁴ (see figure 1). Furthermore, studies show that MSCs¹³⁰ and human neural stem cells improve axonal sprouting and neurite plasticity by increasing the expression of factors like VEGF and Slit¹³¹. Results from our group show that transplanted MSCs themselves do not differentiate into neurons and oligodendrocytes, suggesting that stimulation of endogenous neural stem cells by MSC is mainly responsible for restoring tissue damage¹³². Hence, current data strongly suggest that stem cells secrete factors that promote neurogenic processes and boost regenerative processes in the HI-injured neonatal brain.

Besides showing promising results as a therapeutic strategy, the use of MSCs as a treatment for HI injury holds some more advantages over other strategies. One major appeal of using MSCs as a therapeutic tool is the considerably longer therapeutic window after HI, as administration of MSCs at 10 days after HI leads to improved motor and histological outcome¹³². MSC treatment has also some advantages over neural or embryonic stem cells therapies, since MSC do not express HLA-DR antigens these cells are low-immunogenic, in contrast to neural stem cells and can be used over the allogeneic barrier. Over the past decade, allogeneic MSCs have been widely used as a treatment for hematopoietic diseases^{133,134}. Another major advantage is that they can be obtained easily and safely from placental tissue, umbilical cord stroma and cord blood, whereas neural stem cells and embryonic stem cells can be only obtained from fetal tissue, thereby raising ethical issues. Transplantation of embryonic stem cells may have undesirable consequences as these cells can transdifferentiate into tumors besides differentiating into the desired tissue-type. Although it has never been shown, the possibility remains that MSCs become HLA-DR⁺ after activation and thus, lead to alloreactivity. However, MSCs only survive a few weeks after administration into the brain which will limit the risk of inducing a host versus graft response in the brain¹³². Nevertheless, autologous MSCs from the stroma or blood of the umbilical cord might be the safest treatment option.

Another important aspect of stem cell therapy is finding an efficient and non-invasive administration route. Recent studies show that intranasally administered MSCs migrate towards other brain regions¹³⁵. This method has some advantages over the more conventional administration routes, *i.e.*, intracranial and intravenous injection, as it is less invasive and may reduce systemic exposure. Indeed results from our own group show that intranasal administration of MSCs after neonatal hypoxia-ischemia in P9 mice is as effective as intracranial MSC transplantation leading to improved motor efficacy of treatment may also depend on the administration route. Recently, it has been shown that intravenously injected mononuclear cells (MNCs)¹³⁶ and neural stem cells¹³⁷ are not only detected in the brain, but also in a substantial amount in the spleen¹³⁶, and liver and lungs, respectively¹³⁷. Hence, significantly less of the injected stem cells will end up in the brain after intravenous delivery as they will circulate throughout the body and may even have an undesired effect in other organs.

6. Conclusion and Future Prospects

It is increasingly evident that the neonatal brain has a limited capacity to adapt and regenerate following a deleterious event, such as cerebral ischemia. Although neurogenesis occurs under physiological conditions and may even increase after an insult, the immature brain is incapable of fully regenerating following cerebral ischemia. This impairment may be due to the extent of cellular loss but also to a possible disturbed expression of growth- and differentiation factors in the neurovascular niche as a consequence of brain damage. Crucial questions to be answered are which factors play a pivotal role during the different phases of neurogenesis under normal conditions and on top of that how neurogenic processes within the brain are affected by an insult. Moreover, the molecular and cellular composition of the neurogenic niche that will favor regeneration has to be defined more precisely.

In the past years significant progress has been made in optimizing stem cell treatment as a tool to boost the limited capacity of the neonatal brain to regenerate, especially by the use of MSCs. The intranasal administration route may represent the most optimal route in rodents, but has still to be verified in humans. Before translating the results to the clinic, more knowledge is also needed on the exact array of molecules that direct MSC migration towards the damaged regions.

Transplantation of MSCs induces regulation of the expression of many genes in the neonatal brain, but research is still scarce about the hierarchy or redundancy of the plethora of factors which are up- and down-regulated after transplantation. Although MSC treatment has a relatively long therapeutic window in animal models, one has to realize that the neonatal brain is still immature, being in a critical developmental phase. One of the most challenging issues to be solved in this area of research is to unravel the mechanism by which MSCs adapt to the developmental and regenerative needs of the environment after injurious events in the neonate. We also propose that MSCs do not integrate into the network but stimulate proliferation and differentiation of endogenous precursors. It will be interesting to know to what extent these new (autologous) neurons and other cell types of the brain survive and integrate in existing functional networks. However, pre-clinical research has shown by now that MSC therapy has the potential to become an efficient therapy to treat neonatal brain damage by boosting the endogenous capacity of the immature brain to regenerate, thereby repairing the lesion and improving motor and cognitive behavior in the long-term. The neonatal brain may even be a better 'target' for stem cell therapy than the adult brain because of the higher availability of endogenous precursors in the neonatal brain.

Acknowledgment

The authors are greatly indebted to Emiel Post-Uiterweer, MD for his contribution in designing the figure. This review was supported by EU-7 Neurobid (HEALTH-F2-2009-241778) from the European Union and Zon-MW Project (no 116002003).

References

1. Altman J, Das GD. Autoradiography and histological evidence of postnatal neurogenesis in rats. *J Comp Neurol* 1965; 124: 319-335.
2. Altman J, Das GD. Autoradiography and histological studies of postnatal neurogenesis. I. A longitudinal investigation of the kinetics, migration and transformation of cells incorporating tritiated thymidine in neonate rats, with special reference to postnatal neurogenesis in some brain regions. *J Comp Neurol* 1966; 126: 337-389.
3. Ramirez-Amaya V, Marrone DF, Gage FH, et al. Integration of new neurons into functional neural networks. *J of Neurosci* 2006; 26: 12237-12241.
4. Eriksson PS, Perfilieva E, Bjork-Eriksson T, et al. Neurogenesis in the adult human hippocampus. *Nat Med* 1998; 4: 1313-1317.
5. Kaplan MS, Hinds JW. Neurogenesis in the adult rat: electron microscopic analysis of light radioautographs. *Science* 1977; 197: 1092-1094.
6. Gould E. How widespread is adult neurogenesis in mammals? *Nat rev Neurosci* 2007; 6: 481-488.
7. Seri B, Garcia-Verdugo JM, Collado-Morente L, et al. Cell types, lineage, and architecture of the germinal zone in the adult dentate gyrus. *J Comp Neurol* 2004; 478: 359-378.
8. Hattiangady B, Rao MS, Shetty GA, et al. Brain-derived neurotrophic factor, phosphorylated cyclic AMP response element binding protein and neuropeptide Y decline as early as middle age in the dentate gyrus and CA1 and CA3 subfields of the hippocampus. *Exp. Neurol* 2005; 195: 353-371.
9. Kuhn HG, Dickinson-Anson H, Gage FH. Neurogenesis in the dentate gyrus of the adult rat: age-related decrease of neuronal progenitor proliferation. *J Neurosci* 1996; 16: 2027-2033.
10. Leuner B, Kozorovitskiy Y, Gross CG, et al. Diminished adult neurogenesis in the marmoset brain precedes old age. *Proc. Natl Acad. Sci. USA* 2007; 104: 17169-17173.
11. Miranda CJ, Braun L, Jiang Y, et al. Aging brain microenvironment decreases hippocampal neurogenesis through Wnt- mediated surviving signalling. *Aging Cell* 2012; 11: 542-552.
12. Scharfman HE, McCloskey DP. Postnatal neurogenesis as a therapeutic target in temporal lobe epilepsy. *Epilepsy Res* 2009; 85: 150-161.
13. Yoo SW, Kim SS, Lee SY, et al. Mesenchymal stem cells promote proliferation of endogenous neural stem cells and survival of newborn cells in a rat stroke model. *Exp Mol Med* 2008; 40: 387-397.
14. Kadam SD, Mulholland JD, McDonald JW, et al. Neurogenesis and neuronal commitment following ischemia in a new mouse model for neonatal stroke. *Brain research* 2008; 1208: 35-45.
15. Yasuhara T, Matsukawa N, Hara K, et al. Transplantation of human neural stem cells exerts neuroprotection in a rat model of Parkinson's disease. *J Neurosci* 2006; 3: e2935.
16. Rodriguez JJ, Jones VC, Tabuchi M, et al. Impaired adult neurogenesis in the dentate gyrus of a triple transgenic mouse model of Alzheimer's disease. *Plos One* 2008; 3: e2935.

17. Volpe JJ. Perinatal brain injury: From pathogenesis to neuroprotection. *Ment Retard Dev Disabil Res Rev* 2001; 7: 56-64.
18. Badr Zahr LK, Purdy I. Brain injury in the infant: the old, the new and the uncertain. *J Perinat Neonatal Nurs* 2006; 20: 163-175.
19. Vexler ZS, Ferriero DM. Molecular and biochemical mechanisms of perinatal brain injury. *Semin Neonatol* 2001; 6: 99-108.
20. Dammann O, Ferriero D, Gressens P. Neonatal encephalopathy or hypoxic-ischemic encephalopathy? Appropriate terminology matters. *Pediatr Res* 2011; 70: 1-2.
21. Azzopardi DV, Strohm B, Edwards AD, et al. Moderate hypothermia to treat perinatal asphyxia encephalopathy. *N Engl J Med* 2009; 361: 1349-1358.
22. Gluckman PD, Wyatt JS, Azzopardi D, et al. Selective head cooling with mild systemic hypothermia after neonatal encephalopathy: multicentre randomised trial. *Lancet* 2005; 365: 663-670.
23. Perlman JM. Intervention strategies for neonatal hypoxic-ischemic cerebral injury. *Clin Ther* 2006; 28: 1353-1365.
24. Nijboer CH, Heijnen CJ, Groenendaal F, et al. Strong neuroprotection by inhibition of NF{ κ }B after neonatal hypoxia-ischemia involves apoptotic mechanisms but is independent of cytokines. *Stroke* 2008; 39: 2129-2137.
25. Nijboer CH, Heijnen CJ, van der Kooij MA, et al. Targeting the p53 pathway to protect the neonatal ischemic brain. *Ann Neurol* 2011; 70: 255-264.
26. Compagnoni G, Pogliani L, Lista G, et al. Hypothermia reduces neurological damage in asphyxiated newborn infants. *Biol Neonate* 2002; 82: 222-227.
27. Ishida A, Trescher WH, Lange MS, et al. Prolonged suppression of brain nitric oxide synthase activity by 7-nitroindazole protects against cerebral hypoxic-ischemic injury in neonatal rat. *Brain Dev* 2001; 23: 349-354.
28. Lin S, Zhang Y, Dodel R, et al. Minocycline blocks nitric oxide-induced neurotoxicity by inhibition p38 MAP kinase in rat cerebellar granule neurons. *Neurosci Lett* 2001; 315: 61-64.
29. Han BH, Xu D, Choi J, et al. Selective, reversible caspase-3 inhibitor is neuroprotective and reveals distinct pathways of cell death after neonatal hypoxic-ischemic brain injury. *J Biol Chem* 2002; 277: 30128-30136.
30. Leonardo CC, Eakin AK, Ajmo JM, et al. Delayed administration of a matrix metalloproteinase inhibitor limits progressive brain injury after hypoxia-ischemia in the neonatal rat. *J Neuroinflamm* 2008; 5: 34-44.
31. Cowper-Smith CD, Anger GJA, Magal E, et al. Delayed administration of a potent cyclin dependent kinase and glycogen synthase kinase 3 β inhibitor produces long-term neuroprotection in a hypoxia-ischemia model of brain injury. *Neuroscience* 2008; 155: 864-875.
32. Han J, Pollak J, Yang T, et al. Delayed administration of a small molecule tropomyosin-related kinase B ligand promotes recovery after hypoxic-ischemic stroke. *Stroke*; 43: 1918-1924.
33. Iwai M, Stetler A, Xing J, et al. Enhanced oligodendrogenesis and recovery of neurological function by erythropoietin following neonatal hypoxic-ischemic brain injury. *Stroke*; 2010: 1032-1037.

34. Daadi MM, Davis AS, Arac A, et al. Human neural stem cell grafts modify microglial response and enhance axonal sprouting in neonatal hypoxic-ischemic brain injury. *Stroke* 2010; 41: 516-523.
35. Van Velthoven CTJ, Kavelaars A, van Bel F, et al. Repeated mesenchymal stem cell treatment after neonatal hypoxia-ischemia has distinct effects on formation and maturation of new neurons and oligodendrocytes leading to restoration of damage, corticospinal motor tract activity, and sensorimotor function. *J Neurosci* 2010; 30: 9603-9611.
36. Bacigaluppi M, Pluchino S, Jametti LP, et al. Delayed post-ischaemic neuroprotection following systemic neural stem cell transplantation involves multiple mechanisms. *Brain* 2009; 132: 2239-2251.
37. Liao W, Xie J, Zhong J, et al. Therapeutic effect of human umbilical cord multipotent mesenchymal stromal cells in a rat model of stroke. *Transplantation* 2009; 87: 350-359.
38. Shen LH, Li Y, Chen J, et al. Intracarotid transplantation of bone marrow stromal cells increases axon-myelin remodelling after stroke. *Neuroscience* 2006; 137: 393-399.
39. Pimentel-Coelho PM, Magalhaes ES, Lopes LM, et al. Human cord blood transplantation in a neonatal rat model of hypoxic-ischemic brain damage: functional outcome related to neuroprotection in the striatum. *Stem Cells Dev* 2010; 19: 351-358.
40. Gage FH. Mammalian neural stem cells. *Science* 2000; 287: 1433-1438.
41. Doetsch F, Caille I, Lim DA, et al. Subventricular zone astrocytes are neural stem cells in the adult mammalian brain. *Cell* 1999; 97: 1-20.
42. Lois C, Alvarez-Buylla A. Long-distance neuronal migration in the adult mammalian brain. 1994; 264: 1145-1148.
43. Belluzzi O, Benedusi M, Ackman J, et al. Electrophysiological differentiation of new neurons in the olfactory bulb. *J Neurosci* 2003; 23: 10411-10418.
44. Filippov V, Kronenberg G, Pivneva T, et al. Subpopulation of nestin-expressing progenitor cells in the adult murine hippocampus shows electrophysiological and morphological characteristics of astrocytes. *Mol Cell Neurosci* 2003; 23: 373-82.
45. Fukuda S, Kato F, Tozuka Y, et al. Two distinct subpopulations of nestin-positive cells in adult mouse dentate gyrus. *J Neurosci* 2003; 23: 9357-9366.
46. Steiner B, Klempin F, Wang L, et al. Type-2 cells as link between glial and neuronal lineage in adult hippocampal neurogenesis. *Glia* 2006; 54: 805-14.
47. Seki T, Arai Y. Highly polysialylated neural cell adhesion molecule (NCAM-H) is expressed by newly generated granule cells in the dentate gyrus of the adult rat. *J Neurosci* 1993; 13: 2351-58.
48. Ohira K, Furuta T, Hioki H, et al. Ischemia-induced neurogenesis of neocortical layer 1 progenitor cells. *Nat Neurosci* 2010; 13: 173-179.
49. Fishell G, Goldman JE. A silver lining to stroke: does ischemia generate new cortical interneurons? *Nat Neurosci* 2010; 13: 145-6.
50. Shihabuddin LS, Horner PJ, Ray J, et al. Adult spinal cord stem cells generate neurons after transplantation in the adult dentate gyrus. *J Neurosci* 2000; 20: 8727-35
51. Zhao C, Deng W, Gage FH. Mechanisms and functional implications of adult neurogenesis. *Cell* 2008; 132: 645-660.

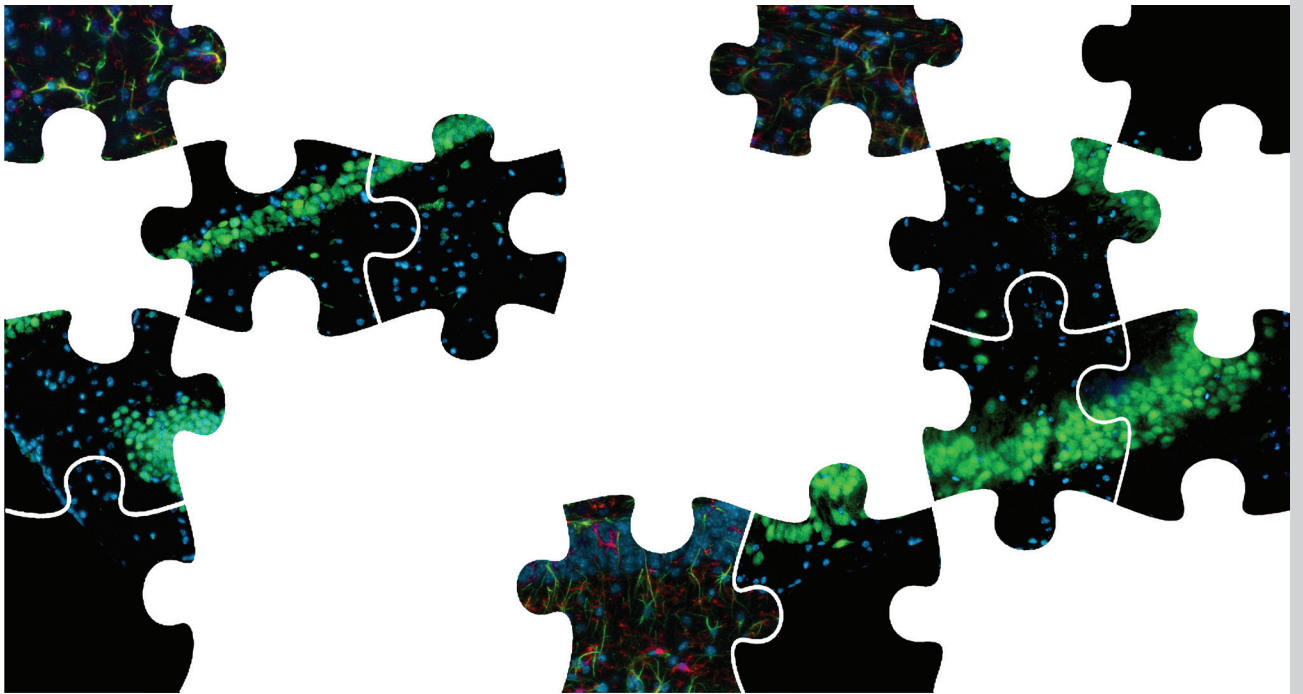
52. Cayre M, Canoll P, Goldman JE. Cell migration in the normal and pathological postnatal mammalian brain. *Prog in Neurobiol* 2009; 88: 41-63.
53. Peretto P, Giachino C, Aimar P, et al. Chain formation and glial tube assembly in the shift from neonatal to adult subventricular zone of the rodent forebrain. *J Comp Neurol* 2005; 487: 407-427.
54. Hinton VJ, Brown WT, Wisniewski K, et al. Analysis of neocortex in three males with the fragile X syndrome. *Am J Med Genet* 1991; 41: 289-294.
55. Irwin SA, Patel B, Idupulapati M, et al. Abnormal dendritic spine characteristics in the temporal and visual cortices of patients with fragile-X syndrome: a quantitative examination. *Am J Med Genet* 2001; 98: 161-167.
56. Spires-Jones TL, Meyer-Luehmann M, Osetek JD, et al. Impaired spine stability underlies plaque-related spine loss in an Alzheimer's disease mouse model. *Am J Pathol* 2007; 171: 1304-1311.
57. Enright LE, Zhang S, Murphy TH. Fine mapping of the spatial relationship between acute ischemia and dendritic structure indicates selective vulnerability of layer V neuron dendritic tufts within single neurons in vivo. *J Cereb Blood Flow Metab* 2007; 27: 1185-2000.
58. Murphy TH, Li P, Betts K, et al. Two-photon imaging of stroke onset in vivo reveals that NMDA-receptor independent ischemic depolarization is the major cause of rapid reversible damage to dendrites and spines. *J Neurosci* 2008; 28: 1756-72.
59. Brown CE, Murphy TH. Livin' on the edge: imaging dendritic spine turnover in the peri-infarct zone during ischemic stroke and recovery. *Neuroscientist* 2008; 14: 139-146.
60. Bhatt DH, Zhang S, Gan WB. Dendritic spine dynamics. *Annu Rev Physiol* 2009; 71: 261-82.
61. Parrish JZ, Emoto K, Kim MD, et al. Mechanisms that regulate establishment, maintenance, and remodelling of dendritic fields. *Annual Review of Neurosci* 2007; 30: 399-423.
62. Vanderhaeghen P, Cheng HJ. Guidance molecules in axon pruning and cell death. *Cold Spring Harbor Perspectives in Biology* 2010 2(6).
63. Kuo CT, Zhu S, Younger S, et al. Identification of E2/E3 ubiquitinating enzymes and caspase activity regulating drosophila sensory neuron dendrite pruning. *Neuron* 2006; 51: 283-290.
64. Tessier CR, Broadie K. Drosophila fragile X mental retardation protein developmentally regulates activity-dependent axon pruning. *Development* 2008; 135: 1547-1557.
65. Bagri A, Cheng HJ, Yaron A, et al. Stereotyped pruning of long hippocampal axon branches triggered by retraction inducers of the semaphoring family. *Cell* 2003; 113: 285-299.
66. Low LK, Liu XB, Faulkner RL, et al. Plexin signalling selectively regulates the stereotyped pruning of corticospinal axons from visual cortex. *Proc Natl Acad Sci USA* 2008; 105: 8136-8141.
67. Liu XB, Low LK, Jones EG, et al. Stereotyped axon pruning via plexin signalling is associated with synaptic complex elimination in the hippocampus. *J Neurosci* 2005; 25: 9124-9134.
68. Cowan WM, Fawcett JW, O'Leary DD, et al. Regressive events in neurogenesis. *Science* 1984; 225: 1258-1265.

69. Innocenti GM, Price DJ. Exuberance in the development of cortical networks. *Nat Rev Neurosci* 2005; 6: 955-965.
70. Singh KK, Park KJ, Hong EJ, et al. Developmental axon pruning mediated by BDNF-p75NTR-dependent axon degeneration. *Nat Neurosci* 2008, 11: 649-658.
71. Yamagata M, Sanes JR, Weiner JA. Synaptic adhesion molecules. *Curr Opin Cell Biol* 2003; 15: 621-632.
72. Tada T, Sheng M. Molecular mechanisms of dendritic spine morphogenesis. *Curr Opin Neurobiol* 2006; 16: 95-101.
73. Craig AM, Kang Y. Neurexin-neuroigin signaling in synapse development. *Curr Opin Neurobiol* 2007; 17: 43-52.
74. Emery B. Regulation of oligodendrocytes differentiation and Myelination. *Science* 2010; 330: 779-782.
75. Nave KA. Myelination and the trophic support of long axons. *Nat Rev Neurosci* 2010; 11: 275-283.
76. Wilkins A, Majed H, Layfield R, et al. Oligodendrocytes promote neuronal survival and axonal length by distinct intracellular mechanisms: a novel role for oligodendrocytes-derived glial cell line-derived neurotrophic factor. *J Neurosci* 2003; 23: 4967-4974.
77. Hayashi T, Iwai M, Ikeda T, et al. Neural precursor cells division and migration in neonatal rat brain after ischemic/hypoxic injury. *Brain Research* 2005; 1038: 41-49.
78. Ong J, Plane JM, Parent JM, et al. Hypoxic-Ischemic Injury Stimulates Subventricular Zone Proliferation and Neurogenesis in the Neonatal Rat. *Pediatric Research* 2005; 58: 600-606.
79. Plane JM, Liu R, Wang TW, et al. Neonatal hypoxic-ischemic injury increases forebrain subventricular zone neurogenesis in the mouse. *Neurobiol Dis* 2004; 16: 585-595.
80. Yang Z, You Y, Levison SW. Neonatal hypoxic/ischemic brain injury induces production of calretinin-expressing interneurons in the striatum. *J Comp Neurol* 2008; 511: 19-33.
81. Yang Z, Levison SW. Perinatal Hypoxic/Ischemic Brain Injury Induces Persistent Production of Striatal Neurons from Subventricular Zone Progenitors. *Developmental Neuroscience* 2007, 29: 331-340.
82. Yang Z, Covey MV, Bitel CL, et al. Sustained neocortical neurogenesis after neonatal hypoxic/ischemic injury. *Ann Neurol* 2007; 61: 199-208.
83. Yang Z, Levison SW. Hypoxia/ischemia expands the regenerative capacity of progenitors in the perinatal subventricular zone. *Neuroscience* 2006; 139: 555-564.
84. Felling RJ, Snyder MJ, Romanko MJ, et al. Neural stem/progenitor cells participate in the regenerative response to perinatal hypoxia/ischemia. *J Neurosci* 2006; 26: 4359-4369.
85. Qiu L, Zhu C, Wang X, et al. Less neurogenesis and inflammation in the immature than in the juvenile brain after cerebral hypoxia-ischemia. *J Cereb Blood Flow Metab* 2007; 27: 785-794.
86. Sheldon RA, Sedik C, Ferriero DM. Strain-related brain injury in neonatal mice subjected to hypoxia-ischemia. *Brain Res* 1998; 810: 114-122.
87. Nakatomi H, Kuriu T, Okabe S, et al. Regeneration of hippocampal pyramidal neurons after ischemic brain injury by recruitment of endogenous neural progenitors. *Cell* 2002; 110: 429-441.

88. Takagi Y, Nozaki K, Takahashi J, et al. Proliferation of neuronal precursor cells in the dentate gyrus is accelerated after transient forebrain ischemia in mice. *Brain Research* 1999; 831: 283-287.
89. Miles DK, Kernie SG. Hypoxic-ischemic brain injury activates early hippocampal stem/progenitor cells to replace vulnerable neuroblasts. *Hippocampus* 2008; 18: 793-806.
90. Rossi DJ, Brady JD, Mohr C. Astrocyte metabolism and signaling during brain ischemia. *Nat Neurosci* 2007; 10: 1377-1386.
91. Sofroniew MV, Vinters HV. Astrocytes: biology and pathology. *Acta Neuropathol* 2010; 119: 7-35.
92. Van Velthoven CTJ, van de Looij Y, Kavelaars A, et al. Mesenchymal stem cells restore cortical rewiring after neonatal ischemia in mice. *Ann Neurol* 2012; 71:785-796.
93. Palmer TD, Willhoite AR, Gage FH. Vascular niche for adult hippocampal neurogenesis. *J Comp Neurol* 2000; 425: 479-494
94. Song H, Stevens CF, Gage FH. Astroglia induce neurogenesis from adult neural stem cells. *Nature* 2002; 417: 39-44.
95. Shen Q, Goderie SK, Jin L, et al. Endothelial cells stimulate self-renewal and expand neurogenesis of neural stem cells. *Science* 2004; 304: 1338-1340.
96. Pathania M, Yan LD, Bordey A. A symphony of signals conducts early and late stages of adult neurogenesis. *Neuropharmacology* 2010; 58: 865-876.
97. Van Velthoven CTJ, Heijnen CJ, van Bel F, et al. Osteopontin enhances endogenous repair after neonatal hypoxic-ischemic brain injury. *Stroke* 2011; 42: 2294-301.
98. Zhao YD, Cheng SY, Ou S, et al. Functional response of hippocampal CA1 pyramidal cells to neonatal hypoxic-ischemic brain damage. *Neurosci Lett* 2012; 10: 5-8.
99. Madri JA. Modeling the neurovascular niche: implications for recovery from CNS injury. *J Physiol Pharmacol* 2009; 60: 95-104.
100. Breunig JJ, Silbereis J, Vaccarino, et al. Notch regulates cell fate and dendritic morphology of newborn neurons in the postnatal dentate gyrus. *PNAS* 2007; 51: 20558-20563.
101. Artavanis-Tsakonas S, Rand MD, Lake RJ. Notch signalling: cell fate control and signal integration in development. *Science* 1999; 284: 770-776.
102. Bray SJ. Notch signalling: a simple pathway becomes complex. *Nat Rev Mol Cell Biol* 2006; 7: 678-689.
103. Schroeter EH, Kisslinger JA, Kopan R. Notch-1 signaling requires ligand-induced proteolytic release of intracellular domain. *Nature* 1998; 393: 382-386.
104. Chojnacki A, Shimazaki T, Gregg C, et al. Glycoprotein 130 signaling regulates Notch1 expression and activation in the self-renewal of mammalian forebrain neural stem cells. *J Neurosci* 2003; 23: 1730-1741.
105. Yarden Y, Sliwkowski MX. Untangling the ErbB signaling network. *Nat Rev Mol Cell Biol* 2001; 2: 127-137.
106. Stavridis MP, Lunn JS, Collins BJ, et al. A discrete period of FGF-induced Erk1/2 signaling is required for vertebrate neural specification. *Development* 2007; 134: 2889-2894.
107. Wagner JP, Black IB, DiCicco-Bloom E. Stimulation of neonatal and adult brain neurogenesis by subcutaneous injection of basic fibroblast growth factor. *J Neurosci* 1999; 19: 6006-6016.

108. Vaccarino FM, Schwartz ML, Raballo R, et al. Fibroblast growth factor signalling regulates growth and morphogenesis at multiple steps during brain development. *Curr Top Dev Biol* 1999; 46: 179-200.
109. Fagel DM, Ganat Y, Cheng E, et al. Fgfr1 is required for cortical regeneration and repair after perinatal hypoxia. *J Neurosci* 2009; 29:1202-1211.
110. Green HF, Treacy E, Keohane AK, et al. A role for interleukin-1 β in determining the lineage fate of embryonic rat hippocampal neural precursor cells. *Molec and Cell Neurosci* 2012; 3: 311-321.
111. Graciarena M, Depino AM, Pitossi FJ. Prenatal inflammation impairs adult neurogenesis and memory related behavior through persistent hippocampal TGF β ₁ downregulation. *Brain Behav and Immun* 2010; 8: 1301-1308.
112. Fedoroff S, Berezovskaya O, Maysinger D. Role of Colony Stimulating Factor-1 in Brain Damage Caused by Ischemia. *Neurosci and Biobehav rev* 1997; 2: 187-197.
113. Yang J, Liu J, Niu G, et al. In vivo MRI of endogenous stem/progenitor cell migration from subventricular zone in normal and injured developing brains. *Neuroimage* 2009; 48: 319-328.
114. Thored P, Arvidsson A, Cacci E, et al. Persistent Production of Neurons from Adult Brain Stem Cells During Recovery after Stroke. *Stem cells* 2006; 24: 739-747.
115. Maddahi A, Chen Q, Edvinsson L. Enhanced cerebrovascular expression of matrix metalloproteinase-9 and tissue inhibitor of metalloproteinase-1 via the MEK/ERK pathway during ischemia in the rat. *BMC Neurosci* 2009; 10: 56.
116. Lee S-R, Kim H-Y, Rogowska J, et al. Involvement of Matrix Metalloproteinase in Neuroblast Cell Migration from the Subventricular Zone after Stroke. *J Neurosci* 2006; 26: 3491-3495.
117. Gashe Y, Fujimura M, Morita-Fujimura Y, et al. Early appearance of activated matrix metalloproteinase-9 after focal cerebral ischemia in mice: a possible role in blood-brain barrier dysfunction. *J Cereb Blood Flow Metab* 1999; 19: 1020-1028.
118. Heo JH, Lucero J, Abumiya T, et al. Matrix metalloproteinases increase very early during experimental focal cerebral ischemia. *J Cereb Blood Flow Metab* 1999; 19: 624-633.
119. Leonardo C, Eakin A, Ajmo J, et al. Delayed administration of a matrix metalloproteinase inhibitor limits progressive brain injury after hypoxia-ischemia in the neonatal rat. *J Neuroinflammation* 2008; 5:34.
120. D'Arcangelo G, Miao GG, Chen SC, et al. A protein related to extracellular matrix proteins deleted in the mouse mutant reeler. *Nature* 1995; 347: 719-723.
121. Tissir F, Goffinet AM. Reelin and brain development. *Nat Rev Neurosci* 2003; 4: 496-505.
122. Alonso M, Viollet C, Gabellec MM, Meas-Yedid V, Olivo-Marin JC, Lledo PM. Olfactory discrimination learning increases the survival of adult-born neurons in the olfactory bulb. *J Neurosci* 2006; 26: 10508-10513.
123. Allan AM, Liang X, Luo Y, et al. The loss of methyl-CpG binding protein 1 leads to autism-like behavioral deficits. *Hum Mol Genet* 2008; 17: 2047-57.
124. Zhao X, Ueba T, Christie BR, et al. Mice lacking methyl-CpG binding protein 1 have deficits in adult neurogenesis and hippocampal function. *Proc Natl Acad Sci U S A* 2003; 100: 6777-82.

125. Horita Y, Honmou O, Harada K, et al. Intravenous administration of glial cell line-derived neurotrophic factor gene-modified human mesenchymal stem cells protects against injury in a cerebral ischemia model in the adult rat. *J Neurosci Res* 2006; 84: 1495-1504.
126. Liu H, Honmou O, Harada K, et al. Neuroprotection by PIGF gene-modified human mesenchymal stem cells after cerebral ischaemia. *Brain* 2006; 129: 2734-2745.
127. Onda T, Honmou O, Harada K, et al. Therapeutic benefits by human mesenchymal stem cells (hMSCs) and Ang-1 gene-modified hMSCs after cerebral ischemia. *J Cereb Blood Flow Metab* 2008; 28: 329-340.
128. Nakano N, Nakai Y, Seo TB, et al. Characterization of conditioned medium of cultured bone marrow stromal cells. *Neurosci Lett* 2010; 483: 57-61.
129. Qu R, Li Y, Gao Q, et al. Neurotrophic and growth factor gene expression profiling of mouse bone marrow stromal cells induced by ischemic brain extracts. *Neuropathology* 2007; 27: 355-363.
130. Van Velthoven CTJ, Kavelaars A, van Bel F, et al. Mesenchymal stem cell transplantation changes the gene expression profile of the neonatal ischemic brain. *Brain Behav Immun* 2011; 25: 1342-1348.
131. Andres RH, Horie N, Slikker W, et al. Human neural stem cells enhance structural plasticity and axonal transport in the ischaemic brain. *Brain* 2011; 134: 1777-1789.
132. van Velthoven CT, Kavelaars A, van Bel F, et al. Nasal administration of stem cells: a promising novel route to treat neonatal ischemic brain damage. *Pediatr Res* 2010; 68: 419-422.
133. Heijnen CJ, Witt O, Wulffraat N, et al. Stem cells in pediatrics: state of the art and future perspectives. *Pediatr Res* 2012; 71: 407-409.
134. Domen J, Gandy K, Dalal J. Emerging uses for pediatric hematopoietic stem cells. *Pediatr Res* 2012; 71: 411-417.
135. Danielyan L, Schafer R, von Ameln-Mayerhofer A, et al. Intranasal delivery of cells to the brain. *Eur J Cell Biol* 2009; 88: 315-324.
136. Yang B, Strong R, Sharma S, et al. Therapeutic time window and dose response of autologous bone marrow mononuclear cells for ischemic stroke. *J Neurosci Res* 2011; 89: 833-839.
137. Pendharkar AV, Chua JY, Andres RH, et al. Biodistribution of neural stem cells after intravascular therapy for hypoxia-ischemia. *Stroke* 2010; 41: 2064-2070.



Chapter 3

Intranasal mesenchymal stem cell treatment for neonatal brain damage: Long-term cognitive and sensorimotor improvement

Vanessa Donega¹, Cindy T.J. van Velthoven^{1*}, Cora H. Nijboer^{1*}, Frank van Bel², Martien J.H. Kas³, Annemieke Kavelaars⁴ and Cobi J. Heijnen^{1,4}

¹Laboratory of Neuroimmunology and Developmental Origins of Disease, University Medical Centre Utrecht, The Netherlands. ²Dept. of Neonatology, University Medical Center Utrecht, Utrecht, The Netherlands. ³Rudolf Magnus Institute of Neuroscience, Dept. of Neuroscience and Pharmacology, University Medical Center Utrecht, Utrecht, The Netherlands. ⁴Department of Symptom Research, MD Anderson Cancer Center, TX, USA.

Plos One (2013) 8: e51253

Abstract

Mesenchymal stem cell (MSC) administration via the intranasal route could become an effective therapy to treat neonatal hypoxic-ischemic (HI) brain damage. We analysed long-term effects of intranasal MSC treatment on lesion size, sensorimotor and cognitive behavior, and determined the therapeutic window and dose response relationships. Furthermore, the appearance of MSCs at the lesion site in relation to the therapeutic window was examined.

Nine day old mice were subjected to unilateral carotid artery occlusion and hypoxia. MSCs were administered intranasally at 3, 10 or 17 days after hypoxia-ischemia (HI). Motor, cognitive and histological outcome was investigated. PKH-26 labeled cells were used to localize MSCs in the brain.

We identified 0.5×10^6 MSCs as the minimal effective dose with a therapeutic window of at least 10 days but less than 17 days after HI. A single dose was sufficient for a marked beneficial effect. MSCs reach the lesion site within 24h when given 3 or 10 days after injury. However, no MSCs were detected in the lesion when administered 17 days following HI. We also show for the first time that intranasal MSC treatment after HI improves cognitive function. Improvement of sensorimotor function and histological outcome was maintained until at least 9 weeks following HI.

The capacity of MSCs to reach the lesion site within 24h after intranasal administration at 10 days but not at 17 days after HI indicates a therapeutic window of at least 10 days. Our data strongly indicate that intranasal MSC treatment may become a promising non-invasive therapeutic tool to effectively reduce neonatal encephalopathy.

Introduction

Neonatal encephalopathy due to perinatal hypoxia-ischemia (HI) remains a significant cause of neonatal mortality and long-term neurological deficits such as cerebral palsy, mental retardation and seizures in babies born at term¹⁻⁶. Presently, the only available treatment, hypothermia, has limited beneficial effects and is only effective in mildly-affected children born at term^{7,8}. Moreover, hypothermia has a narrow therapeutic window of 6 hours. Hence, there is an urgent need to develop therapeutic strategies with a longer therapeutic window.

One emerging strategy with therapeutic potential is mesenchymal stem cell (MSC) treatment. A growing number of studies in rodent models show that MSC treatment significantly improves motor outcome and reduces lesion volume after neonatal brain injury⁹⁻¹⁸. Currently, in most studies, MSCs are administered intracranially, which has serious disadvantages for clinical application. In a previous study, we explored the potential of intranasal MSC administration in a mouse model of neonatal HI brain damage. Our results showed that intranasal MSC treatment improved sensorimotor behaviour and decreased lesion volume 4 weeks after HI, suggesting a therapeutic potential¹⁶.

Neonatal encephalopathy in humans is often associated with cognitive impairment^{2,3,5}. Therefore, we investigated for the first time whether intranasal MSC treatment after neonatal HI brain damage restores cognitive function and sensorimotor function 8 weeks after HI. We also determined the dose response relationships and therapeutic window of intranasal treatment in the HI mouse model. Moreover, we explored the early presence of MSCs at the lesion site in relation to the therapeutic window.

Materials and methods

Ethics statement

Experiments were performed according to the international guidelines and approved by the Experimental Animal Committee Utrecht (University Utrecht, Utrecht, Netherlands).

Animals

Unilateral HI cerebral damage was induced in 9 day old C57BL/6 mice by permanent occlusion of the right common carotid artery under isoflurane anesthesia followed by 45 min 10% oxygen at 35°C¹⁴. Our HI induction procedure has a 10% death rate. Sham-controls underwent anesthesia and incision only. Pups from at least five litters were randomly assigned to experimental groups. Analyses were performed in a blinded set-up.

Mesenchymal stem cells from C57BL/6 mice were purchased from Invitrogen (GIBCO mouse C57BL/6 MSCs, Life Technologies, UK) and cultured according to the manufacturer's instructions. Characterization of cell specific antigens was performed in a previous study from our group¹⁶. 3 µl of hyaluronidase in PBS (100 U, Sigma-Aldrich, St. Louis, MO) was administered to each nostril. Thirty minutes later animals received 3 µl MSCs or 3 µl PBS (Vehicle) twice in each nostril.

Sensorimotor function

Unilateral sensorimotor deficits were evaluated in the cylinder rearing test (CRT). Weight-bearing left (impaired), right (unimpaired) or both paw(s) contacting the wall during full rear were counted. Paw preference was calculated as $((\text{right} - \text{left}) / (\text{right} + \text{left} + \text{both})) \times 100\%$.

Cognitive function

To assess cognitive function, we used the social discrimination test as described¹⁹. After 10 min of habituation to the test environment, the test mouse was allowed to explore a novel conspecific of the same gender (Mouse 1), which is placed in a wire cage for 10 min. Five minutes later, the test mouse is exposed to a novel mouse (Mouse 2), which is placed in the empty wire cage while Mouse 1 remains in the other side chamber. This session is repeated 5 min and 3h later with a novel unfamiliar mouse (Mouse 3 and Mouse 4) and the now familiar Mouse 2. Time spent interacting with the familiar or unfamiliar conspecific was scored. Percent time spent with the novel mouse was calculated as $((\text{interaction time novel mouse}) / (\text{total interaction time}))$.

Histology

Coronal paraffin sections (8 µm) of paraformaldehyde (PFA)-fixed brains were incubated with mouse-anti-myelin basic protein (MBP) (Sternberger Monoclonals,

Lutherville, MD,) or mouse-anti-microtubuli-associated protein 2 (MAP2) (Sigma-Aldrich) followed by biotinylated horse-anti-mouse antibody (Vector Laboratories, Burlingame, CA). Binding was visualized with Vectastain ABC kit (Vector Laboratories) and diaminobenzamidine. Ipsilateral MAP2 and MBP area loss were determined on sections -1.85 mm from bregma²⁰. MBP and MAP2 staining were quantified using ImageJ software (<http://rsb.info.nih.gov/ij/>) and Adobe Photoshop CS5, respectively.

MSC tracking

MSCs were labeled with PKH-26 Red fluorescent cell linker kit (Sigma-Aldrich) and administered intranasally. 24h after MSC treatment brains were fixed in 4% PFA. Coronal cryosections (8 μ m) were stained with DAPI. Fluorescent images were captured using a EMCCD camera (Leica Microsystems, Benelux) and Softworx software (Applied Precision, Washington).

Statistical analysis

Data were analyzed using (repeated measures) one-way ANOVA followed by Bonferroni post-tests. Significance for social discrimination was analyzed with the one sample t-test. $p < 0.05$ was considered statistically significant. Data are presented as mean \pm SEM.

Results

Dose of intranasally administered MSC

To determine the MSC dose response relationship, we administered 0.25×10^6 , 0.5×10^6 , 1×10^6 MSCs or Vehicle intranasally at 10 days after HI. Exposure to HI markedly impaired sensorimotor performance in the CRT (Fig 1A). The doses of 0.5×10^6 and 1×10^6 MSCs significantly improved sensorimotor function as determined 3, 4 and 5 weeks after HI (data shown for 5 weeks; Fig 1A). The beneficial effect of MSC treatment on sensorimotor function was lost when the dose was reduced to 0.25×10^6 MSCs.

We analyzed MAP2 loss as a measure of gray matter damage and MBP loss as a parameter of white matter loss at 5 weeks post-insult¹⁴. HI-mice receiving 0.5×10^6 or 1×10^6 MSCs on day 10 showed a substantial decrease in MAP2 loss (Fig 1B) and MBP loss (Fig 1C). When a lower dose of 0.25×10^6 MSCs was used, we no longer observed a beneficial effect on MAP2 or MBP loss.

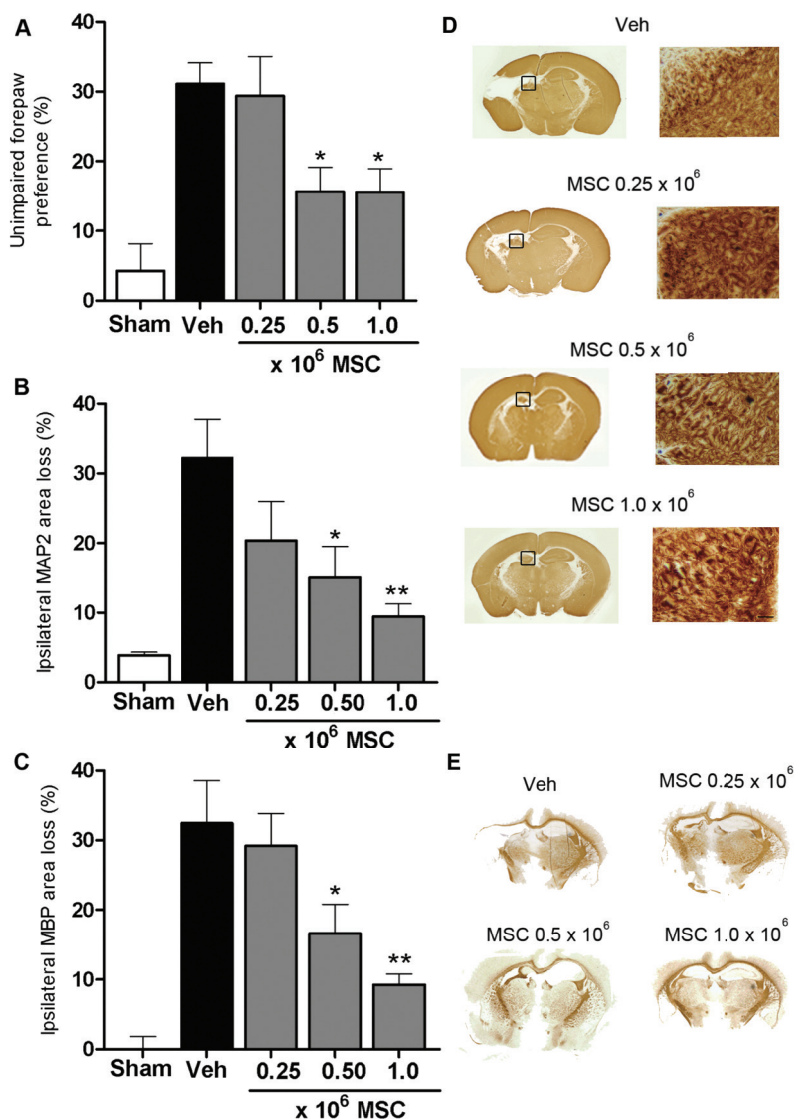


Figure 1. Dose effect of MSCs on motor performance and lesion volume at 35 days after HI. Mice received 0.25x10⁶, 0.5x10⁶, 1x10⁶ MSCs or Vehicle treatment at 10 days after induction of HI. (A) Paw preference to use the unimpaired forepaw in the cylinder rearing test (CRT) was assessed at 5 weeks following HI. Sham-operated littermates (Sham) were used as controls. Quantification of ipsilateral MAP2 (B) and MBP(C) area loss measured as 1- (ipsi-/contralateral MAP2- or MBP-positive area) at 5 weeks after HI. (D) Representative sections of MAP2 loss. Insets show higher magnification of corresponding MAP2 sections. Scale bar = 100 μ m. (E) Representative sections of MBP area loss. Data represent mean \pm SEM. Sham n=8; Veh n=10; 0.25x10⁶ MSC n=11; 0.5x10⁶ MSC n=10; 1x10⁶ MSC n=13. *p<0.05; **p<0.01 vs Veh. Data presented in this figure are results from pooled experiments out of 8 different litters. Treatment groups were randomly distributed between litters.

Therapeutic window

To determine the therapeutic window of intranasal MSC treatment, we administered 0.5×10^6 MSCs at 3, 10 or 17 days after HI and assessed sensorimotor performance in the CRT. Our data show that MSC treatment given 3 or 10 days post-insult is effective in improving motor behavior significantly. However, when we postponed MSC treatment to 17 days after HI, we no longer observed improvement of sensorimotor function as analyzed 5 weeks post-insult (Fig 2A). With respect to lesion volume, MSC treatment at 3 or 10 days, but not 17 days after HI significantly reduced MAP2 and MBP loss (Fig 2B, C).

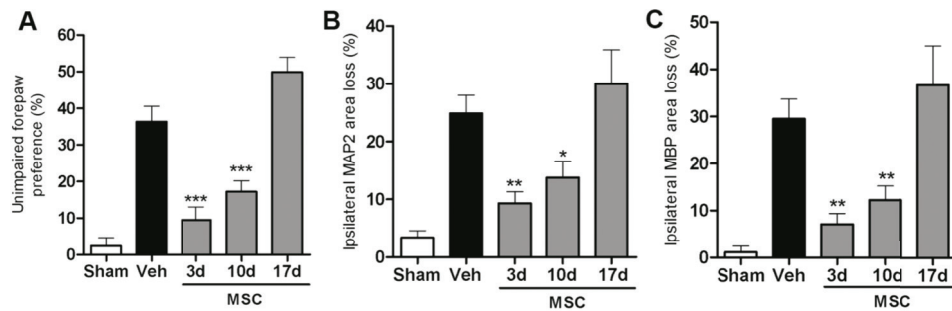


Figure 2. Therapeutic window for MSC treatment. Mice received 0.5×10^6 MSCs or Vehicle at 3, 10 or 17 days following HI. Because no significant difference was found between Vehicle groups treated at different time-points we pooled all animals into one group. (A) Unimpaired forepaw preference in the CRT at 5 weeks post-insult. Quantification of ipsilateral MAP2 (B) and MBP (C) area loss measured as 1- (ipsi-/contralateral MAP2- or MBP-positive area) at 5 weeks post-insult. Insets show representative examples of MAP2 or MBP staining. Data represent mean \pm SEM. Sham n=8; Vehicle n=19; MSC 3 days n=12; MSC 10 days n=17; MSC 17 days n=9; *p < 0.05; **p < 0.01; ***p < 0.001 vs. Vehicle. Data presented in this figure are results from pooled experiments out of 12 different litters. Treatment groups were randomly distributed between litters.

Effect of two MSC dosages

Previous results from our group showed that two intracranial MSC injections at 3+10 days compared to a single injection 3 days after HI, further improved motor performance and decreased neuronal and white matter loss¹⁴. The data in Figure 3A show that one intranasal dose at either 3 or 10 days is as effective in restoring sensorimotor function as two intranasal doses at 3+10 days following insult. Histological data on MAP2 or MBP staining confirmed the functional CRT analyses, showing that one single intranasal dose at 3 or 10 days is as effective as two doses at

3+10 days analyzed at 5 weeks after HI (Fig 3B, C). Furthermore, the positive effects of either one or two intranasal doses of MSCs on sensorimotor and histological outcome can still be observed at respectively 8 and 9 weeks after HI, and no additive effect of two doses was observed at this time-point either (Fig 4).

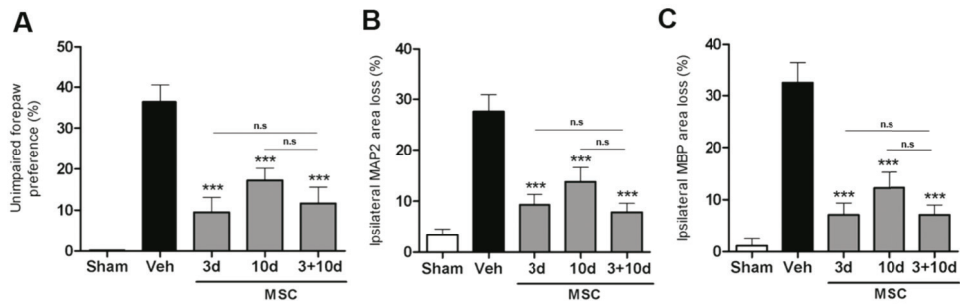


Figure 3. Effect of two MSC treatments on sensorimotor function and lesion size. Mice received 0.5×10^6 MSCs or Vehicle at 3, 10 or 3+10 days after insult. Because no significant difference was found between Vehicle groups treated at different time-points we pooled all animals into one group. (A) Unimpaired forepaw preference in the CRT at 5 weeks following HI. Quantification of ipsilateral MAP2 (B) and MBP (C) area loss measured as 1- (ipsi-/contralateral MAP2- or MBP-positive area) at 5 weeks after HI. Insets show representative examples of MAP2 or MBP staining. Data represent mean \pm SEM. Sham n=7; Vehicle n=19; MSC 3+10 days n=13; MSC 10+17 days n=11; MSC 10 days n=17. ***p<0.001 vs. Vehicle, n.s. = non-significant. Data presented in this figure are results from pooled experiments out of 14 different litters. Treatment groups were randomly distributed between litters.

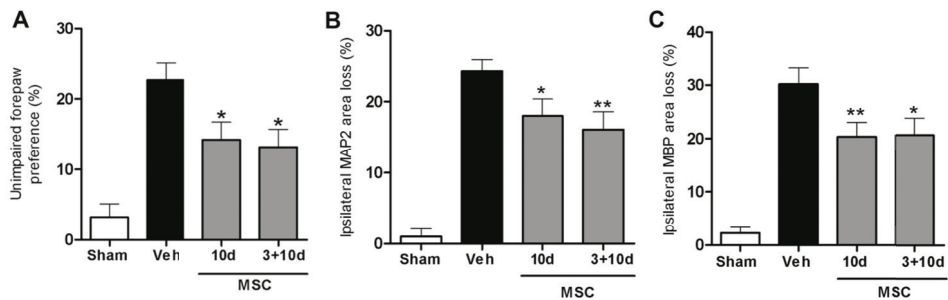


Figure 4. Long-term effect of MSC treatment on sensorimotor function and lesion volume. Mice received 0.5×10^6 MSCs or Vehicle at 3, 10 or 3+10 days after HI. Because no significant difference was found between Vehicle groups treated at different time-points we pooled all animals into one group. (A) Unimpaired forepaw preference in the CRT at 8 weeks after HI. Quantification of ipsilateral MAP2 (B) and MBP (C) area loss measured as 1- (ipsi-/contralateral MAP2- or MBP-positive area). Insets show representative examples of MAP2 or MBP staining at 9 weeks post-insult. Data represent mean \pm SEM. Sham n=23; Vehicle n=23; MSC 10 days n=23; MSC 3+10 days n=12. *p<0.05; **p<0.01 vs. Vehicle. Data presented in this figure are results from pooled experiments out of 13 different litters. Treatment groups were randomly distributed between litters.

Effect of MSC treatment on cognitive function

To determine whether MSC treatment improves HI-induced cognitive impairment, we used the social discrimination test at 7 weeks after HI. This test uses the preference for social novelty as a measure of cognitive function *i.e.* the ability to discriminate between known or unknown conspecific.

As anticipated, sham-control mice showed preference for the novel mouse at 5 min and 3h after the training session (Fig 5A, B). Vehicle-treated HI mice lost the capability to discriminate between the novel and familiar mouse at both time-points. Interestingly, performance in the social discrimination test normalized in the groups treated with MSCs at 10 days or 3+10 days following HI. During the training session we did not observe group differences in social interaction times (Fig 5C).

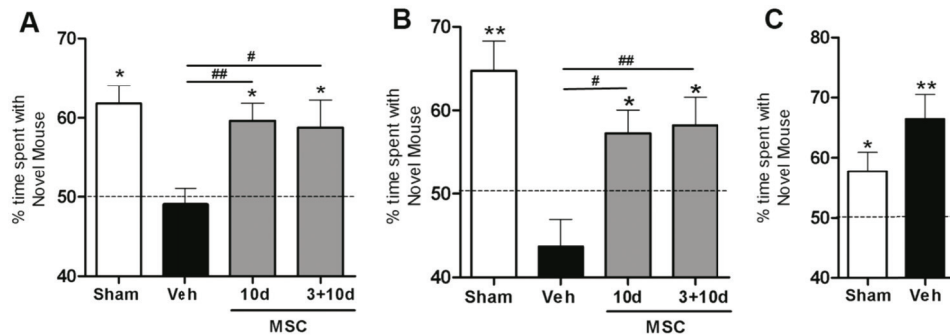


Figure 5. Effect of MSC treatment on cognitive behavior. Mice received 0.5×10^6 MSCs or Vehicle at 10 or 3+10 days following HI. Because no significant difference was found between Vehicle groups treated at different time-points we pooled all animals into one group. Animals were tested for cognitive function using the social discrimination test at 7 weeks after HI. Preference for novel conspecific is expressed as exploratory ratio. The total social interaction time did not differ between groups. (A) Preference for novel mouse after a 5 min interval. (B) Preference for novel mouse after a 3h interval. (C) Training session to measure preference for social novelty as an indication for social avoidance. Sham $n=23$; Vehicle $n=23$; MSC 10 days $n=23$; MSC 3+10 days $n=12$. * $p<0.05$; ** $p<0.01$ in relation to 50% (no discrimination); # $p<0.05$; ## $p<0.01$ vs. Vehicle. Data presented in this figure are results from pooled experiments out of 13 different litters. Treatment groups were randomly distributed between litters.

MSC migration towards lesion site

To determine whether MSCs migrate from the nose to the lesion site, we used PKH-26 labeled MSCs and analyzed brain sections 24h after intranasal administration. PKH-26⁺ MSCs administered 3 days after HI are present predominantly in the damaged hippocampus (Fig 6A; ipsilateral).

MSCs given 10 days after HI localize in the area surrounding the lesion site. At this time-point, the entire hippocampus was lost and PKH-26⁺ cells were now present in cortical layers 5 and 6 (Fig 6B; ipsilateral) and in the dorsal and epithalamic regions (data not shown). Interestingly, hardly any MSCs could be detected in the brain when given 17 days following HI (Fig 6C; ipsilateral).

No labeled MSCs were present in the contralateral hemisphere, although MSCs were given to both nostrils (Fig 6A to C). In addition, no PKH-26⁺ cells were observed in brains from sham-operated mice (Fig 6D; sham 3d and 10d). Furthermore, we found no evidence for tissue autofluorescence after HI either 3 or 10 days following the insult (Fig 6D; Vehicle).

Discussion

In the present study we show that intranasally administered MSCs reach the brain within just 24h after intranasal administration. Interestingly, the MSCs migrate specifically towards the lesion site. We determined the dose response relationship of MSC administration and demonstrate that one single intranasal MSC administration is sufficient to induce maximal improvement of functional outcome and reduction in brain damage. A single intranasal dose of MSC has long-lasting effects on motor, cognitive and histological outcome up to 9 weeks following HI injury. Moreover, we are the first to show that intranasal MSC treatment also improves cognitive function, which holds significant clinical relevance.

To determine whether the beneficial effects of intranasal MSC application are associated with migration of MSCs from the nasal mucosa to the lesion site, we used the cell tracking dye PKH-26. In contrast to other commonly used cell tracking dyes, PKH-26 does not have any adverse effects on cell proliferation or survival. Furthermore, no significant cell to cell transfer or dye leakage from cells was measured²¹. No PKH-26⁺ MSCs were observed at the hippocampal level of sham-operated mice treated at 3 or 10 days after HI. Interestingly, we clearly detected PKH-26 labeled MSCs at the HI lesion site, but not in the contralateral hemisphere of mice subjected to HI that were treated with MSCs via both the ipsilateral and contralateral nostril. MSCs given at 3 days following HI migrate specifically to the damaged hippocampus. At 10 days the damage has evolved into an extensive lesion site, including the entire hippocampus and part of the cortex.

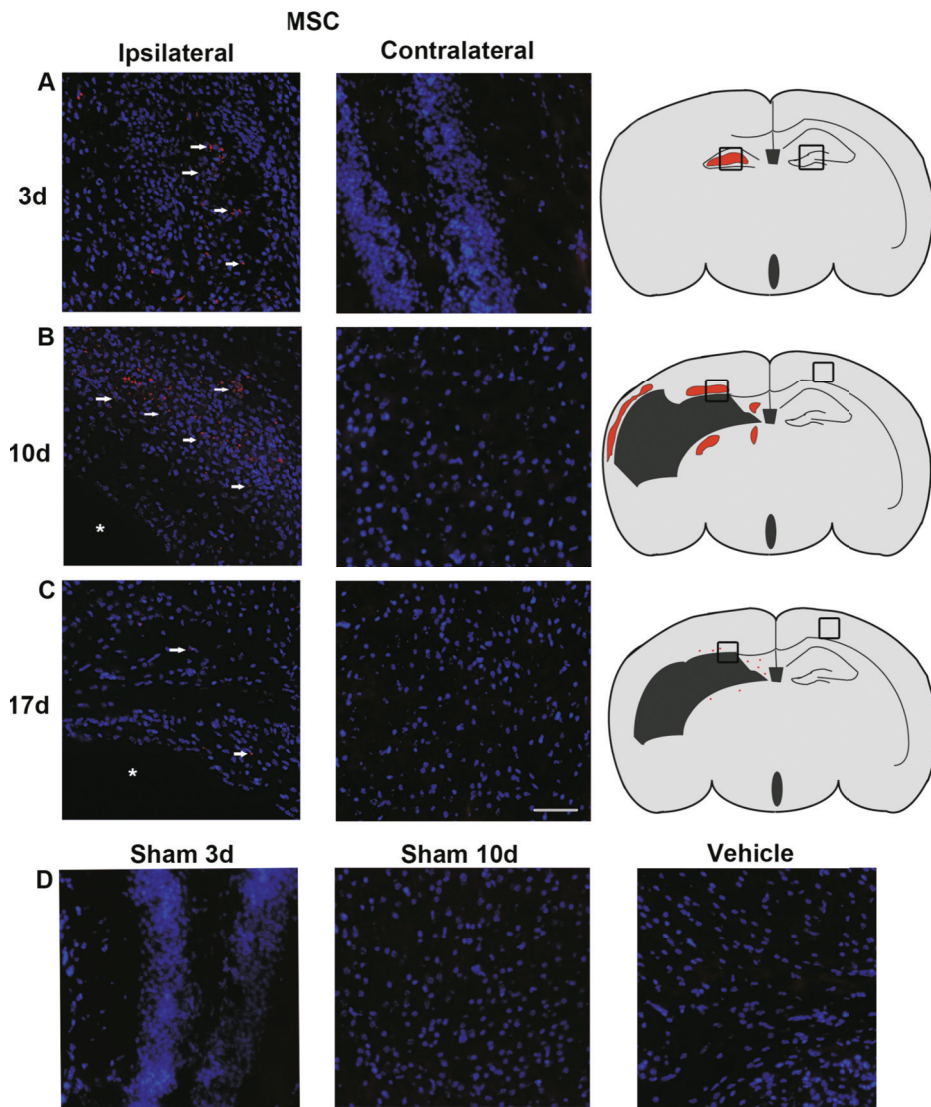


Figure 6. Presence of MSCs in the brain. PKH-26 labeled 1.0×10^6 MSCs were administered intranasally at 3, 10 and 17 days after HI. Because no significant difference was found between Veh groups treated at different time-points we pooled all animals into one group. (A, B, C) Notice the severe HI-induced damage, as the layer structure of the ipsilateral cortex and hippocampus are lost. (A) MSCs (red) in the ipsilateral hippocampus (see arrow heads) 24h after administration at 3 days following HI. (B) MSCs (see arrow heads) in the ipsilateral damaged cortex 24h after administration at 10 days after HI. (C) Lack of MSCs (see arrow heads) in the ipsilateral cortical areas surrounding the lesion site when MSCs are given at 17 days following HI. Contralateral pictures depict hippocampal area (in A) and cortical area (in B and C). (D) Control groups showing lack of MSCs in the hippocampal area and cortical area at 3 and 10 days, respectively, after MSC administration in sham-operated animals and HI-Vehicle treated brain without MSC treatment. Asterisk = lesion site. Blue = Dapi staining. Scale bar 50 μm . Data presented in this figure are results from pooled experiments out of 10 different litters. Treatment groups were randomly distributed between litters.

When MSCs are administered intranasally at 10 days following injury, 24h later MSCs are located in the remaining regions of the cortex and thalamus. In contrast, when MSCs were administered at 17 days after HI, only a sporadic PKH-26⁺ MSC was detected in the lesion, although there is still substantial injury at 17 days post-insult. Notably, MSC treatment at this time-point did not have any effect on lesion size nor on sensorimotor function. Combined, these findings indicate that the loss of effect of MSCs given at 17 days after the insult will be due to reduced migration of MSC to the lesion site when cells are given at this time-point.

The social discrimination test was used to assess cognitive performance following HI. This test was chosen as it is a very sensitive measure for short-term and long-term recognition memory function¹⁹. This type of memory describes the ability to discriminate between familiar and unfamiliar stimuli. The social discrimination test exploits the natural interest of an adult mouse to explore an unknown conspecific over a known conspecific. The molecular mechanisms and neuro-anatomical structures underlying this behavioural paradigm remain elusive. Studies have shown that performance on the social discrimination test requires functional olfactory bulb, bed nucleus of the stria terminalis and amygdalo-hippocampal network²²⁻²³. The hippocampus is known to be important in memory consolidation, which is essential for long-term memory storage in other cortical areas²⁴. We are the first to establish that intranasal MSC treatment not only improves sensorimotor but also cognitive behavior.

The exact mechanisms underlying MSC-induced improvement of short-term memory after neonatal HI brain damage have yet to be clarified. HI injury leads to extensive unilateral loss in cortical and hippocampal areas, which explains the inability of Vehicle-treated group to form and/or store new information. Intranasal MSC treatment significantly reduces loss of cortical and hippocampal areas, which are both important in memory formation and storage.

Our present and previous findings¹⁴ indicate that there is no further increase in lesion size after day 10 following HI. Therefore, we propose that the major effect of MSC treatment is not mediated by inhibition of injurious processes, but rather by stimulating repair. We indeed have evidence from earlier studies in which we applied MSC intracranially that formation of new cells and differentiation of these new cells into neurons and oligodendrocytes is promoted by MSC treatment^{14,15}. Moreover, we showed that only a very small proportion of cells of donor origin survived in the brain¹⁶.

Therefore, it is highly likely that MSC treatment restores cognitive as well as motor circuitries in the brain through stimulation of endogenous regenerative processes. However, it may well be possible that inhibition of injurious processes contributes to the observed beneficial effects of MSC treatment. If so, this will especially be the case when MSC are administered early after the insult. In our experiments this is 3 days after the insult as at this time-point the damage has not yet fully developed.

We also propose that beneficial effects of MSC transplantation are cell-specific, because intracranial fibroblast (3T3) administration did not affect performance in the CRT as well as on lesion size (unpublished observations). Although we now studied the effect of intranasal administration, we anticipate that the same cellular specificity will apply for intranasal administration, give an effect on repair, it should anyhow occur when cells are given directly at the lesion site.

In preparation for clinical translation of our finding that nasally administered MSCs improve cognitive as well as sensorimotor outcome and reduce lesion size, we investigated the therapeutic window, the treatment dose and frequency. We report here that sensorimotor function improves and lesion size reduces significantly when 0.5×10^6 cells are administered via the nasal route. Decreasing the dose to 0.25×10^6 MSCs had no significant effect on either the CRT performance or MAP2 and MBP outcome, while increasing the dose to 1.0×10^6 did not further improve sensorimotor function or reduce lesion size. Thus, a minimum of 0.5×10^6 MSCs per mouse is required to have a long-lasting beneficial effect on behavior and lesion size in our model of HI-induced brain damage.

In the present study, we demonstrate that multiple doses at 3+10 days via the intranasal route did not have an additional effect on sensorimotor performance and brain damage compared to a single dose. This finding is clinically important as it would mean that only one intranasal dose of MSCs will be sufficient for optimal therapeutic benefit in the neonate. In contrast, we showed earlier that when MSCs are administered intracranially, two gifts of MSC have a stronger beneficial effect on outcome than one gift. One possible explanation for the finding that one intranasal MSC treatment already provides optimal effects is that intranasally administered MSCs may perform better as migration from the nasal mucosa towards the lesion may allow adaptation to the detrimental milieu in the brain. In contrast, intracranially administered cells were directly injected adjacent to the lesion size, consisting of an apoptotic/inflammatory milieu which may partially impair the functionality of MSCs.

Conclusions

In conclusion, this study shows that intranasal MSC treatment has a wide therapeutic window, leads to long-term improvement in sensorimotor and cognitive function and decreases gray and white matter damage after HI. MSCs migrate specifically to the site of injury, despite contralateral administration. Our results clearly establish that intranasal MSC treatment has the potential to become a novel therapeutic strategy for neonatal encephalopathy.

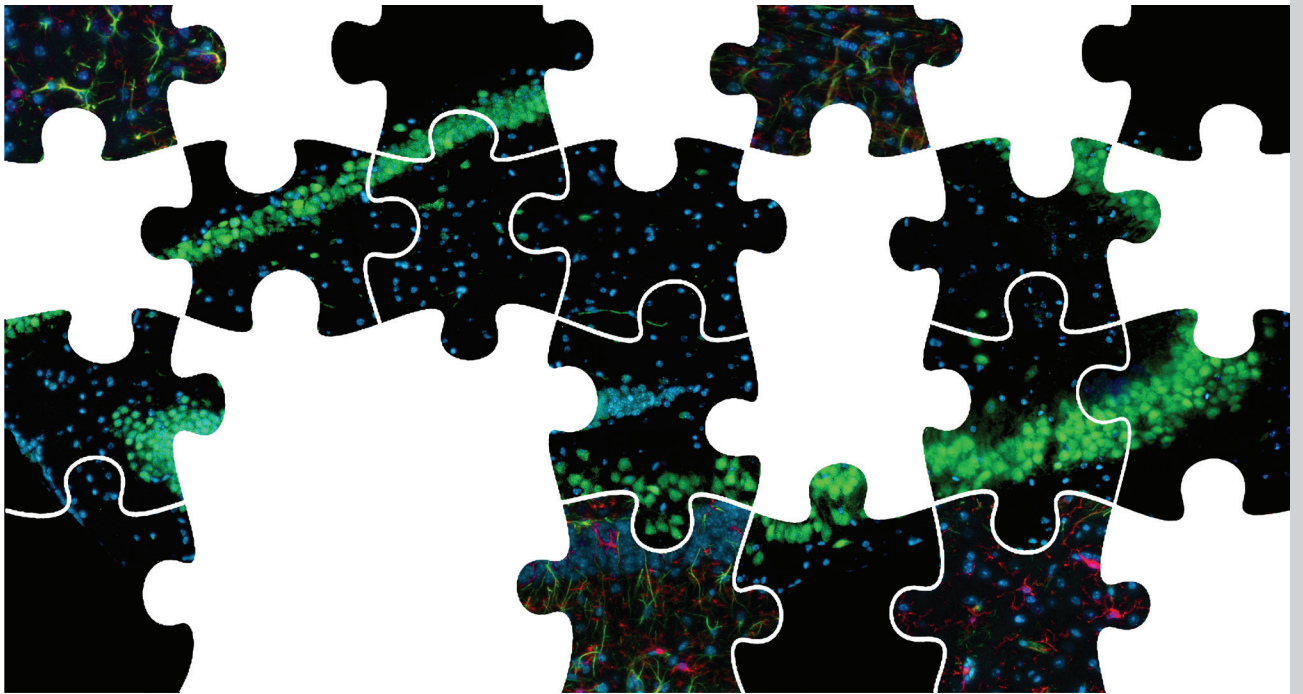
Acknowledgments

The authors are greatly indebted to Dr. Marijke Laarakker, Jitske Zijlstra, Marijke Tersteeg-Kamperman and Karima Amarouchi for technical assistance. This work was supported by EU-7 Neurobid (HEALTH-F2-2009-241778) from the European Union and Zon-MW Project (no 116002003).

References

1. Dammann O, Ferriero D, Gressens P. Neonatal encephalopathy or hypoxic ischemic encephalopathy? Appropriate terminology matters. *Pediatr Res* 2011; 70: 1-2.
2. De Haan M, Wyatt JS, Roth S, et al. Brain and cognitive-behavioural development after asphyxia at term birth. *Dev Sci* 2006; 9: 350-358.
3. Ferriero DM. Neonatal brain injury. *N Engl J Med* 2004; 351: 1985-1995.
4. Graham EM, Ruis KA, Hartman AL, et al. A systematic review of the role of intrapartum hypoxia-ischemia in the causation of neonatal encephalopathy. *Am J Obstet Gynecol* 2008; 199: 587-595.
5. van Handel M, Swaab H, de Vries LS, et al. Long-term cognitive and behavioural consequences of neonatal encephalopathy following perinatal asphyxia: a review. *Eur J Pediatr* 2007; 166: 645-654.
6. Volpe JJ. Perinatal brain injury: from pathogenesis to neuroprotection. *Ment Retard Dev Disabil Res Rev* 2001; 7: 56-64.
7. Edwards AD, Brocklehurst P, Gunn AJ, et al. Neurological outcomes at 18 months of age after moderate hypothermia for perinatal hypoxic ischaemic encephalopathy: synthesis and meta-analysis of trial data. *BMJ* 2010; 340: c363-370.
8. Azzopardi DV, Strohm B, Edwards AD, et al. Moderate hypothermia to treat perinatal asphyxial encephalopathy. *N Engl J Med* 2009; 361: 1349-1358.
9. Borlongan CV, Weiss MD. Baby STEPS: A giant leap for cell therapy in neonatal brain injury. *Pediatr Res* 2011; 70: 3-9.
10. Lee JA, Kim BI, Jo CH, et al. Mesenchymal stem-cell transplantation for hypoxic-ischemic brain injury in neonatal rat model. *Pediatr Res* 2010; 67: 42-46.
11. Pimentel-Coelho PM, Mendez-Otero R. Cell therapy for neonatal hypoxic-ischemic encephalopathy. *Stem Cells Dev* 2010; 19: 299-310.
12. Titomanlio L, Kavelaars A, Dalous J, et al. Stem cell therapy for neonatal brain injury: perspectives and challenges. *Ann of Neurol* 2011; 70: 698-712.
13. van Velthoven CT, Kavelaars A, Heijnen CJ. Mesenchymal stem cells as a treatment for neonatal ischemic brain damage. *Pediatr Res* 2012; 71: 474-481.
14. van Velthoven CT, Kavelaars A, van Bel F, et al. Mesenchymal stem cell treatment after neonatal hypoxic-ischemic brain injury improves behavioral outcome and induces neuronal and oligodendrocyte regeneration. *Brain Behav Immun* 2010; 24: 387-393.
15. van Velthoven CT, Kavelaars A, van Bel F, et al. Repeated mesenchymal stem cell treatment after neonatal hypoxia-ischemia has distinct effects on formation and maturation of new neurons and oligodendrocytes leading to restoration of damage, corticospinal motor tract activity, and sensorimotor function. *J Neurosci* 2010; 30: 9603-9611.
16. van Velthoven CT, Kavelaars A, van Bel F, et al. Nasal administration of stem cells: a promising novel route to treat neonatal ischemic brain damage. *Pediatr Res* 2010; 68: 419-422.
17. Yasuhara T, Matsukawa N, Yu G, et al. Behavioral and histological characterization of intrahippocampal grafts of human bone marrow-derived multipotent progenitor cells in neonatal rats with hypoxic-ischemic injury. *Cell Transplant* 2006; 15: 231-238.

18. Yasuhara T, Hara K, Maki M, et al. Intravenous grafts recapitulate the neurorestoration afforded by intracerebrally delivered multipotent adult progenitor cells in neonatal hypoxic-ischemic rats. *J Cereb Blood Flow Metab* 2008; 28: 1804-1810.
19. Nadler JJ, Moy SS, Dold G, et al. Automated apparatus for quantitation of social approach behaviors in mice. *Genes Brain Behav* 2004; 3: 303-314.
20. Nijboer CH, Kavelaars A, Vroon A, et al. Low endogenous G-protein-coupled receptor kinase 2 sensitizes the immature brain to hypoxia-ischemia-induced gray and white matter damage. *J Neurosci* 2008; 28: 3324-3332.
21. Ashley DM, Bol SJ, Waugh C, et al. A novel approach to the measurement of different in vitro leukaemic cell growth parameters: The use of PKH GL fluorescent probes. *Leuk Res* 1993; 17: 873-882.
22. Auger CJ, Vanzo RJ. Progesterone Treatment of Adult Male Rats Suppresses Arginine Vasopressin Expression in the Bed Nucleus of the Stria Terminalis and the Centromedial Amygdala. *J of Neuroendoc* 2005; 18: 187-194.
23. Ferguson JN, Young LJ, Insel TR. The neuroendocrine basis of social recognition. *Front Neuroendocrinol* 2002; 23: 200-224.
24. Morgado-Bernal I. Learning and memory consolidation: Linking molecular and behavioural data. *Neurosci* 2011; 176: 12-19.



Chapter 4

Intranasally administered mesenchymal stem cells promote a regenerative niche for repair of neonatal ischemic brain injury

Vanessa Donega^a, Cora H. Nijboer^a, Geralda van Tilborg^b,
Rick M. Dijkhuizen^b, Annemieke Kavelaars^c and Cobi J. Heijnen^{a,c*}

^aLab. of Neuroimmunology and Developmental Origins of Disease, University Medical Center Utrecht, Utrecht, The Netherlands. ^bBiomedical MR Imaging and Spectroscopy Group, Image Sciences Institute, University Medical Center Utrecht, The Netherlands. ^cLab. of Neuroimmunology, Department of Symptom Research, The University of Texas, MD Anderson Cancer Center, Houston, Texas, USA.

Experimental Neurology, in press

Abstract

Previous work from our group has shown that intranasal MSC treatment decreases lesion volume and improves motor and cognitive behavior after hypoxic-ischemic (HI) brain damage in neonatal mice. Our aim was to determine the kinetics of MSC migration after intranasal administration, and the early effects of MSCs on neurogenic processes and gliosis at the lesion site.

HI brain injury was induced in 9 day old mice and MSCs were administered intranasally at 10 days after HI. The kinetics of MSC migration were investigated by immunofluorescence and MRI analysis. BDNF and NGF gene expression was determined by qPCR analysis following MSC co-culture with HI brain extract. Nestin, Doublecortin, NeuN, GFAP, Iba-1 and M1/M2 phenotypic expression was assessed over time.

MRI and immunohistochemistry analyses showed that MSCs reach the lesion site already within 2h after intranasal administration. At 12h after administration the number of MSCs at the lesion site peaks and decreases significantly at 72h. The number of DCX⁺ cells increased 1 to 3 days after MSC administration in the SVZ. At the lesion, GFAP⁺/nestin⁺ and DCX⁺ expression increased 3 to 5 days after MSC treatment. The number of NeuN⁺ cells increased within 5 days, leading to a dramatic regeneration of the somatosensory cortex and hippocampus at 18 days after intranasal MSC administration. Interestingly, MSCs expressed significantly more BDNF gene when exposed to HI brain extract *in vitro*. Furthermore, MSC treatment resulted in resolution of the glial scar surrounding the lesion, represented by a decrease in reactive astrocytes and microglia and polarization of microglia towards the M2 phenotype.

In view of the current lack of therapeutic strategies, we propose that intranasal MSC administration is a powerful therapeutic option through its functional repair of the lesion represented by regeneration of the cortical and hippocampal structure and decrease of gliosis.

Introduction

Encephalopathy caused by neonatal hypoxia-ischemia (HI) results in cerebral tissue loss leading to long-term neurological deficits *e.g.* mental retardation and motor impairment¹⁻⁵.

The capacity of stem cells to treat neonatal encephalopathy is gaining support from an increasing number of studies⁶⁻¹⁵. These studies describe the therapeutic potential of intracranially and intravenously delivered neural stem cells (NSC) or mesenchymal stem cells (MSCs) in rodent models of neonatal HI or neonatal stroke. We have shown recently that both intracranial and intranasal MSC treatment at 10 days after HI in neonatal mice significantly decreases cerebral lesion volume and improves long-term motor and cognitive behavior^{8,13}.

In view of the therapeutic potential of non-invasive intranasal MSC administration, we investigated the mechanism underlying MSC mediated repair. Firstly, we studied the kinetics of MSC migration to the lesion site after intranasal administration. To visualize the arrival of MSCs in the brain, we used fluorescence microscopy and Magnetic Resonance Imaging (MRI). We determined the short- and long-term effects of MSCs on regeneration of the lesion by systematic quantification and characterization of precursor cells (type B cells; uncommitted precursors), neural progenitor cells (type A cells; neuronally-committed), neurons, microglia and astrocytes.

Material and Methods

Ethics statement

Experiments were performed according to the international guidelines from the EU Directive 2010/63/EU for animals experiments and approved by the Experimental Animal Committee Utrecht (University Utrecht, Utrecht, Netherlands).

Animals

Unilateral HI brain damage was induced in 9 day old C57BL/6 mice (Harlan Laboratories, The Netherlands) by permanent occlusion of the right common carotid artery under isoflurane anesthesia followed by hypoxia (45 min at 10% oxygen). Sham-controls underwent anesthesia and incision only.

MSCs were purchased from Invitrogen (GIBCO mouse C57BL/6 MSCs, Life Technologies, UK) and cultured according to the manufacturer's instructions. Characterization of cell specific antigens has been described previously by us¹⁴. Before administering 1×10^6 MSCs intranasally, each nostril was treated with $3 \mu\text{l}$ of hyaluronidase (100 U, Sigma-Aldrich, St. Louis, MO) in PBS to increase permeability of nasal mucosa. Thirty minutes later, pups received $3 \mu\text{l}$ of MSCs or PBS (Vehicle) twice in each nostril.

Histology

Coronal paraffin sections ($8 \mu\text{m}$) of paraformaldehyde (PFA)-fixed brains were incubated with mouse-anti-myelin basic protein (MBP) (Sternberger Monoclonals, Lutherville, MD,) or mouse-anti-microtubule-associated protein 2 (MAP2) (Sigma-Aldrich) followed by biotinylated horse-anti-mouse antibody (Vector Laboratories, Burlingame, CA). Binding was visualized with Vectastain ABC kit (Vector Laboratories) and diaminobenzamide.

Immunohistochemistry

MSCs were labeled with PKH-26 Red fluorescent cell linker kit (Sigma-Aldrich). Coronal frozen sections ($8 \mu\text{m}$) were incubated overnight at 4°C with primary antibodies; goat anti-DCX (1:300) (Santa Cruz Biotechnology, TX, USA), rabbit anti-Iba1 (1:500) (Wako Chemicals, Osaka, Japan), mouse anti-GFAP (1:100) (Acris antibodies, Herford, Germany), mouse anti-NeuN (1:200) (Chemicon, Temecula, CA), mouse anti-nestin (1:200) (BD Biosciences, Breda, The Netherlands), rat anti-CD16/CD32 (1:300) (BD Pharmingen, Breda, The Netherlands), goat anti-CD206 (1:300) (R&D systems, Abingdon, UK). Primary antibody binding was detected by incubating with corresponding secondary antibodies for 1h at room temperature. Nuclei were counterstained with DAPI (Invitrogen, Paisley, UK) and mounted with FluoroSave reagent (Calbiochem, Nottingham, UK). Fluorescent images were captured using an EMCCD camera (Leica Microsystems, Benelux) and Softworx Software (Applied Precision, Washington, USA) or an AxioCam MRm (Carl Zeiss, Sliedrecht, The Netherlands) on an Axio Observer Microscope with Axiovision Rel 4.6 software (Carl Zeiss).

MSC labeling for MRI

Culture flasks were coated with Poly-L-Lysine (0.02 mg/mL) before seeding MSCs. 48h later, MSCs were incubated with 0.01 mg Fe/mL fluorescent micron-sized superparamagnetic iron-oxide particles (MPIO; 0.86 μm) (Bangs Laboratories Inc., IN, USA) diluted in GlutaMAX DMEM medium (Life Technologies). After 4h, excessive MPIO particles were removed by washing 4 times with PBS. About 70% of the cells were labeled with MPIO particles. Images were taken on an Axio-Observer microscope (Carl Zeiss Microscopy, Jena, Germany) with Axiovision rel. 4.6 software (Carl Zeiss Microscopy).

MRI

MRI was performed on a 9.4T horizontal bore preclinical MRI system (Varian Inc., Palo Alto, CA). T_2^* -weighted gradient echo images of cells in agarose were acquired with TR/TE = 1000/15 ms and 100 μm x 100 μm x 200 μm spatial resolution. T_2^* -weighted gradient echo images of *ex-vivo* mouse brain were acquired with TR/TE = 40/15 ms and a voxel size of 75 μm in all directions.

To verify the detectability of MPIO-labeled MSCs with MRI, cells were homogeneously distributed in 0.4% agarose in PBS at concentrations between 0 and 1000 cells/ μl . T_2^* -weighted gradient echo images were acquired with a Millipede™ coil (Varian Inc.), using the following parameters: TR = 1 s, TE = 15 ms, flip angle = 90°, 4 averages, field-of-view 25.6 mm x 25.6 mm, matrix size 256 x 256 and slice thickness 0.2 mm. For the detection of MPIO-labeled cells in *ex-vivo* mouse brain, mice were perfused transcardially with 4% PFA at 2h after MSC-treatment. T_2^* -weighted images were acquired with a 3D GE sequence, with TR = 40 ms, TE = 15 ms, flip angle = 15°, 32 averages, field-of-view = 22mm x 12mm x 10mm and a voxel size of 75 μm in all directions.

MSCs co-culture with brain extracts

10 days after HI- or sham-operation, mice were euthanized by pentobarbital overdose, decapitated and brains were removed. The ipsilateral hemisphere was dissected on ice at -2.0—2 mm from bregma and was subsequently pulverized on liquid nitrogen. Dissected brains were dissolved in KO-DMEM medium (Life Technologies) at a final concentration of 150 mg/mL and centrifuged for 10 min at 3.000 g at 4°C. Supernatants were collected as 'brain extract' and protein concentration was measured with the

protein assay (Bio-Rad, Hercules, CA). MSCs were cultured at a concentration of 40.000 cells per well in a 24 wells-plate for 24h before replacing the medium with knock-out medium containing 1mg/mL brain extract. RNA was isolated from the MSCs 72h after culture with brain extracts.

RNA isolation and qPCR

Total RNA was isolated with the RNAmuni kit according to the manufacturer's instructions (Invitrogen). The amount of RNA was measured with the nanodrop 2000 (Thermo Scientific, Waltham, MA, USA). The RNA quality was determined with the OD 260/280 ratio, which was between 1,9 and 2,1. cDNA was synthesized with SuperScript Reverse Transcriptase (Invitrogen). The expression of BDNF and NGF genes was measured by quantitative reverse transcription (qRT)-PCR (Biorad IQ5, Thermo Scientific) analysis on individual samples. We chose these genes as they are important neurotrophic factors that have been shown to be secreted by MSCs¹⁶. Data was normalized for the expression of GAPDH and actin.

SDS-PAGE gel and Western Blot

To assess the expression of BDNF and NGF in sham and HI brain extracts used for co-culture with MSCs, equal amounts of brain extract were loaded on a 15% SDS-PAGE gel (Bio-Rad) and transferred to a nitrocellulose membrane (Hybond C; Amersham Biosciences, Roosendaal, Netherlands). Membranes were blocked with 5% skimmed milk for 1 hour, followed by overnight incubation with primary antibodies for rabbit anti-BDNF 1:400 (Santa Cruz Biotechnology, Dallas, Texas) and rabbit anti-NGF 1:1000 (Sigma-Aldrich). Expression was detected by incubation with donkey anti-rabbit-HRP 1:5000 (Amersham Biosciences) and developed by enhanced chemiluminescence (ECL) (Advansta, Isogen Life Science, De Meern, The Netherlands) on a ProXima Imager (Isogen Life Science). To control for equal loading, membranes were reprobed for β -actin followed by donkey anti-goat-HRP 1:5000 (both Santa Cruz Biotechnology).

Data analysis

Analyses were performed in a blinded set-up. PKH-26⁺ signal was determined by measuring pixel intensity with ImageJ 1.47f Software (Wayne Rasband, National Institutes of Health, USA). Co-localization of GFAP and nestin, CD16/CD32 and Iba-1, CD206 and Iba-1 pixels was assessed with the co-localization macro of ImageJ 1.47f Software. GFAP and Iba-1 positive signal was also measured by using the ImageJ software. The number of DCX⁺ and NeuN⁺ cells was counted manually. Statistical significance in relative mRNA expression was determined with an unpaired two-tailed T-test. Statistical significance between M1 and M2 phenotype was determined by Multiple T-test corrected for multiple comparisons using the Holm-Sidak method. Statistical significance was analyzed by using (repeated measures) one-way ANOVA followed by Bonferroni post-tests, when not mentioned otherwise. $p < 0.05$ was considered statistically significant. Data are presented as mean \pm SEM. Outliers were identified with the Grubbs test ($Q=2\%$) or the ROUT test ($Q=2\%$).

Results

Kinetics of MSC migration to the lesion site

We have previously shown that intranasal MSC treatment significantly decreases HI brain injury at 25 days after MSC treatment (*i.e.* 35 days after HI)⁸. We assessed HI-induced loss of MAP2 and MBP staining as measures for gray and white matter damage, respectively. The results in Figure 1 confirm our previous data and show that intranasal treatment with $0,5 \times 10^6$ MSCs leads to substantial repair of both the somatosensory cortex and hippocampus, which are both severely damaged after HI.

We have shown in a previous study that MSCs administered intranasally to both nostrils, migrate specifically to the ipsilateral side, but not to the contralateral hemisphere⁸. To assess the kinetics of MSC migration to the lesion site, we administered PKH-26 labeled MSCs intranasally via both nostrils at 10 days after HI. We analyzed sections of the lesion at 2, 6, 12, 24, 48 and 72h after administration. PKH-26⁺-MSCs form clusters around the lesion site and appear to home exclusively to the ipsilateral side. Our results show that PKH-26⁺-MSCs reach the lesion site as early as 2h after administration and peak at 12h. At 72h, the PKH-26⁺-MSC signal decreases by more than 50% compared to levels at 12h after administration (Fig 2).

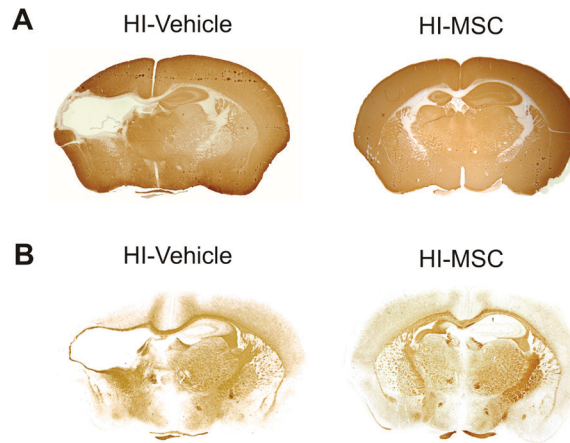


Figure 1. Intranasal MSC treatment decreases HI lesion size. Representative images of (A) MAP2 and (B) MBP staining from HI-Vehicle and HI-MSC animals at 18 days after MSC administration (*i.e.* 28 days after HI).

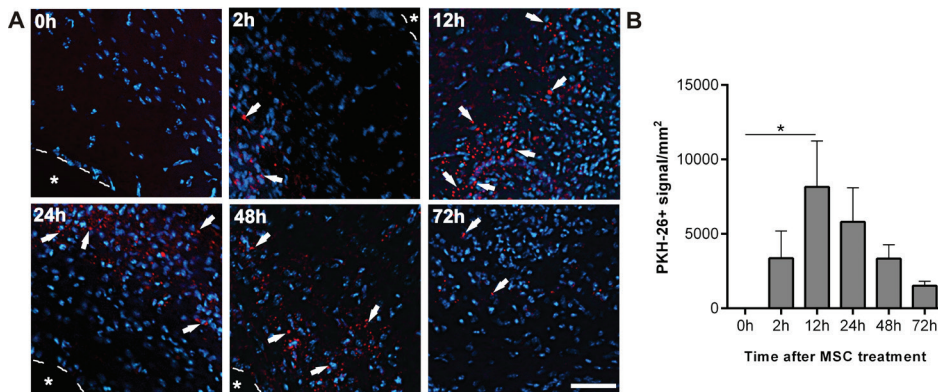


Figure 2. MSCs reach the lesion site within 2 hours after administration. 1×10^6 PKH-26 labeled MSCs were administered intranasally 10 days after HI. (A) Representative images of PKH-26⁺ cells (see arrows) at the lesion site at 2, 6, 12, 24, 48 and 72h following MSC administration. (B) Quantification of PKH-26⁺ signal/mm² at 2, 6, 12, 24, 48 and 72h. Data represent mean \pm SEM. * $p < 0.05$ by ANOVA and Bonferroni post-hoc test. (n=5 per group) Red = PKH-26; Blue = DAPI; Asterisk = lesion; Dashed line = lesion border. scale bar = 50 μ m.

MRI of MPIO-labeled MSCs

To corroborate our observation that MSCs reach the lesion site within 2h, we performed *ex-vivo* MRI analysis of mouse brains using MSCs loaded with micron-sized superparamagnetic iron-oxide particles (MPIO) co-labeled with the fluorescent label Dragon Green. *In vitro* pre-screening of MPIO-labeled MSCs showed strong fluorescent signal indicating that MSCs had ingested MPIO particles (Fig 3A). To verify that contrast-induced signal intensity changes represent changes in MPIO-MSC numbers, increasing numbers of MPIO-MSCs were assessed *in vitro* with MRI. The results clearly showed that MPIO signal intensity correlated with MSC concentration (Fig 3B).

MPIO-labeled MSCs were administered to both nostrils 10 days after HI or sham-operation and mice were sacrificed 2h later. Hypo-intensities in T_2^* -weighted images were detected specifically in regions adjacent to the lesion site (Fig 3C). No hypo-intensities were observed in the brains of sham-operated mice (Fig 3D). To validate the MRI results, we analyzed brain sections for Dragon Green fluorescence. In the HI-injured brain we observed a strong fluorescent signal clustered in the somatosensory cortex adjacent to the lesion, in a pattern comparable to the MPIO signal observed with MRI (Fig 3E). In agreement with our MRI results, no Dragon Green signal was observed in brains from sham-operated mice (Fig 3F, F').

To control for the possibility that dying MPIO-labeled MSCs or free MPIO had been taken up by microglia *in vivo*, we also analyzed colocalization of Iba-1 and Dragon Green. The results show that Iba-1⁺ cells surround the Dragon Green fluorescent signal without overlapping (Fig 3E').

Neurotrophic factor expression by MSCs

To determine whether the HI brain environment stimulates MSCs to express the neurotrophic factors BDNF and NGF, we co-cultured MSCs with HI or sham-operated brain extracts from 10 days post-insult. Our results show that BDNF mRNA expression significantly increases after co-culture with HI brain extract, but not with sham-operated brain extract (Fig 4C). NGF gene expression increased after co-culture with both HI and sham brain extracts (Fig 4C).

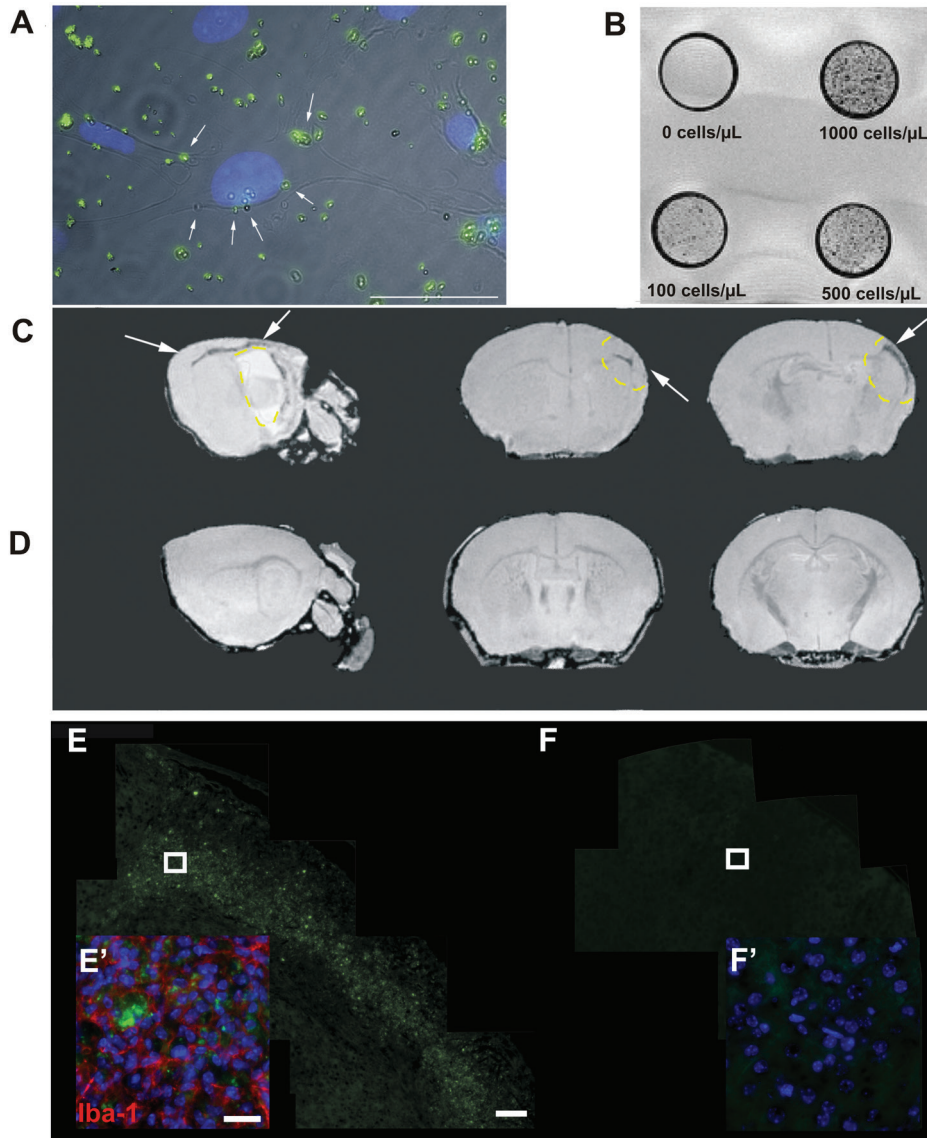


Figure 3. Magnetic Resonance Imaging of MPIO labeled MSCs. 1×10^6 MPIO-labeled MSCs were administered intranasally at 10 days after HI or sham-operation. (A) Representative phase-contrast and fluorescent image of MPIO-(Dragon Green) labeled MSCs. Dragon Green MPIOs are taken up by the MSCs. Scale bar = 10 μm . (B) T_2^* -weighted gradient echo image of cell samples acquired at $100 \times 100 \times 200 \mu\text{m}^3$ spatial resolution, with TE = 15 ms. Note the increase in contrast as cell concentration increases. (C, D) *Ex-vivo* T_2^* -weighted images of mouse brain ($75 \times 75 \times 75 \mu\text{m}^3$ resolution, TE = 15 ms), 2h following intranasal administration of MPIO-labeled MSC at 10 days after HI (C) or sham-operation (D). (C) Arrows show signal contrast from MPIO-labeled MSCs surrounding damaged region (yellow dashed line). (E, F) Panorama of ipsilateral cortex from HI (E) or sham-operated (F) mice. Note the Dragon Green signal in (E). scale bar = 200 μm . (E') Iba-1 (red) staining on sections from brain shown in (E). (F') Insert of sham-operated mice. Blue = DAPI; scale bar = 20 μm .

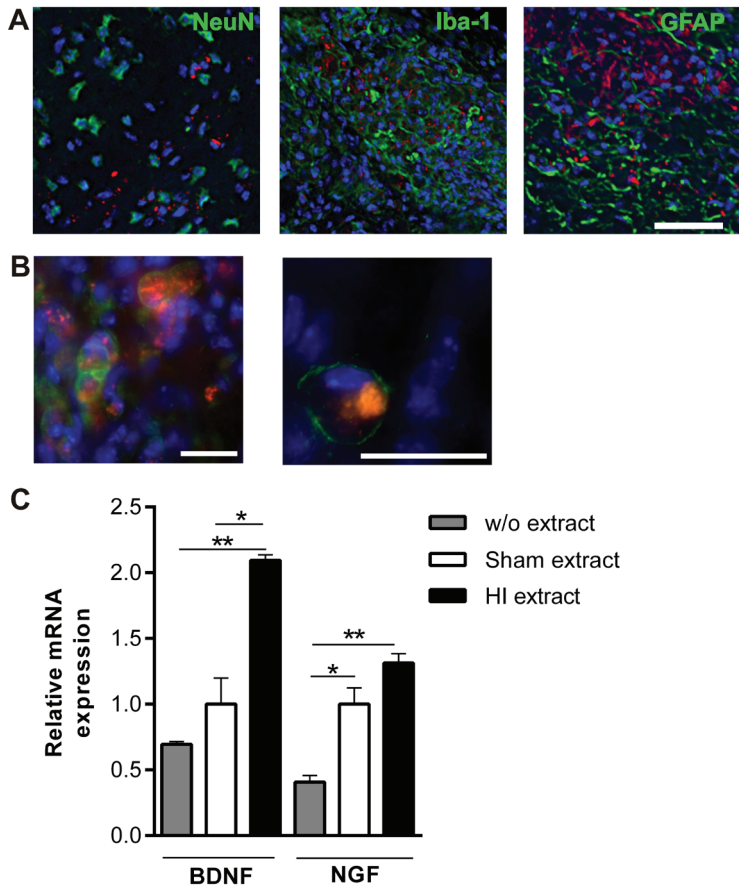


Figure 4. Characterization of the cellular niche at the lesion and neurotrophic factor expression by MSCs. (A) Brain sections from 24h after MSC-treatment were stained for NeuN (Green), Iba-1 (Green) and GFAP (Green) expression. (n=3 per group); Red = PKH-26; Blue = DAPI; scale bar = 50 μ m. (B) Overlap between Iba-1⁺ cells and PKH-26⁺ signal at 2h after MSC administration. Green = Iba-1; Red = PKH-26; scale bar = 20 μ m. (C) Relative mRNA expression of BDNF and NGF by MSCs at 72h after co-culture without brain extract or with either HI or sham-operated brain extract (n=2). Data represent mean \pm SEM. * p < 0.05; **p < 0.01 by unpaired two-tailed T-test.

Characterization of the early regenerative niche at the lesion

To characterize the cellular environment surrounding the MSCs at the lesion site, we stained ipsilateral brain sections at 1 day after MSC treatment for NeuN, GFAP and Iba-1. PKH-26⁺-MSCs were primarily surrounded by Iba-1⁺ cells (Fig 4A). NeuN⁺ cells were found scattered around the MSCs. GFAP⁺ cells formed a boundary border around the PKH-26⁺-MSCs. There was no overlap between PKH-26⁺ MSCs and NeuN⁺, GFAP⁺ or

Iba-1⁺ cells at 1 day. To determine whether Iba-1⁺ cells overlapped with PKH-26⁺-MSCs at an earlier time-point, we stained brain sections at 2h following MSC treatment for Iba-1. At this early time-point, we estimate that around 80% of the Iba-1⁺ cells overlapped with the PKH-26⁺-MSC-derived signal suggesting that Iba-1⁺ cells may phagocytose dying MSCs (Fig. 4B).

MSCs increase the number of DCX⁺ cells in the SVZ

First, we investigated whether MSCs affect neurogenesis in the SVZ. To this end, we assessed the number of neuronally-committed type A progenitor cells, *i.e.* neuroblasts, which have the phenotype of young migrating neurons. Coronal sections from the SVZ were stained for doublecortin (DCX) at 1, 3 and 5 days after MSC or Vehicle treatment. MSC administration significantly increased the number of DCX⁺ cells in the SVZ at 1 and 3 days (Fig 5A-C). At 5 days after MSC treatment, the number of DCX⁺ cells had returned to the level observed in sham-operated mice (Fig 5D). DCX⁺ cell numbers increased in the contralateral SVZ at 1 days. HI alone did not lead to a significant increase in the number of DCX⁺ cells at any of the time-points measured (Fig 5).

Early effect of MSCs on neural progenitor cells at the lesion

Next, we determined the number of type B precursor cells (*i.e.* uncommitted precursors) at the lesion site, by quantifying the expression of GFAP⁺/nestin⁺ pixels in 10 fields, at 1, 3 and 5 days after MSC or Vehicle administration (Fig 6A). Our results show that the number of GFAP⁺/nestin⁺ pixels at 1 day after MSC treatment is almost two times higher than in HI-Vehicle or sham-operated animals (Fig 6B, C). At 5 days the amount of GFAP⁺/nestin⁺ pixels had returned to sham level. HI only led to a small significant increase in GFAP⁺/nestin⁺ expression on day 3. In sham-operated mice, GFAP⁺/nestin⁺ expression remained stable over time. In HI-Vehicle and HI-MSC animals, GFAP⁺/nestin⁺ cells were located at the lesion border. These data show that MSC enhance the number of type B precursor cells at the lesion, which suggests the formation of a neurogenic niche.

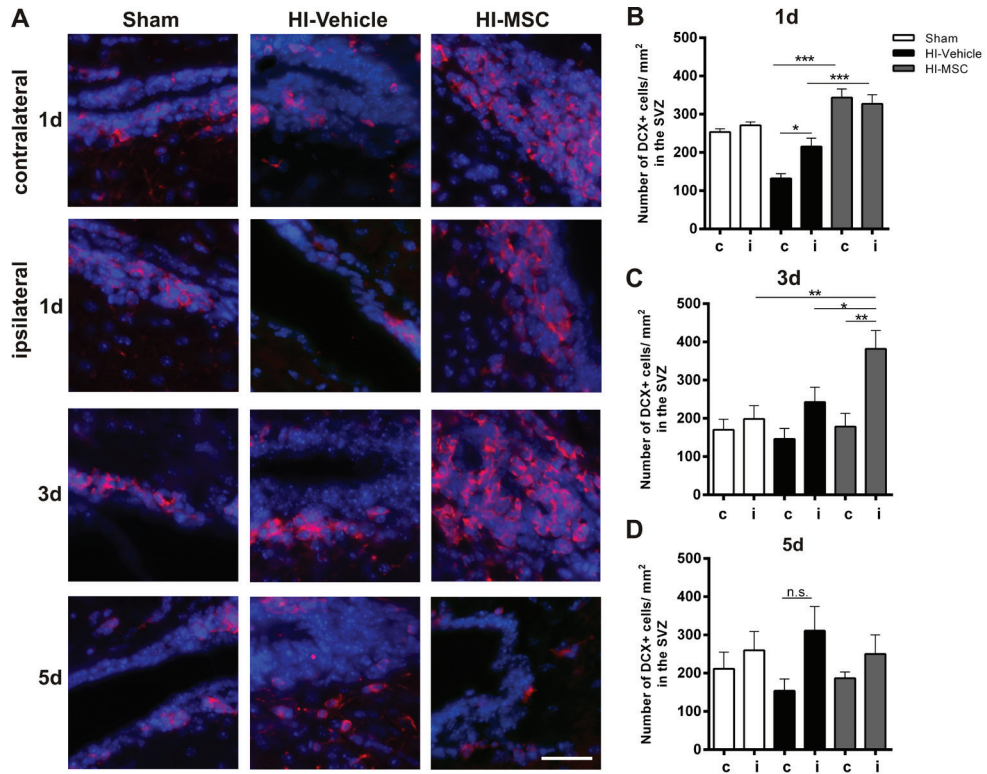


Figure 5. MSCs increase the expression of DCX in the SVZ. DCX expression in the SVZ at 1, 3 and 5 days after MSC or Vehicle administration and in sham-operated brain. (A) Representative images of sham, HI-Vehicle or HI-MSC at 1, 3 and 5 days after treatment. (B-D) Quantification of DCX⁺ cells in the contra- and ipsilateral SVZ at 1 day (B), 3 day (C) and 5 day (D). Data represent mean \pm SEM. * $p < 0.05$; ** $p < 0.01$; *** $p < 0.001$; n.s. = not significant by ANOVA and Bonferroni post-hoc test. (n=6 per group); Red = DCX; Blue = DAPI; scale bar = 32 μ m.

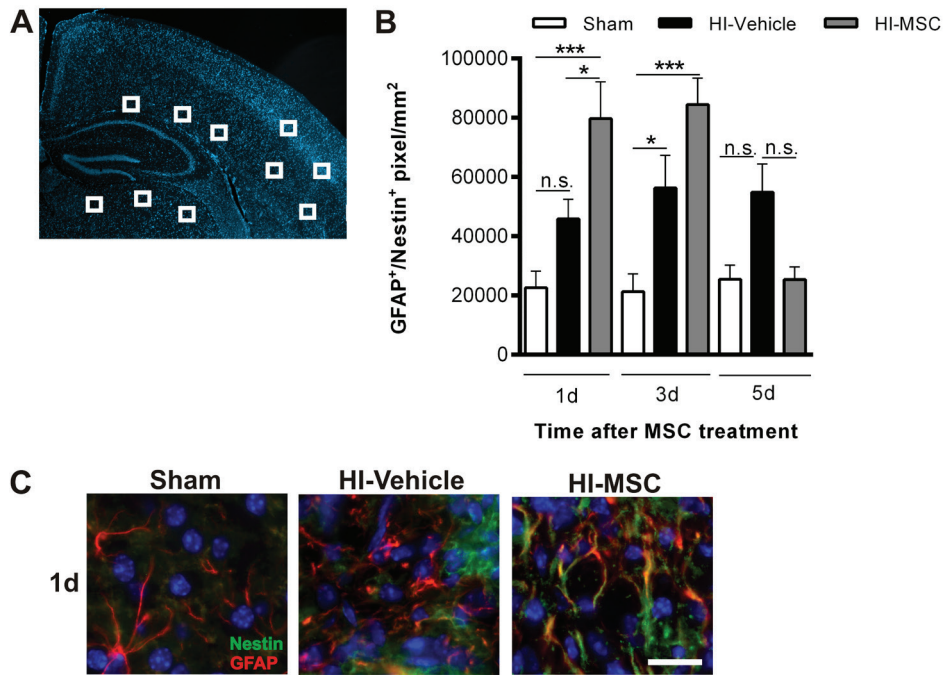


Figure 6. Expression of neural precursor cells increases following MSC-treatment. GFAP and nestin expression at the lesion site at 1, 3 and 5 days after MSC or Vehicle treatment and in sham-operated brain. (A) Schematic illustration of regions that were quantified. (B) Quantification of GFAP⁺/nestin⁺ pixels at 1, 3 and 5 days. (C) Representative images of sham, HI-Vehicle or HI-MSc at 1 day after treatment. Data represent mean \pm SEM. * $p < 0.05$; *** $p < 0.001$; n.s. = not significant by ANOVA and Bonferroni post-hoc test. (n=6 per group); Green = Nestin; Red = GFAP; Blue = DAPI; scale bar = 20 μ m.

Next, we quantified the number of DCX⁺ cells at the lesion. At both 1 and 3 days after MSC-treatment there was a significant increase in DCX⁺ cells in the corpus callosum, and in the ipsilateral cortical and thalamic regions adjacent to the lesion (Fig 7A,C). At 5 days, the number of DCX⁺ cells in the ipsilateral hemisphere had returned to sham level (Fig 7A,D). However, at this time-point the number of DCX⁺ cells in the ipsilateral hemisphere of MSC-treated mice was significantly higher than in the contralateral area (Fig 7D). In HI-Vehicle mice, DCX expression at the lesion or contralateral side was not changed at 1 to 5 days (*i.e.* 11-15 days post-HI) (Fig 7). DCX expression remained constant in sham-operated mice. These results demonstrate that MSCs also enhance the number of neuronally committed progenitor cells at the lesion.

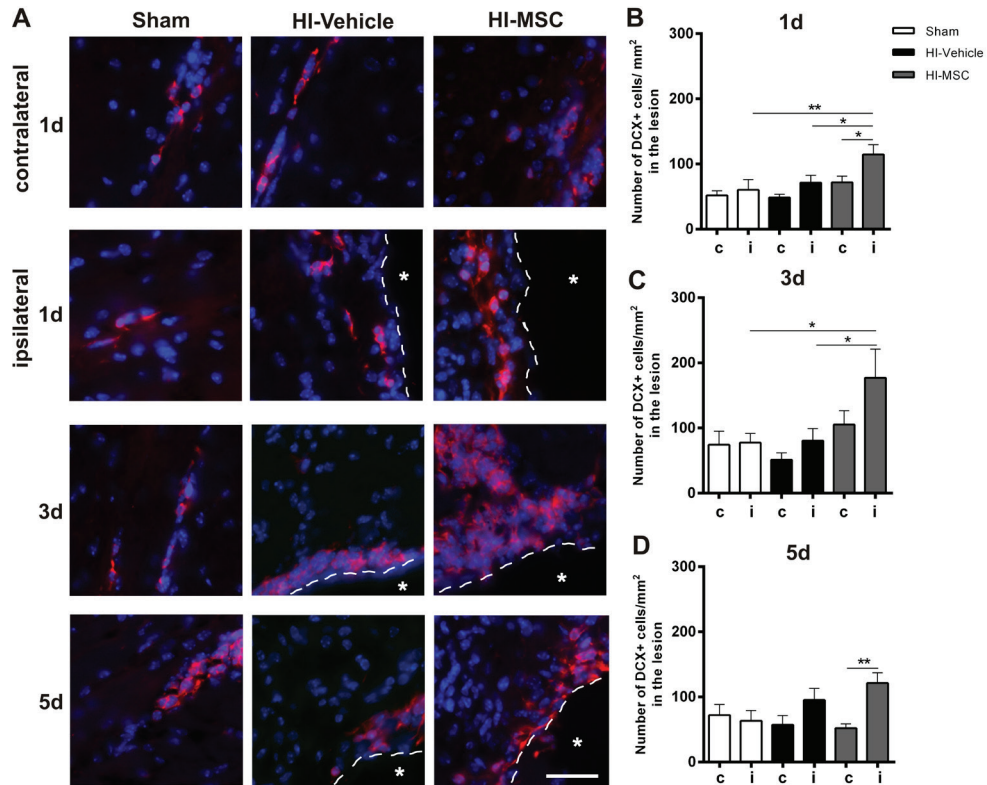


Figure 7. DCX expression is increased at the lesion site following MSC-treatment. DCX expression at the lesion at 1, 3 and 5 days after MSC or Vehicle administration and in sham-operated brains. (A) Representative images of sham, HI-Vehicle or HI-MSC at 1, 3 and 5 days after treatment. (B-D) Quantification of DCX⁺ cells adjacent to the lesion and at the undamaged contralateral side at 1 day (B), 3 days (C) and 5 days (D). Data represent mean \pm SEM. * $p < 0.05$; ** $p < 0.01$ by ANOVA and Bonferroni post-hoc test. (n=6 per group); Red = DCX; Blue = DAPI; Asterisk = lesion; Dashed line = lesion border. scale bar = 32 μ m.

MSCs regenerate the lesioned brain

Next, we investigated whether MSC treatment leads to increased repopulation of lost brain structures. We determined the number of NeuN⁺ cells in the damaged somatosensory cortex and hippocampus at 1, 5 and 18 days after MSC or Vehicle treatment. Our results show a significant loss of tissue, encompassing the hippocampus and somatosensory cortex, which can be clearly discerned as a cavity at 11 days after HI (*i.e.* 1 day after MSC or Vehicle treatment) (Fig 8A). In HI-Vehicle mice this cavity was still discernible at 18 days (Fig 8A). The lesion in the somatosensory region

was repopulated by NeuN⁺ cells at 5 days following MSC treatment, and the number of neurons had significantly increased compared to HI-Vehicle mice, and reached sham-level (Fig 8B, C). At 18 days after MSC treatment, NeuN expression in the somatosensory cortex was still increased. At 5 days following MSC treatment, an area with hippocampal morphology started to emerge (Fig 8D). At this time-point, NeuN⁺ cells repopulated the dentate gyrus and we also observed a partial recovery of the CA1, CA2 and CA3 regions. At 18 days, the dentate gyrus, CA1, CA2 and CA3 regions had further regenerated and the hippocampal structure was clearly discernible (Fig 8D).

Effect of MSCs on astrocyte and microglia activation

To assess whether MSC treatment has an effect on the number of astrocytes and microglia, we quantified expression of GFAP⁺ and Iba-1⁺ cells at 1, 5 and 18 days after MSC or Vehicle treatment. Figure 9A and B show that the number of microglia and astrocytes are substantially upregulated at the lesion at all time-points. Following HI, Iba-1⁺ cells show morphological characteristics that correlate with an activated state (amoeboid phenotype) (Fig 9A). GFAP⁺ cells change their star shape morphology to a more rounded, multipolar morphology. A dense network of reactive astrocytes demarcates the entire lesion (Fig 9B). At 1 day after MSC treatment, no significant difference in either Iba-1⁺ or GFAP⁺ expression was observed between Vehicle- and MSC-treated mice (Fig 9A, B). However, at 18 days following MSC treatment, GFAP and Iba-1 expression levels are substantially decreased compared to levels in Vehicle-treated HI mice and have returned to sham level (Fig 9A, B).

Polarization of microglial cells following MSC-treatment

As microglia can have distinct phenotypes, *e.g.* pro-inflammatory (M1) or regenerative/anti-inflammatory (M2a/b), we assessed whether MSC treatment affects microglia polarization. We double-stained coronal sections for CD16/32 (M1) or CD206 (M2) and Iba-1. Our data show that HI-Vehicle mice have a higher expression of both M1 and M2 microglia than sham-operated mice, but no significant polarization towards the M1 or the M2 phenotype (Fig 9C, D). MSC treatment induced polarization towards the M2 phenotype.

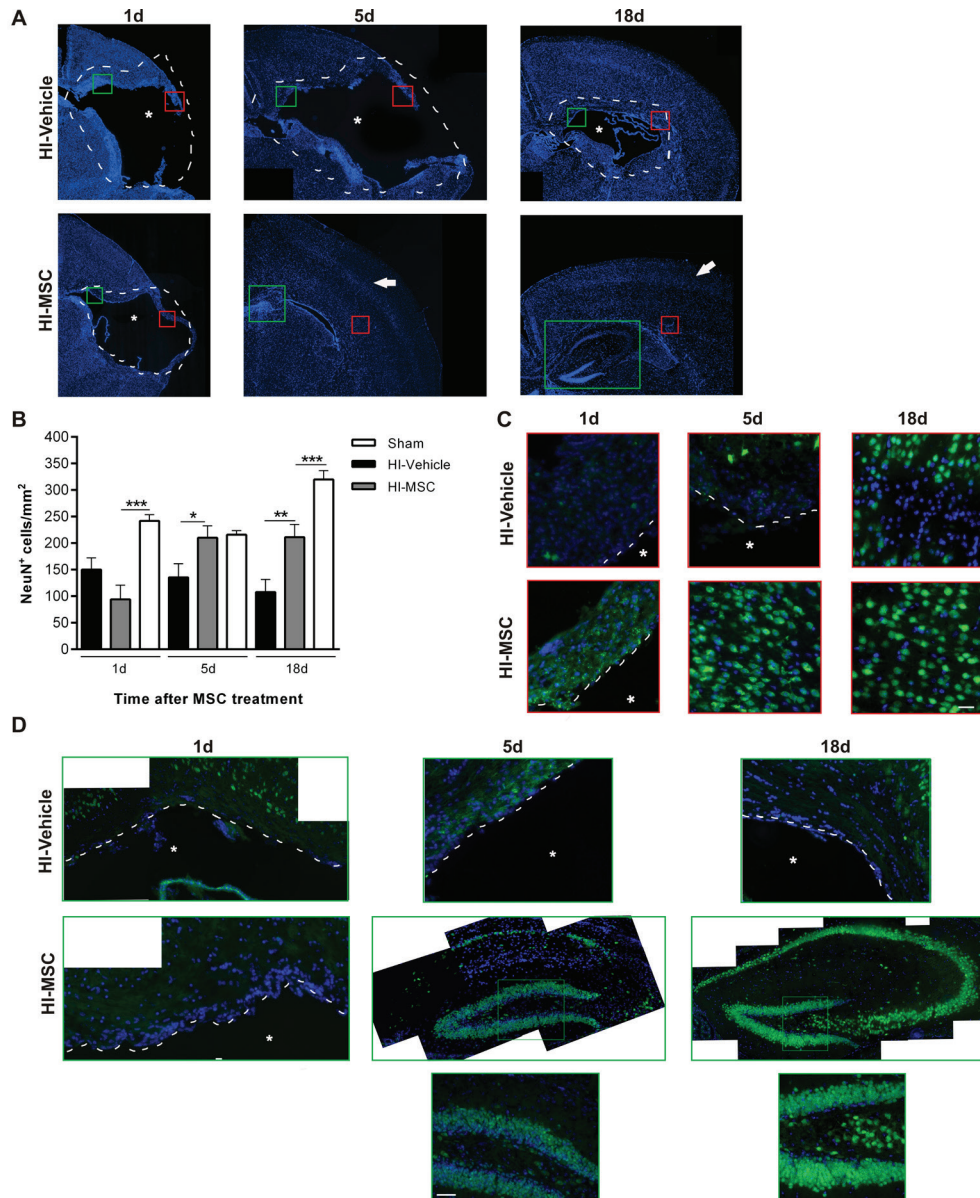


Figure 8. Regeneration following MSC administration. NeuN expression at 1, 5 and 18 days following Vehicle or MSC administration. (A) Overview of macroscopic lesion site at 1, 5 and 18 days after Vehicle or MSC treatment. Note cortical Layer 4 (arrow) at 5 and 18 days after MSC treatment. Red square = insert shown in (C); Green square = insert shown in (D). (B) Quantification of NeuN⁺ cells in 4 random fields in the ipsilateral somatosensory cortex. (C) Representative images of NeuN expression in the somatosensory cortex of HI-Vehicle and HI-MSC. (D) Representative images of NeuN expression in the hippocampal structure at 1, 5 and 18 days following MSC or Vehicle treatment. Data represent mean ± SEM. *p<0.05; **p<0.01; ***p<0.001 by ANOVA and Bonferroni post-hoc test. (n=6 per group). Green = NeuN; Blue = DAPI; Asterisk = lesion site; Dashed line = boundary lesion. scale bar = 50 μm in C, D.

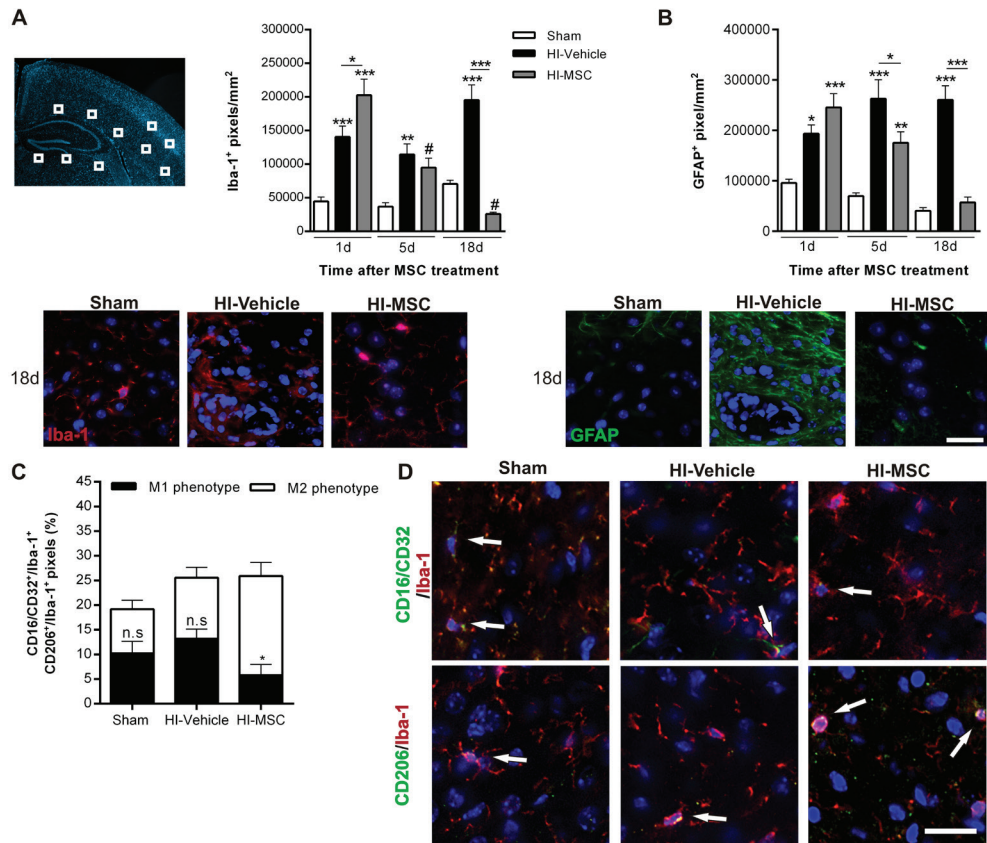


Figure 9. MSCs revert astrogliosis at the damaged region. Iba-1 and GFAP expression at the lesion at 1, 5 and 18 days after MSC or Vehicle administration. (A) Upper: Quantification of Iba-1⁺ at 1, 5 and 18 days and a schematic view of the regions that were quantified in (A), (B) and (C). Lower: Representative images of Iba-1⁺ cells in sham, HI-Vehicle and HI-MSC at 18 days. (B) Upper: Quantification of GFAP⁺ pixels at 1, 5 and 18 days. Lower: Representative images of GFAP⁺ cells in sham, HI-Vehicle and HI-MSC at 18 days. (C) Quantification of CD16/32⁺/Iba-1⁺ pixels and CD206⁺/Iba-1⁺ pixels at 5 days. (D) Representative images of CD16/32⁺/Iba-1⁺ cells and CD206⁺/Iba-1⁺ cells at 5 days after MSC-treatment. Data represent mean \pm SEM. (A, B) * p <0.05; ** p <0.01; *** p <0.001; # = not significant for Sham 5 days vs HI-MSC 5 days and Sham 18 days vs HI-MSC 18 days by ANOVA and Bonferroni post-hoc test. (C) * p <0.05 by multiple T-test corrected with the Holm-Sidak method. (n =6 per group); Red = Iba-1 (A,D); Green = GFAP (B), CD206, CD16/CD32 (D); Blue = DAPI; scale bar = 20 μ m.

Discussion

In view of the pre-clinical efficacy of MSC treatment and the lack of effective therapies for infants with neonatal brain damage, intranasal MSC administration might become a powerful therapeutic strategy in the future. In previous studies we described the potent effect that MSCs have in decreasing lesion size and improving motor and cognitive behavior following HI injury^{8, 13-15}. Yet, how MSCs mediate this effect is unclear. Here, we describe the effect of intranasally administered MSCs on the cellular composition of the 'regenerative niche' in the SVZ and lesion. Moreover, we followed repair of the lesion by quantifying the number of GFAP⁺/nestin⁺, DCX⁺ and NeuN⁺ cells, astrocytes and microglia until 18 days after MSC-treatment (*i.e.* 28 days after HI). Following application of MSCs, cells migrate from the ipsi- and contralateral nasal cavities to the unilateral lesion within 2h after administration. The number of MSCs decreases sharply at 72h, which is in accordance with previous findings¹⁴. This indicates that MSCs *induce* a cascade of events leading to tissue repair. MSCs not only increase the number of GFAP⁺/nestin⁺ and DCX⁺ cells at the lesion within 1 day after intranasal administration, but also induce maturation of neuroblasts following HI brain injury (Fig 10). Moreover, MSCs induce microglial polarization towards a M2 phenotype and decrease the number of activated astroglial cells at 18 days after treatment. Our key finding is that intranasal MSC treatment leads to a remarkably fast regeneration of the lesion, as repopulation of the somatosensory and hippocampal regions starts within 5 days after administration.

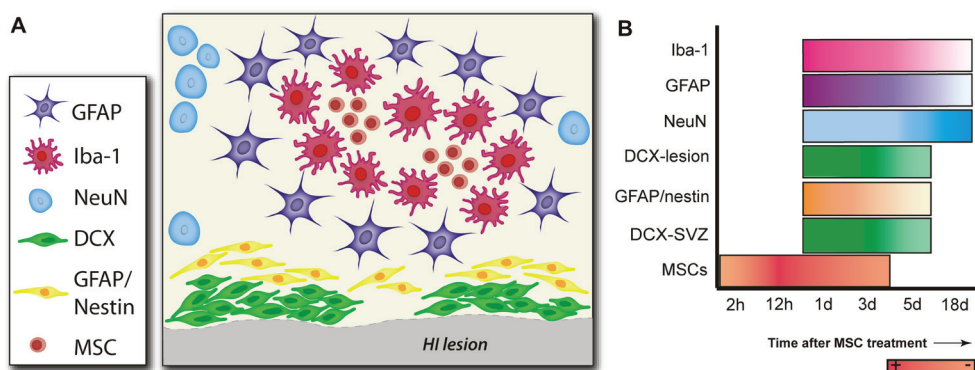


Figure 10. Schematic overview of location and changes in number of MSCs, precursor cells and glial cells. (A) Schematic figure showing location of MSCs, GFAP⁺/nestin⁺, DCX⁺, GFAP⁺ and Iba-1⁺ cells at the lesion at 1 day after administration. (B) Diagram depicting changes in MSC, GFAP/nestin, DCX, NeuN, GFAP and Iba-1 expression over time.

The MSC signal detected with MRI and Dragon Green fluorescence surrounding the lesion at 2h after administration (Fig 3) closely resembles the PKH-26⁺ MSC signal, which forms clusters alongside the lesion (Fig 2). We checked for the possibility that MPIOs are phagocytosed by microglia, thereby leading to false positive results. However, Iba-1 staining showed no overlap with the MPIO-labeled MSCs, further supporting that the MRI signal and the Dragon Green fluorescence correspond to the presence of MSCs at the lesion. Yet, at 2h after MSC administration, around 80% of the PKH26⁺ signal overlapped with Iba-1⁺ microglia (Fig 4B). In contrast, at 1 day there was no overlap between the Iba-1⁺ signal and the PKH26⁺ signal (Fig 4A). To explain the apparent discrepancy between results we postulate that the first MSCs reaching the lesion at 2h will be phagocytosed by activated microglia, which may in its turn affect the local brain environment that will shift towards an environment more receptive for MSCs. Hence, at 12h, when there is a peak in the number of MSCs in the lesion, the environment is more receptive to the MSCs, which are no longer phagocytosed. The fact that we did not observe an overlap between Dragon Green signal and the Iba-1⁺ signal at 2h after MSC administration might be due to the relatively strong Dragon Green staining (Fig 3E').

Our finding that MSCs reach the damaged area within 2h makes it unlikely that MSCs migrate to the lesion through the brain parenchyma. Neural precursor cells have been shown to migrate $94\mu\text{m} \pm 20\mu\text{m}$ per hour along the rostral migratory stream (RMS)¹⁷. Hence, if one would assume that MSCs migrate at a similar rate it would take several days to reach the damaged region. Therefore, it seems more plausible that MSCs migrate from the intranasal cavity towards the lesion through the meningeal circulation or along blood vessels in the lamina propria or via the cerebral spinal fluid.

In order to study whether MSCs increase the number of neuronally-committed cells in the neurogenic niche in the SVZ, we determined the presence of DCX⁺ cells in the SVZ. We show that MSCs increase the number of neuroblasts in the ipsilateral SVZ at 1 and 3 days after treatment (Fig 5). As we did not find MSCs in the SVZ region at any time-point, we postulate that MSCs at the lesion induce neurotrophic factor production in the SVZ, possibly through paracrine signaling by MSCs, which in turn promotes differentiation of type B precursor cells towards neuroblasts in the SVZ. The fact that most of the increase in DCX⁺ cells in the SVZ was detected in the ipsilateral side indicates that MSC presence at the lesion leads to increased precursor cells in the SVZ. These results raise the interesting possibility that neuroblasts in the SVZ may migrate towards the lesion to repopulate the damaged cortical areas¹⁸⁻²⁰.

Anderova *et al.*, 2011, described that HI increases the number of GFAP⁺/nestin⁺ NSCs in the hippocampus in adult rats. Neonatal HI has also been demonstrated to increase the number of neuroblasts in the lesion 1-3 weeks post-insult²²⁻²⁴. We detected a small increase of GFAP⁺/nestin⁺ expression at the lesion at 3 days (*i.e.* 13 days after HI) after Vehicle treatment. We did not observe any change in DCX expression after Vehicle treatment. Therefore, we conclude from our data that neurogenesis is impaired following neonatal HI, which is in accordance with current literature²⁵. In contrast, 1 day after MSC treatment, the number of GFAP⁺/nestin⁺ cells surrounding the lesion had increased almost two times in comparison to HI-Vehicle mice (Fig 6). At 5 days after MSC administration the number of precursor cells had returned to sham level. Moreover, we found a substantial increase in DCX⁺ cells at 1 and 3 days after MSC, which declined to sham level at 5 days (Fig 7).

Our results show that this increase in the number of DCX⁺ cells was short-lasting as at 5 days after MSC administration it had returned to sham level suggesting that the DCX⁺ cells had either differentiated to a more mature phenotype or died. As GFAP⁺/nestin⁺ cells first become nestin⁺ before differentiating towards DCX⁺ cells, we also investigated whether the GFAP⁺/nestin⁺ cells had differentiated towards the nestin⁺ intermediate phenotype at 5 days. We found that at 5 days, nestin⁺ cells are still significantly increased in the lesion in comparison to sham, which suggests that the GFAP⁺/nestin⁺ cells have become type 2 precursor cells at 5 days (data not shown). These data suggest that the differentiation of nestin⁺ cells into adult neurons and astrocytes may continue after 5 days following MSC treatment.

Next, we investigated whether the DCX⁺ cells had further differentiated into more mature neurons, by assessing the number of NeuN⁺ cells after MSC and Vehicle treatment. Our results show extensive tissue loss encompassing the somatosensory cortex and hippocampus 1 day (*i.e.* 11 days after HI) following Vehicle or MSC treatment. Furthermore, we observed that in the Vehicle-treated mice the lesion size did not aggravate any further after 11 days following HI. However, at 5 days after MSC treatment the number of NeuN⁺ cells increases significantly reaching sham level. These NeuN⁺ cells will repopulate the damaged somatosensory cortex resulting in cortical lamination, as Layer 4 can be clearly distinguished (Fig 8A-C). The hippocampal region also starts to regenerate at 5 days after MSC treatment. The dentate gyrus is well defined and the CA1, CA2 and CA3 regions are beginning to repopulate. The CA1, CA2 and CA3 regions develop further at 18 days. The fact that at 10 days after

HI, there is significant tissue loss and the lesion does not augment, does not support a neuroprotective role for MSCs in our model. Instead, the results strongly support that MSC induced lesion repair is due to increased neuroregeneration.

MSCs are known to have strong immunomodulatory capacity and to decrease inflammatory responses following injury²⁶⁻²⁸. Astrocytes have been shown to be a (functionally) heterogeneous cell population that can be either detrimental to neurogenesis or support neuronal function^{27,29,30,31}. Whether astrocytes will lead to astrogliosis and impair regeneration or promote neurogenesis and repair, depends on a plethora of signals including pro-inflammatory (*e.g.* IFN- γ and IL-1) and damage signals (*e.g.* DAMPs and PAMPs)³¹. At 1 day after Vehicle or MSC treatment we observed a significant amount of GFAP⁺ cells surrounding the lesion. Interestingly, 18 days after MSC treatment the amount of GFAP⁺ expressing cells had decreased back to sham level (Fig 9), which suggests that MSCs may also decrease gliosis, since in HI-Vehicle animals there is still a dense network of reactive astrocytes at the lesion border.

Microglia, like astrocytes, can have either a pro-inflammatory effect (M1) or promote tissue repair and anti-inflammation (M2)³²⁻³⁵. We show that MSCs stimulate microglia polarization towards a M2 phenotype (Fig 9). This may be mediated by the immunosuppressive effects of MSCs. In this respect, it is of interest that we have shown increased IL-10 mRNA expression after MSC transplantation¹⁴. MSC treatment decreases the number of microglia at 28 days after HI, the time-point when repair of the lesion by NeuN⁺ cells was observed. These findings suggest that lesion repair is associated with an anti-inflammatory environment and that the immunosuppressive capacity of MSCs play an important role in mediating regeneration following HI injury³⁶.

In conclusion, the results in this study demonstrate that intranasal MSCs decrease lesion volume by promoting formation of a 'neurogenic niche' leading to a dramatic reconstruction of the hippocampus and somatosensory cortex (Fig 8). This is crucial as the regenerative signal induced by HI is largely insufficient²⁵. Our present study demonstrates that MSCs boost the endogenous regenerative capacity by promoting neurogenesis and neuronal survival. Importantly, we show evidence that MSCs are directly involved in inducing and supporting a shift to a neurogenesis supportive environment, as we found that MSCs express more BDNF following contact with a HI environment. Co-culture of MSCs with brain extract from sham-operated mice doubles the mRNA expression of NGF. In contrast to BDNF, co-culture with HI brain

extract does not further increase the production of NGF. This may suggest that factors present in the brain of sham animals stimulate MSCs to maintain production of NGF. Following injury, endogenous stimuli in the brain will increase the production of BDNF by MSCs to promote neurogenesis. Therefore, this suggests that the HI brain environment stimulates MSCs to secrete specific neurotrophic factors. The neurotrophic factor BDNF plays an important role in proliferation, migration, differentiation and survival of neuronal cells³⁷. Moreover, we have previously shown that intracranially-administered MSCs upregulate gene expression of several neurotrophic factors¹⁴. Both the SVZ and lesion site may be sources of progenitor cells. MSCs may induce migration of DCX⁺ cells from the SVZ to the lesion and also stimulate a subset of reactive astrocytes in the lesion to develop stem cell potential. MSCs also revert scar formation, which is known to impair neurogenesis. These findings are of clinical importance as they further delineate the power of MSCs as a future therapeutic strategy for neonatal HI brain damage.

Acknowledgments

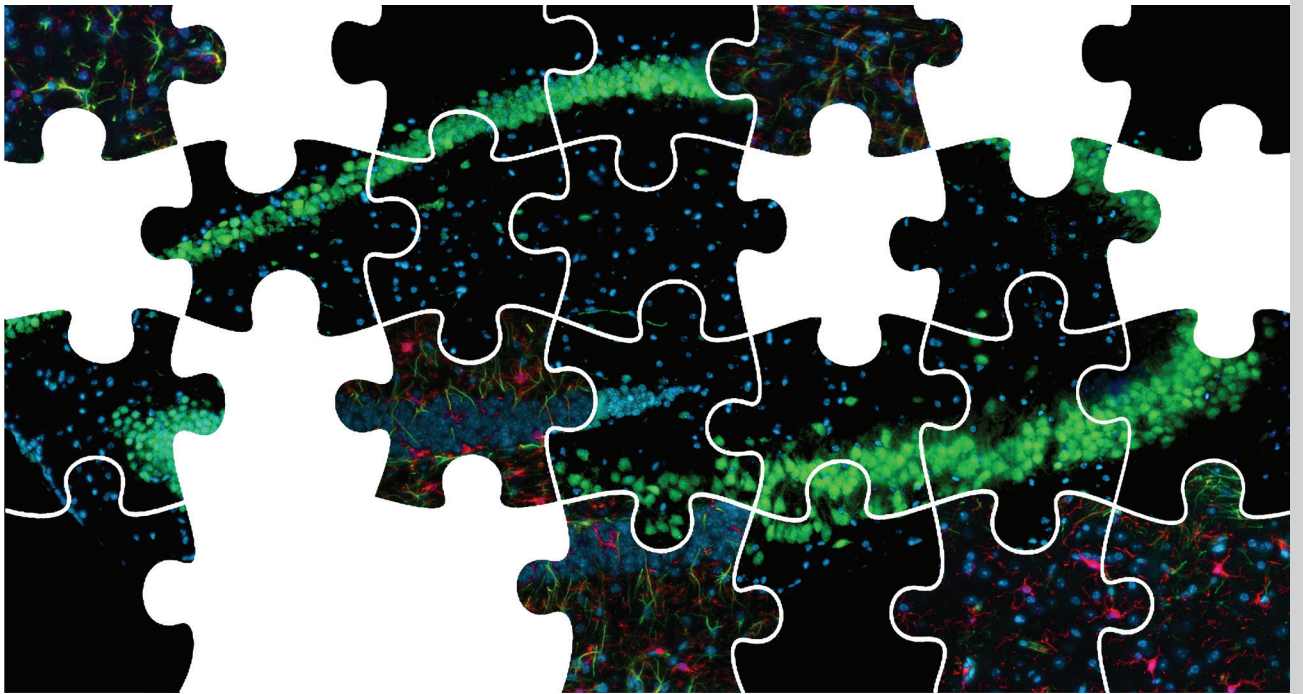
This study was supported by Zon-MW Project (no 116002003) and EU-7 Neurobid (HEALTH-F2-2009-241778) from the European Union.

References

1. De Haan M, Wyatt JS, Roth S, et al. Brain and cognitive-behavioural development after asphyxia at term birth. *Dev Sci* 2006;9:350–358.
2. Ferriero DM. Neonatal brain injury. *N Engl J Med* 2004;351:1985–1995.
3. Graham EM, Ruis KA, Hartman AL, et al. A systematic review of the role of intrapartum hypoxia-ischemia in the causation of neonatal encephalopathy. *Am J Obstet Gynecol* 2008;199:587–595.
4. Van Handel M, Swaab H, de Vries LS, et al. Long-term cognitive and behavioural consequences of neonatal encephalopathy following perinatal asphyxia: a review. *Eur J Pediatr* 2007;166:645–654.
5. Volpe JJ. Perinatal brain injury: from pathogenesis to neuroprotection. *Ment Retard Dev Disabil Res Rev* 2001;7:56–64.
6. Bacigaluppi M, Pluchino S, Jametti LP, et al. Delayed post-ischaemic neuroprotection following systemic neural stem cell transplantation involves multiple mechanisms. *Brain* 2009;132:2239–2251.
7. Daadi MM, Davis AS, Arac A, et al. Human neural stem cells grafts modify microglial response and enhance axonal sprouting in neonatal hypoxic-ischemic brain injury. *Stroke* 2010;41:516–523.
8. Donega V, van Velthoven CT, Nijboer CH, et al. Intranasal Mesenchymal Stem Cell Treatment for Neonatal Brain Damage: Long-Term Cognitive and Sensorimotor Improvement. *PLoS ONE* 2013a;8:e51253.
9. Lee JA, Kim BI, Jo CH, et al. Mesenchymal stem cell transplantation for hypoxic-ischemic brain injury in a neonatal rat model. *Pediatric Res* 2010;67:42–46.
10. Pimentel-Coelho PM, Magalhaes ES, Lopes LM, et al. Human cord blood transplantation in a neonatal rat model of hypoxic-ischemic brain damage: functional outcome related to neuroprotection in the striatum. *Stem Cells Dev* 2010;19:351–358.
11. Titomanlio L, Kavelaars A, Dalous J, et al. Stem cell therapy for neonatal brain injury: perspectives and challenges. *Ann of Neurol* 2011;70:698–712.
12. Yasahura T, Hara K, Maki M, et al. Intravenous grafts recapitulate the neurorestoration afforded by intracerebrally delivered multipotent adult progenitor cells in neonatal hypoxic-ischemic rats. *J Cereb Blood Flow Metab* 2008;28:1804–1810.
13. Van Velthoven CT, Kavelaars A, van Bel F, et al. Repeated mesenchymal stem cell treatment after neonatal hypoxia-ischemia has distinct effects on formation and maturation of new neurons and oligodendrocytes leading to restoration of damage, corticospinal motor tract activity, and sensorimotor function. *J Neurosci* 2010;30:9603–11.
14. Van Velthoven CT, Kavelaars A, van Bel F, et al. Mesenchymal stem cell transplantation changes the gene expression profile of the neonatal ischemic brain. *Brain Behav Immun* 2011;25:1342–1350.
15. Van Velthoven CT, Braccioli L, Willems HL, et al. Therapeutic potential of genetically modified mesenchymal stem cells after neonatal hypoxic-ischemic brain damage. *Mol Ther* 2013 [epub ahead of print].

16. Crigler L, Robey RC, Asawachaicharn A, et al. Human mesenchymal stem cell subpopulations express a variety of neuro-regulatory molecules and promote neuronal cell survival and neurogenesis. *Exp Neurol* 2006;198:54-64.
17. Murase SI, Horwitz AF. Deleted in colorectal carcinoma and differentially expressed integrins mediate the directional migration of neural precursors in the rostral migratory stream. *J Neurosci* 2002;22:3568-3579.
18. Inta D, Alfonso J, von Engelhardt, et al. Neurogenesis and widespread forebrain migration of distinct GABAergic neurons from postnatal subventricular zone. *Proc Natl Acad Sci USA* 2008;105:20994-9.
19. Kempermann G, Jessberger S, Steiner B, et al. Milestones of neuronal development in the adult hippocampus. *Trends Neurosci* 2004;27:447-452.
20. Zhao C, Deng W, Gage FH. Mechanisms and functional implications of adult neurogenesis. *Cell* 2008;132:645-660.
21. Anderova M, Vorisek I, Pivonkova H, et al. Cell death/proliferation and alterations in glial morphology contribute to changes in diffusivity in the rat hippocampus after hypoxia-ischemia. *J Cereb Blood Flow Metab* 2011;31:894-907.
22. Fagel DM, Ganat Y, Silbereis J, et al. Cortical neurogenesis enhanced by chronic perinatal hypoxia. *Exp Neurol* 2006;199:77-91.
23. Felling RJ, Snyder MJ, Romanko MJ, et al. Neural stem/progenitor cells participate in the regenerative response to perinatal hypoxia-ischemia. *J Neurosci* 2006;26:4359-4369.
24. Kadam SD, Mulholland JD, McDonald JW, et al. Neurogenesis and neuronal commitment following ischemia in a new mouse model for neonatal stroke. *Brain Res* 2008;1208:35-45.
25. Donega V, Velthoven C, Nijboer CH, et al. The endogenous regenerative capacity of the damaged newborn brain: boosting neurogenesis with mesenchymal stem cell treatment. *J Cereb Blood Flow Metab* 2013b;33:625-634.
26. Tse WT, Pendleton JD, Beyer WM, et al. Suppression of allogeneic T-cell proliferation by human marrow stromal cells: implications in transplantation. *Transplantation* 2003;75:389-397.
27. Salem HK, Thiemermann C. Mesenchymal stromal cells: Current understanding and clinical status. *Stem Cells* 2010;28:585-596.
28. Zhang R, Liu Y, Yan K, et al. Anti-inflammatory and immunomodulatory mechanisms of mesenchymal stem cell transplantation in experimental traumatic brain injury. *J Neuroinflammation* 2013;10:106-118.
29. Rusnakova V, Honsa P, Dzamba D, et al. Heterogeneity of Astrocytes: from development to injury-single cell gene expression. *PLOS One* 2013;8:e69734.
30. Garcia DR, Doan NB, Imura T, et al. GFAP-expressing progenitors are the principal source of constitutive neurogenesis in adult mouse forebrain. *Nat Neurosci* 2004;7:1233-1241.
31. Sofroniew MV. Multiple Roles for astrocytes as effectors of cytokines and inflammatory mediators. *Neuroscientist* 2013; epub ahead of print.
32. Chor V, Charpentier TL, Lebon S, et al. Characterization of phenotype markers and neuronotoxic potential of polarized primary microglia in vitro. *Brain Behav Immun* 2013;32:70-85.

33. Czeh M, Gressens P, Kaindl AM. The Yin and Yang of microglia. *Dev Neurosci* 2011;33:199-209.
34. Neumann J, Gunzer M, Gutzeit HO, et al. Microglia provide neuroprotection after ischemia. *FASEB J* 2006;20:714-720.
35. Wake H, Moorhouse AJ, Miyamoto A, et al. Microglia: actively surveying and shaping neuronal circuit structure and function. *Trends Neurosci* 2013;36:209-217.
36. Kokaia Z, Martino G, Schwartz M, et al. Cross-talk between neural stem cells and immune cells: the key to better brain repair? *Nat Rev Neurosci* 2012;15:1078-1087.
37. Yuan TF. BDNF signaling during olfactory bulb neurogenesis. *J Neurosci* 2008;28:5139-5140.



Chapter 5

Intranasal administration of human MSC for ischemic brain injury in the mouse: In vitro and in vivo neuroregenerative functions

Vanessa Donega¹, Cora H. Nijboer¹, Luca Braccioli¹, Ineke Slaper-Cortenbach², Annemieke Kavelaars³, Frank van Bel⁴ and Cobi J. Heijnen^{1,3}

¹Lab. of Neuroimmunology and Developmental Origins of Disease, University Medical Center Utrecht, Utrecht, The Netherlands, ²Cell Therapy Facility, Dept. of Clinical Pharmacy, University Medical Center Utrecht, ³Dept. of Symptom Research, MD Anderson Cancer Center, Houston TX, USA, ⁴Dept. of Neonatology, University Medical Center Utrecht.

submitted to Plos One

Abstract

Intranasal treatment with C57BL/6 MSCs reduces lesion volume and improves motor and cognitive behavior in the neonatal hypoxic-ischemic (HI) mouse model. In this study, we investigated the potential of human MSCs (hMSCs) to treat HI brain injury in the neonatal mouse. Assessing the regenerative capacity of hMSCs is crucial for translation of our knowledge to the clinic. We determined the neuroregenerative potential of hMSCs *in vitro* and *in vivo* by intranasal administration 10 days following HI in neonatal mice.

HI was induced in P9 mouse pups. 1×10^6 or 2×10^6 hMSCs were administered intranasally 10 days after HI. Motor behavior and lesion volume were measured 28 days following HI. The *in vitro* capacity of hMSCs to induce differentiation of mouse neural stem cell (mNSC) was determined using a transwell co-culture differentiation assay. To determine which chemotactic factors may play a role in mediating migration of MSCs to the lesion, we performed a PCR array on 84 chemotactic factors 10 days following sham-operation, and at 10 and 17 days after HI.

Our results show that 2×10^6 hMSCs decrease lesion volume, improve motor behavior, and reduce scar formation and microglia activity. Moreover, we demonstrate that the differentiation assay reflects the neuroregenerative potential of hMSCs *in vivo*, as hMSCs induce mNSCs to differentiate into neurons *in vitro*. We also provide evidence that the chemotactic factor CXCL10 may play an important role in hMSC migration to the lesion site. This is suggested by our finding that CXCL10 is significantly upregulated at 10 days following HI, but not at 17 days after HI, a time when MSCs no longer reach the lesion when given intranasally. The results described in this work also tempt us to contemplate hMSCs not only as a potential treatment option for neonatal encephalopathy, but also for a plethora of degenerative and traumatic injuries of the nervous system.

Introduction

Neonatal encephalopathy due to perinatal hypoxia-ischemia (HI) is an important cause of mortality and long-term neurological deficits such as cerebral palsy, seizures and mental retardation in babies born at term¹⁻⁵. However, therapeutic strategies for neonatal encephalopathy remain scarce. Hence, developing new treatment options for the newborn infant that effectively prevent or diminish the development of encephalopathy is of pivotal importance.

Bone marrow-derived mesenchymal stem/stromal cells (MSCs) have been shown to promote tissue repair in various disease models ranging from cardiovascular⁶ to graft-versus-host disease⁷. MSCs are valuable as a therapeutic tool as they are hardly immunogenic due to a lack of MHC class II expression and co-stimulatory proteins (*e.g.* CD80, CD86 and CD40)^{8,9}. Therefore, several clinical trials are currently investigating the efficacy and safety of MSCs as a treatment option for various pathologies¹⁰.

We have previously shown in a mouse model of neonatal HI brain damage that intranasal administration of *murine* MSCs significantly improves motor and cognitive behavior and reduces cerebral lesion volume¹¹. In contrast to current pharmacological therapies for neonatal HI¹², we found that MSC treatment has a long therapeutic window of 10 days after the insult. Studies from our group and others have shown that intracranial and intravenous injection of murine MSCs actively promote proliferation and differentiation of neuronal and glial precursor cells as well as axonal regeneration¹³⁻¹⁷. Moreover, MSCs have been shown to exert strong anti-inflammatory properties and to modulate immune responses, for example by suppressing the proliferation of T cells and B cells in various disease models such as graft-versus-host disease^{7,18}.

Before MSCs can be used in the clinic for the treatment of neonatal brain damage, the neuroregenerative potential of *human* MSCs (hMSCs) has to be determined. A few studies in the adult rodent MCAO model for stroke have investigated the efficacy of hMSCs to repair stroke induced brain lesion and behavioral deficits, but none have studied the effects of hMSCs on neonatal encephalopathy¹⁹⁻²¹. The results from these studies show that hMSCs improve motor behavior, decrease lesion size and enhance angiogenesis. In our study, we used an *in vitro* assay to assess the capacity of hMSCs to induce mouse neural stem cell (mNSC) to differentiate towards neuronal and glial cell fates. Moreover, we determined *in vivo* whether hMSCs are able to migrate towards

the injury site in our mouse model of neonatal HI brain injury and which chemotactic factors may mediate MSC migration to the lesion. Most importantly, we investigated whether treatment with hMSCs improves motor behavior and decreases lesion size and gliosis following HI injury in the neonatal mice.

Material and Methods

Ethics statement, hMSCs isolation, culture and characterization

MSCs are classified as Advanced Therapy Medicinal Products and expanded in the GMP-accredited Cell Therapy Facility of the UMC Utrecht. Bone marrow from healthy donors is harvested for the expansion of MSCs as approved by the Dutch Central Committee on Research Involving Human Subjects (CCMO) (Biobanking bone marrow for MSC expansion, NL41015.041.12). Either the bone marrow donor or the parent or legal guardian of the donor signed the informed consent approved by the CCMO. The MSCs are isolated from the bone marrow by plastic adherence and expanded using platelet lysate. Optimal MSC expansion is achieved using human platelet lysate as substitute for fetal bovine serum in alpha-MEM (Macopharma, Utrecht, The Netherlands)²². Briefly, mononuclear cells from bone marrow are isolated using a density separation method. Isolation and expansion of MSCs is done by plastic adherence using 2-layer CellStacks in combination with Macopharma seeding sets, medium exchange sets and harvesting sets. MSCs are harvested using TripLE and Passage 3 MSCs are cryopreserved in bags in Physiological Salt solution containing human serum albumin and 10% DMSO for clinical trials. The bags are stored in the vapour phase of liquid nitrogen. After thawing, \pm 95% of the hMSCs are alive and positive for CD73, CD90 and CD105 and contain less than 0.1% CD-45 positive cells. Thus the hMSCs used in this study are in agreement with the release criteria described by the International Society for Cellular Therapy being >70% of the MSCs are CD73, CD90 and CD105 positive and contain <10% CD45-positive cells and <1% T cells^{23,24} (Supplemental Figure 1). Furthermore, the MSCs are sterile (negative for bacteria, yeast, funghi, mycoplasma (<10CFU) and endotoxin (<5EU/kg/hr)).

Ethics statement, HI induction and intranasal MSC administration

Experiments were performed according to the Dutch and European international guidelines (Directive 86/609, ETS 123, Annex II) and approved by the Experimental Animal Committee Utrecht (University Utrecht, Utrecht, Netherlands). All efforts were made to minimize suffering.

An unilateral HI lesion was induced in 9 day old C57BL/6 mouse pups (Harlan Laboratories, Boxmeer, The Netherlands) under isoflurane anesthesia, by permanent occlusion of the right common carotid artery followed by hypoxia for 45 min at 10% oxygen. Control sham-operated mouse pups underwent anesthesia and incision only. The HI procedure resulted in a mortality rate of 10%. Pups from 11 litters were randomly assigned to the different experimental groups. Analyses were performed in a blinded set-up. At 10 days after HI, either 1×10^6 or 2×10^6 human MSCs (Passage 3) or PBS (Vehicle treatment) was administered intranasally. 3 μ L of hyaluronidase in PBS (100 U, Sigma-Aldrich, St. Louis, MO) was administered twice to each nostril to increase the permeability of the nasal mucosa. Thirty minutes later animals received 3 μ L twice to each nostril with a total volume of 12 μ L.

In vitro proliferation assay and differentiation assay

Cell proliferation was determined with a ^3H -thymidine incorporation assay (Perkin Elmer, Waltham, USA). MSCs were plated in a 96 wells-plate at a concentration of 1000 cells per well. 25 μ L of ^3H -thymidine (5mCi (185MBq)) was added to the wells at 0, 24, 48 and 96h after plating. Time-point 0h (T0) was designated as 4h after plating, allowing the MSCs to attach to the plate. Incorporated ^3H -thymidine was measured 16h later with a micro beta-plate counter (Perkin Elmer).

For the (non-contact) transwell co-culture differentiation assay^{25,26}, 80.000 hMSCs were embedded in 0.2% HydroMatrix gel (Sigma-Aldrich) and cultured in transwell inserts for 48h (Millipore, Amsterdam, The Netherlands) in alpha-MEM with human platelet lysate supplement. 24 wells-plates were coated with 10 μ g/mL Poly-L-Ornithine and 5 μ g/mL Laminin (both Sigma-Aldrich) before plating mouse cortical neural stem cells (mNSC) (R&D systems, Minneapolis, USA) at a concentration of 25.000 cells per well in DMEM:F12 + B27 medium (Life Technologies). 20 ng/mL of human recombinant EGF (Peprotech, Rocky Hill, NJ, USA) and 20 ng/mL of mouse b-FGF (Peprotech) was added to the mNSCs cultures daily for the following 2 days. 48h after plating the mNSCs, co-culture was started by transferring the inserts containing

hMSCs (in HydroMatrix gel) into the 24-wells plates with mNSCs. The assay was stopped by fixing the mNSCs with 4% paraformaldehyde (PFA) at T0 (unstimulated mNSCs) and at T96 after starting co-culture with hMSCs. Differentiation of the mNSCs was assessed by immunocytochemistry.

Immunocytochemistry

Briefly, PFA-fixed mNSCs from the co-culture assay were blocked with 5% BSA and 0.1% saponin for 30 min followed by incubation for 1h at room temperature with primary antibodies: mouse anti-nestin (1:200) (BD Biosciences, Breda, The Netherlands), rabbit anti-Olig2 (1:400) (Millipore), mouse anti-GFAP (1:100) (Acris antibodies, Herford, Germany) or rabbit-anti β III-Tubulin (1:1000) (Abcam antibodies, Cambridge, UK). Secondary antibodies goat anti-mouse AF488 or goat anti-rabbit AF594 (Invitrogen, Paisley, UK) were incubated for one hour at room temperature. Nuclei were counterstained with 4'-6-diamidino-2-phenylindole (DAPI; Invitrogen) and mounted with FluoroSave reagent (Calbiochem, Nottingham, UK). Fluorescent images were taken with an AxioCam MRm (Carl Zeiss, Sliedrecht, The Netherlands) on an Axio Observer Microscope with Axiovision Rel 4.6 software (Carl Zeiss).

MSC tracking

1×10^6 hMSCs were labeled with PKH-26 Red fluorescent cell linker kit (Sigma-Aldrich) and administered intranasally to mouse pups at 10 days after induction of HI. 24h later, mice were perfused intracardially with PBS followed by 4% PFA. Fixed brains were cryoprotected in a sucrose gradient (15% followed by 30% overnight) and embedded in OCT compound (VWR BDH Prolab, Boxmeer, The Netherlands). Coronal cryosections (8 μ m) were stained with DAPI (Invitrogen) for nuclei counterstaining. Fluorescent images were captured using an EMCCD camera (Leica Microsystems, Benelux) and Softworx software (Applied Precision, Washington, USA).

Gene expression profiling

Real-time PCR analysis was done on pooled samples from 10 HI mouse pups and 6 sham-operated mouse pups on the RT² Profiler PCR array (PAMM-022, SABiosciences, Venlo, Netherlands). A standard brain region was isolated at 10 and 17 days following HI induction or sham-operation by dissecting the ipsilateral hemisphere at bregma and 2 mm from bregma on ice and pulverizing on liquid nitrogen. Total RNA was

isolated by TRIzol according to the manufacturer's instructions (Invitrogen). The amount of RNA was measured by spectrophotometry at 260 nm. The RNA quality was determined with the OD 260/280 ratio, which was between 1,9 and 2,1. To confirm that there was no RNA degradation, all samples were run on a 1% agarose gel. cDNA was synthesized with SuperScript Reverse Transcriptase (Invitrogen). Expression of 84 genes was measured according to the producer's guidelines by using the RT² Real-Time SYBR green PCR master Mix (SABiosciences) on the Bio-rad IQ5 (Thermo Scientific, Waltham, MA, USA). Data was normalized for the expression of GAPDH and actin. Analysis was done with the PCR Array Data Analysis Software (SABiosciences). Two separate comparisons were made, *i.e.* the sham-operated group was compared to the 10 days after HI group and the 10 days after HI group was compared to the 17 days after HI group. Changes in gene expression were determined as significant by an arbitrary cut-off of > 2-fold. The PCR array results were validated by quantitative reverse transcription (qRT)-PCR analysis on individual samples and pooled samples.

MSCs co-culture with brain extracts

10 days after HI-surgery, mice were euthanized by pentobarbital overdose, decapitated and brains were removed. The ipsilateral hemisphere was dissected on ice at 0 mm to 2 mm from bregma and was subsequently pulverized on liquid nitrogen. Dissected brains were dissolved in KO-DMEM medium (Gibco Life Technologies) at a final concentration of 150 mg/mL and centrifuged for 10 min at 3000g at 4°C. Supernatants were collected as 'brain extract' and protein concentration was measured using a protein assay with BSA as a standard on a Multiskan GO (Thermo Scientific). hMSCs were cultured at a concentration of 40.000 cells per well in a 24 wells-plate for 24h before replacing the medium with knock-out medium with either 1 mg/mL HI brain extract or without extract. After 72h of culture with brain extracts, hMSCs were lysed for RNA isolation.

RNA isolation and qPCR

Total RNA was isolated with the RNAmuni kit according to the manufacturer's instructions (Invitrogen). The amount of RNA was measured with the nanodrop 2000 (Thermo Scientific). RNA quality was determined with the OD 260/280 ratio, which was between 1,9 and 2,1. cDNA was synthesized with SuperScript Reverse Transcriptase (Invitrogen). The expression of CXCR3 gene was measured by

quantitative reverse transcription (qRT)-PCR (Biorad IQ5) analysis on individual samples. Data was normalized for the expression of GAPDH and β -actin.

Sensorimotor function

Unilateral sensorimotor impairments were measured in the cylinder rearing test (CRT). Mice were placed in a transparent cylinder and the weight-bearing paw (left (impaired), right (unimpaired) or both) contacting the cylinder wall during full rear was scored. Paw preference was calculated as $((\text{right} - \text{left}) / (\text{right} + \text{left} + \text{both})) \times 100\%$.

Histology

Coronal paraffin sections (8 μm) of paraformaldehyde (PFA)-fixed brains were incubated with mouse-anti-myelin basic protein (MBP) (Sternberger Monoclonals, Lutherville, MD) or mouse-anti-microtubule-associated protein 2 (MAP2) (Sigma-Aldrich) followed by biotinylated horse-anti-mouse antibody (Vector Laboratories, Burlingame, CA). Binding was visualized with Vectastain ABC kit (Vector Laboratories) and diaminobenzamide. Ipsilateral MAP2 and MBP area loss was determined on sections corresponding to -1.85 mm from bregma in adult mouse brain. MBP and MAP2 staining were quantified using ImageJ software (<http://rsb.info.nih.gov/ij/>) and Adobe Photoshop CS5, respectively.

Immunofluorescence

Coronal paraffin sections (8 μm) were blocked with 2% BSA and 0.1% saponin, incubated for 2h with primary antibodies rabbit anti-Iba1 (1:200) (Wako Chemicals, Osaka, Japan) and mouse anti-GFAP (1:100) (Acris antibodies) followed by incubation with secondary antibodies goat anti-rabbit AF594 and goat anti-mouse AF488 (both Invitrogen). Nuclei were counterstained with DAPI (Invitrogen) and mounted with FluoroSave reagent (Calbiochem). Fluorescent images were captured with an AxioCam MRm (Carl Zeiss, Sliedrecht, The Netherlands) on an Axio Observer Microscope with Axiovision Rel 4.6 (Carl Zeiss).

Statistical analysis

Quantification of the differentiation assay, and GFAP and Iba-1 staining was done by measuring pixel intensity with ImageJ software (<http://rsb.info.nih.gov/ij/>). Analysis

was performed blind to treatment groups to avoid bias. Similar thresholds were used for all treatment groups. The mean of all signal intensities from all individual pictures per sample were combined and this number was entered in the graph. For the GFAP and Iba-1 staining, we quantified one section per animal and 10 regions of interest with a 20x magnification. 7 cortical regions (3 fields in the motor cortex and 4 fields in the somatosensory cortex) were quantified. Of these 7 regions: 3 regions were just adjacent to the lesion border, in sham operated animals just above the corpus callosum (Cortical layer 6), 2 in the upper layers of the motor cortex and 2 in Layer 4 of the cortex. We also quantified 3 ROI's in the thalamic regions of the brain bordering the lesion cavity or the hippocampal structure in sham operated animals. We ensured consistency across animals by maintaining recognizable regions in the brain as landmarks. Examples of such landmarks are Layer 4 in the cortex and the corpus callosum for the vertical line and the size and structure of the hippocampus and corpus callosum for the horizontal line. Data are presented as mean \pm SEM. Statistical significance was determined by using one-way ANOVA followed by Bonferroni post-hoc tests. For the differentiation assay, statistical significance was assessed by Two-tailed unpaired T-test. $p < 0.05$ was considered statistically significant.

Results

Pre-treatment characterization of human MSCs

Before intranasal administration of hMSCs, we assessed expression of stem cell markers by the hMSCs. MSCs expressed CD73, CD90 and CD105 and contained less than 10% CD45 positive cells as confirmed by FACS analysis (data not shown). We also show that hMSCs are capable of proliferating *in vitro* (Fig 1A).

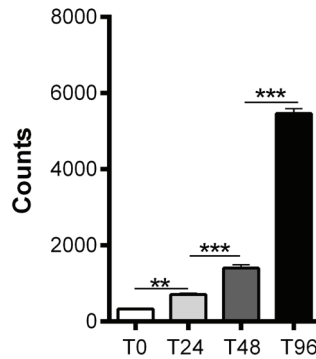


Figure 1. *In vitro* proliferation of hMSCs. Proliferating capacity of hMSCs *in vitro*. 1000 hMSCs were plated (T0) and proliferation was assessed at 4(T0), 24(T24), 48(T48) and 96(T96) hours after plating the MSCs by adding ^3H -thymidine to the culture and measuring ^3H -thymidine uptake 16h later. Data represent mean \pm SEM. ** $p < 0.01$; *** $p < 0.001$ by ANOVA and Bonferroni post-hoc test. (n=10 wells for each condition)

Human MSCs induce mouse NSCs to differentiate in vitro

To investigate the effect of hMSCs on murine neurogenesis, mouse neural stem cells (mNSCs) were co-cultured with hMSCs in a non-contact transwell assay. This assay assesses whether hMSCs can induce murine neurogenesis and whether MSCs can do so in a paracrine way. hMSCs were placed in a transwell insert on top of adherent mNSCs in a 24 wells-plate and co-cultured for 96h. Markers for nestin, Olig2, GFAP and $\beta\text{III-Tubulin}$ were used for cell fate determination. Our results show that the number of nestin⁺ cells, as a marker for undifferentiated stem cells, increased after co-culture with hMSCs (Fig 2A, E). Expression of the oligodendrocyte-progenitor marker Olig2 decreased after co-culture with hMSCs (Fig 2B, E). Figure 2C shows that hMSCs were capable of inducing mNSC differentiation towards neuronal (*i.e.* $\beta\text{III-Tubulin}$ positive) cell fate (Fig 2C, E). Moreover, our data show that hMSCs also induce mNSC differentiation into GFAP⁺/astrocytic cell fate (Fig 2D, E).

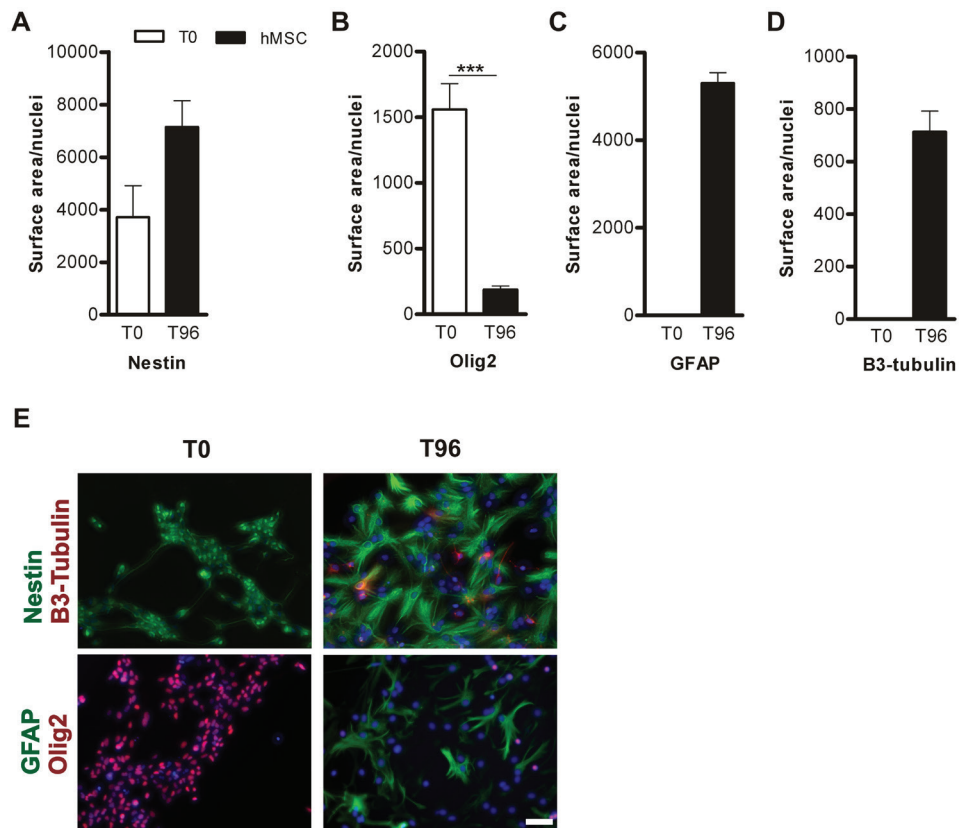


Figure 2. hMSCs induce differentiation of mouse NSCs *in vitro*. *In vitro* mNSC transwell differentiation assay in co-culture with hMSCs. mNSCs were fixed at 4 (T0) and 96 (T96) hours after co-culture with hMSCs and stained for (A) nestin (green), (B) Olig2 (red), (C) GFAP (green) and (D) β III-Tubulin (red). Data represent mean \pm SEM. *** $p < 0.001$ by Unpaired two-tailed T-test. Scale bar = 100 μ m. (n=4 wells per condition)

hMSCs migrate towards the HI-induced cerebral lesion site

In a previous study we showed that PKH-26-labeled C57BL/6 MSCs migrate specifically towards the HI damaged brain region within 24h after intranasal administration¹¹. We demonstrated that the PKH-26⁺ signal is specific and not due to auto-fluorescence of damaged tissue as we did not see any positive signal in the HI-damaged brain after Vehicle treatment. As we are applying human MSCs to the mouse brain, we first established if intranasal delivery is an efficient administration route before investigating the therapeutic potential of hMSCs *in vivo*. We administered 1×10^6 PKH-26-labeled hMSCs intranasally at 10 days after HI and sacrificed the mice 24h later.

At 10 days after HI, *i.e.* the time-point when hMSCs are administered intranasally, the entire hippocampus and part of the cortex had degenerated and an evident cyst could be discerned in the ipsilateral hemisphere. 24h after hMSC administration we observed a strong PKH-26⁺ signal, *i.e.* hMSCs, in the sensorimotor and epithalamic regions of the damaged brain, surrounding the cyst (Fig 3A). We did not detect any PKH-26⁺ signal in the contralateral hemisphere (Fig 3B).

We have previously shown that *mouse* MSCs no longer reach the lesion site when given at 17 days after HI¹¹. Therefore, we investigated which chemotactic factors may be involved in regulating MSC migration towards the lesion, by comparing the expression profile of chemotactic factors at the lesion site from 17 days after HI with 10 days after the insult. First, we analyzed the chemokine profile induced by HI by comparing the gene expression profiles from HI mice to sham-operated mice at 10 days following the insult. To this end a 2mm region from -2 bregma at the ipsilateral hemisphere was dissected and the expression of 84 chemotactic factors was analyzed by PCR array using an arbitrary cut off of > 2.00 fold change (Table 1). We validated the results from the PCR array by qPCR, which confirmed that the factors Ccl4, Ccl5, Cxcl10 and Itgb-2 were significantly upregulated at 10 days following HI (Fig 3C). Next we compared the gene expression profile of 84 chemotactic factors at the lesion site at 10 and 17 days following HI (Table 2). Validation of the PCR array results on individual samples by qPCR analysis confirmed that the expression of the chemokines Ccl5 and Cxcl10 were significantly down-regulated at 17 days in comparison to 10 days after HI. The expression of Ccl4 and Itgb-2 did not change significantly at 17 days (Fig 3C).

To determine whether CXCL10 may be involved in mediating the migration of hMSCs towards the lesion, we performed a qPCR to assess whether hMSCs *in vitro* express CXCR3, the receptor for CXCL10. Our qPCR results show that hMSCs express CXCR3, without co-culturing the cells with HI brain extract. Interestingly, following 72h of co-culture with brain extracts from 10 days after HI we observed an increase in CXCR3 mRNA expression.

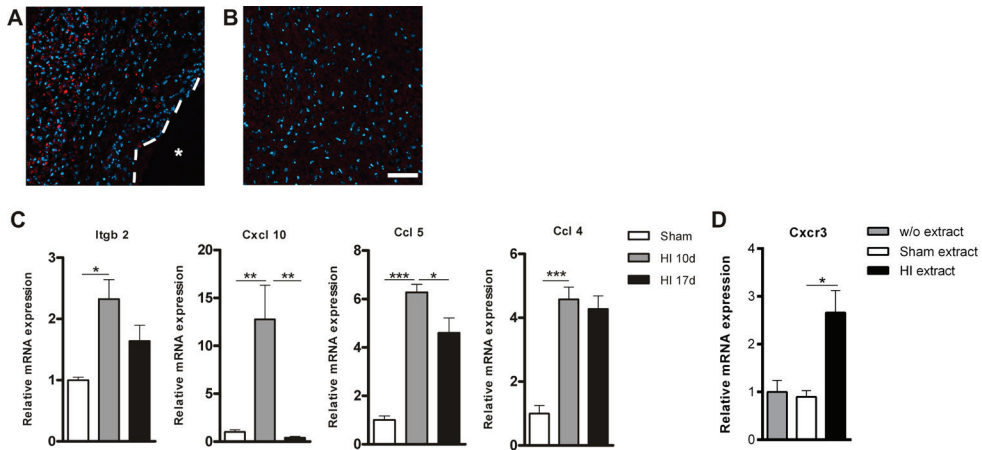


Figure 3. PKH-26 labeled hMSCs migrate to the lesion site. 1×10^6 hMSCs were labeled with PKH-26 and administered intranasally at 10 days after HI. (A+B) Mice were terminated 24h following hMSC treatment. (A) PKH-26⁺ hMSCs in the ipsilateral damaged cortex. (B) Contralateral cortex shows no PKH-26⁺ signal. (C) qPCR validation of PCR array confirmed the upregulation of five genes 10 days after HI. At 17 days after HI 2 genes were down-regulated in comparison to 10 days following HI. (HI n=10; sham n=6). (D) hMSCs express CXCR3, which increases after co-culture with HI brain extract (n=2). Data represent mean \pm S.E.M. *p<0.05; **p<0.01; ***p<0.001 by ANOVA and Bonferroni post-hoc test. Dashed line = lesion border; Asterisk = lesion site. Blue = Dapi staining. Scale bar = 50 μ m.

Intranasal hMSC treatment improves sensorimotor outcome and lesion volume after HI

Next, we investigated whether hMSCs were also capable of improving sensorimotor behavior and decreasing lesion size in HI mice *in vivo*. To assess motor function we used the cylinder rearing test that measures the preference to use the unimpaired forepaw. We treated mouse pups at 10 days after HI with 1×10^6 or 2×10^6 hMSC or Vehicle treatment. Our results show that both doses of hMSCs significantly improved sensorimotor function at 21 (data not shown) and 28 days after HI as measured in the cylinder rearing test (Fig 4A).

Next we analyzed loss of MAP2 and MBP staining as measures for gray and white matter damage, respectively. Treatment with 2×10^6 hMSCs substantially decreased MAP2 loss (Fig 4B, D) and MBP loss (Fig 4C, E) at 28 days after HI. Treatment with the lower dose of 1×10^6 hMSCs was not sufficient to significantly reduce either gray (Fig 4B, D) or white matter injury (Fig 4C, E).

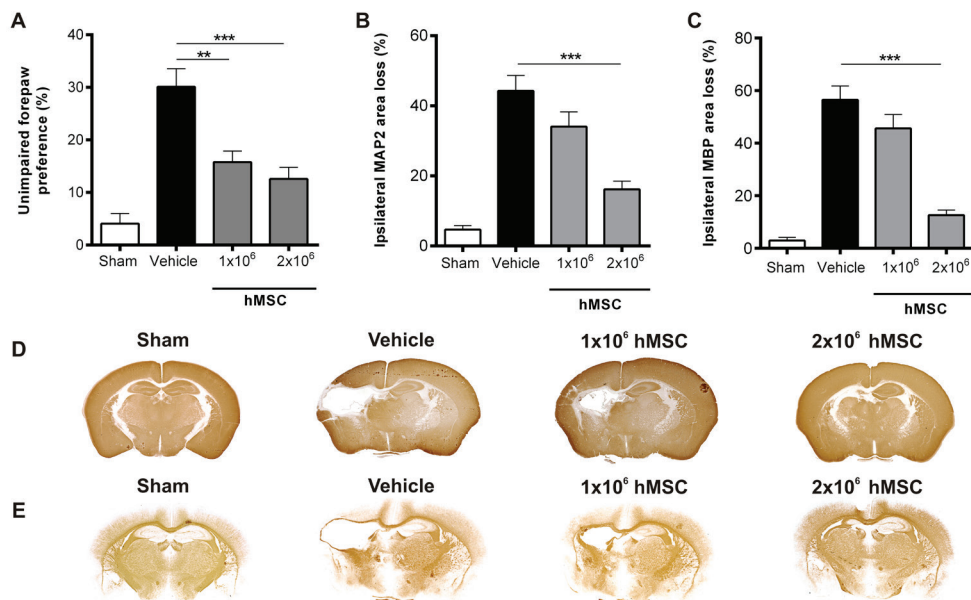


Figure 4. Dose effect of hMSC on motor performance and lesion volume. Mice were treated intranasally with either 1×10^6 or 2×10^6 hMSCs or Vehicle at 10 days after HI. (A) Preference to use the unimpaired forepaw in the cylinder rearing test (CRT) was assessed at 28 days after HI. Sham-operated littermates (Sham) were used as controls. (B-C) Quantification of ipsilateral MAP2 (B) and MBP (C) area loss measured as 1- (ipsi-/contralateral MAP2- or MBP-positive area) at 28 days after HI. Representative sections of MAP2 (D) and MBP (E) staining. Data represent mean \pm SEM. ** $p < 0.01$; *** $p < 0.001$ by ANOVA and Bonferroni post-hoc test. Sham $n=13$; Vehicle $n=21$; 1×10^6 hMSC $n=11$; 2×10^6 hMSC $n=12$. Data presented in this figure are results from pups pooled out of 11 different litters. Treatment groups were randomly distributed between litters.

GFAP and Iba-1 expression following hMSC treatment

To assess whether treatment with hMSCs reduced scar formation in the long-term, we stained brain sections at 28 days after HI for astrocytes and microglia with the markers GFAP and Iba-1, respectively. We analyzed 10 regions in the brain as depicted in figure 5A. Following HI, a long-lasting upregulation of GFAP⁺ and Iba-1⁺ signal in the region adjacent to the cystic lesion can be discerned (Fig 5B, C, E). Treatment with either 1 or 2×10^6 hMSCs decreased Iba-1 expression to sham level (Fig 5B, F, G). Furthermore, the highest dose of 2×10^6 hMSCs also significantly reduced GFAP expression to sham level (Fig 5B, C, G), whereas the lower dose of 1×10^6 hMSCs had no effect on GFAP expression (Fig 5C, F).

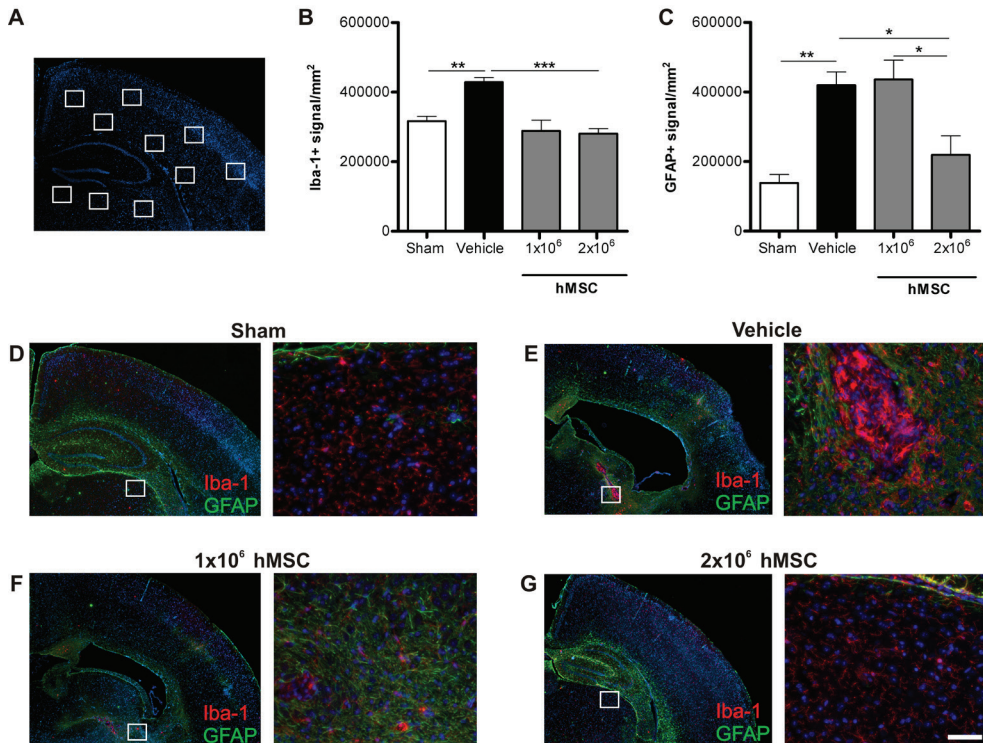


Figure 5. hMSCs reduce the activation of glial cells at 28 days after HI. Mice were treated with either 1×10^6 or 2×10^6 hMSCs or Vehicle intranasally at 10 days following HI. Mice were sacrificed 28 days after HI. (A) Schematic overview of fields quantified. (B) Quantification of Iba-1⁺ signal/mm² or (C) GFAP⁺ signal/mm². (D-G) Representative sections of Iba-1 (red) and GFAP (green) expression after sham-operation (D), Vehicle (E), 1×10^6 hMSCs (F) or 2×10^6 hMSCs (G). Sections are counterstained with DAPI (blue). Scale bar = 100 μ m. Data represent mean \pm SEM. * $p < 0.05$; ** $p < 0.01$; *** $p < 0.001$ by ANOVA and Bonferroni post-hoc test. (Sham and Vehicle $n=4$; 1×10^6 and 2×10^6 MSC $n=3$)

Discussion

Our study shows that *human* MSCs have the capacity to promote neuroregeneration. This finding is reflected by our results showing that intranasal administration of hMSCs significantly improves motor behavior, and decreases lesion size and scar formation at 28 days after HI brain damage in neonatal mice. Furthermore, our *in vitro* results demonstrate that *human* MSCs are capable of inducing mNCSs to differentiate towards astrocytic and neuronal cell fate. This suggests that hMSCs do not need cell to

cell contact with neural stem cells, but rather promote endogenous neurogenesis and lesion repair by the secretion of neurotrophic factors. We also show that hMSCs reach the damaged brain region in the mouse within 24h after intranasal administration. Importantly, our work also provides new insight into the chemotactic factors that may regulate MSC migration towards the lesion site. Our results show that the chemokine CXCL10 is strongly upregulated at 10 days following HI.

We have previously shown that intranasal treatment with both 0.5×10^6 and 1×10^6 murine MSCs decreased HI lesion volume substantially by 53% and 71%, respectively¹¹ and improved motor behavior by 47%. In the present work we demonstrate that hMSCs decrease gray and white matter lesion volume with respectively 63% and 78% and improve motor behavior by 58%. Our present work indicates that, provided that the optimal dose is used, hMSCs can be as effective as mouse MSCs and have a remarkable effect on both motor behavior and cerebral lesion size after HI (Fig 4). These positive effects may result from increased neurogenesis as we observed that hMSCs have the capacity to induce mNSCs to differentiate into neurons *in vitro*. We also observed that hMSCs repair white matter structures, since MBP expression increases significantly at 28 days after HI (*i.e.* 18 days after MSC treatment). Although, the results of our *in vitro* differentiation assay did not show differentiation into oligodendrocyte lineage, unpublished work from our group, shows that *in vitro* Olig2 expression increases when MSCs are genetically engineered to promote differentiation towards the oligodendrocyte lineage. These findings are in line with previous studies showing that neuronal cell differentiation requires downregulation of oligodendrocyte transcription factor 2 (Olig2), as this is a strong inhibitor of neurogenesis *in vitro* and *in vivo*^{27,28}.

Recent work from our group on the development of the brain lesion following neonatal HI demonstrates that at 10 days after HI the lesion is fully developed and does not deteriorate any further (unpublished results). MAP2 and HE staining showed that the hippocampus degenerates resulting in a cystic lesion in the ipsilateral hemisphere. These data illustrate that MSCs given 10 days after HI will act by neuroregenerative processes leading to repair of the lesion and not neuroprotection, *i.e.* the prevention of cell death (unpublished results). Furthermore, recent work from our group shows that intranasal MSC administration leads to a significant increase in GFAP/nestin-

and DCX-positive precursor cells, which further supports our hypothesis that MSCs operate via regenerative pathways (unpublished results).

Interestingly, the lower dose of hMSCs, which did not have an effect on lesion volume, only decreased microglia activation and had no effect on astrocyte activation. Moreover, the lower dose of hMSC (1×10^6) improved motor behavior, but did not decrease gray or white matter loss. In a previous study by Lee JA *et al.*,²⁹ hMSCs were administered intracardially 3 days after HI induction in the neonatal rat without any positive effect on lesion size. However, in contrast to our study, the authors only tested one dose of hMSCs *i.e.* 1×10^6 , which also had no effect in our study. Furthermore, the intracardial administration route may be a less efficient delivery method than the intranasal route, as systemic delivery may result in a smaller number of hMSCs homing to the injured brain. There are other studies on stem cell administration following HI injury, that describe restoration of behavior without significant decrease of lesion volume. One possible explanation is that downregulation of inflammation may restore motor neuron function and thus also motor behavior.

We observed that Vehicle-treated mice with extensive HI-induced cerebral cell loss also show substantial scar formation at 28 days after HI (*i.e.* 18 days after MSC treatment) (Fig 5). In contrast, mice that received hMSC treatment showed decreased lesion size, which is associated with decreased astrocyte and microglia activation. Reactive astrocytes contribute to a process called glial scar formation, which forms a physical and chemical barrier that prevents inflammation from spreading through the tissue, thus restricting the progression of the injury. However, a downside of scar formation is that it also inhibits growth cone motility, thereby impairing axon regeneration³⁰⁻³². This may be one of the reasons underlying impaired neurogenesis following a HI insult in the neonatal brain³³. Hence, our data suggest that hMSC-induced reduction in astrocyte activation is crucial for repair of the lesion after HI brain damage. The decrease in astrocyte and microglia activity may be mediated by anti-inflammatory cytokines secreted by the hMSCs. We and others have previously shown that MSCs secrete IL-10^{9,16}, which is known to suppress the pro-inflammatory phenotype of both microglia and astrocytes³⁴. Future studies should focus on the mechanisms underlying MSC-mediated reduction of astrocytic scar in brain lesions, which may be crucial in promoting a pro-neurogenic microenvironment that supports tissue repair.

Besides showing the potential of hMSCs to repair the HI injured brain, we also provide new insight into factors that may be involved in MSC migration from the nose to the injury site. Our results show that expression of the integrin beta 2 protein (Itgb-2) is upregulated at 10 days after HI. Itgb-2 together with the Intercellular Adhesion Molecule 1 (ICAM-1) mediates the migration of leukocytes along endothelial cells^{35,36} and may be involved in the migration of MSCs through blood vessels and regulate transmigration into the brain tissue. The results from the PCR array show that CXCL10 is the chemotactic factor with the highest fold change at 10 days following HI. Interestingly, at 17 days after HI, the expression level of this chemokine has returned to sham level (Fig 3C). We also show that the expression of the CXCL10 receptor, CXCR3, increases following co-culture of hMSCs with brain extract from 10 days after HI (Fig 3D). Together these results suggest that CXCL10 may play an important role in regulating homing of MSCs to the lesion site. We also found that Ccl5 significantly decreases at 17 days following HI, which also suggests a role for this chemokine in MSC homing to lesion. Hence, our data propose that Cxcl10 and Ccl5 secreted by astrocytes, microglia and neurons³⁷ at the lesion site attract MSCs to home at the lesion site.

Conclusions

To our knowledge this is the first study that shows the potent regenerative effects of intranasally administered *human* MSCs on HI brain damage in the neonatal mouse. Moreover, our results suggest that the decrease in glial scar formation induced by hMSCs is a crucial step in promoting neurogenesis. Finally, the efficiency of the intranasal delivery route was confirmed, as hMSCs migrate specifically towards the lesion site in the mouse brain. The results in this study strongly support the therapeutic potential of hMSCs for neonatal HI.

Acknowledgments

The authors are grateful to Dr. Mark Klein, Miss Karima Amarouchi, Miss Mirjam Maas, Miss Marcelle van Gelder and Mr. Kasper Westinga for technical assistance. This work was supported by EU-7 Neurobid (HEALTH-F2-2009-241778) from the European Union and Zon-MW Project (no 116002003).

Table 1. Down- or upregulated genes at 10 days after HI in comparison to sham-operated mice.

RefSeq	Symbol	Description	Fold Up- or Down-regulation
NM_001173550.1	C5ar1	Complement component 5a receptor 1	-3,39
NM_021609.3	Ccbp2	Chemokine binding protein 2	-1,19
NM_011329.3	Ccl1	Chemokine (C-C motif) ligand 1	-1,24
NM_011330.3	Ccl11	Chemokine (C-C motif) ligand 11	1,44
NM_011331.2	Ccl12	Chemokine (C-C motif) ligand 12	3,52
NM_011332.3	Ccl17	Chemokine (C-C motif) ligand 17	1,15
NM_011888.2	Ccl19	Chemokine (C-C motif) ligand 19	1,35
NM_011333.3	Ccl2	Chemokine (C-C motif) ligand 2	7,66
NM_001159738.1	Ccl20	Chemokine (C-C motif) ligand 20	1,87
NM_009137.2	Ccl22	Chemokine (C-C motif) ligand 22	1,22
NM_019577.4	Ccl24	Chemokine (C-C motif) ligand 24	-1,34
NM_009138.3	Ccl25	Chemokine (C-C motif) ligand 25	-1,34
NM_001013412.2	Ccl26	Chemokine (C-C motif) ligand 26	-1,99
NM_020279.3	Ccl28	Chemokine (C-C motif) ligand 28	1,08
NM_011337.2	Ccl3	Chemokine (C-C motif) ligand 3	3,78
NM_013652.2	Ccl4	Chemokine (C-C motif) ligand 4	3,40
NM_013653.3	Ccl5	Chemokine (C-C motif) ligand 5	4,98
NM_009139.3	Ccl6	Chemokine (C-C motif) ligand 6	2,09
NM_013654.3	Ccl7	Chemokine (C-C motif) ligand 7	4,37
NM_021443.3	Ccl8	Chemokine (C-C motif) ligand 8	1,81
NM_011338.2	Ccl9	Chemokine (C-C motif) ligand 9	1,17
NM_009912.4	Ccr1	Chemokine (C-C motif) receptor 1	1,21
NM_007721.4	Ccr10	Chemokine (C-C motif) receptor 10	-1,14
NM_007718.3	Ccr11	Chemokine (C-C motif) receptor 1-like 1	1,08
NM_009915.2	Ccr2	Chemokine (C-C motif) receptor 2	3,02
NM_009914.4	Ccr3	Chemokine (C-C motif) receptor 3	1,36
NM_009916.2	Ccr4	Chemokine (C-C motif) receptor 4	-4,15
NM_009917.5	Ccr5	Chemokine (C-C motif) receptor 5	1,31
NM_001190333.1	Ccr6	Chemokine (C-C motif) receptor 6	-1,56
NM_007719.2	Ccr7	Chemokine (C-C motif) receptor 7	1,49
NM_007720.2	Ccr8	Chemokine (C-C motif) receptor 8	-1,32
NM_001166625.1	Ccr9	Chemokine (C-C motif) receptor 9	1,19
NM_145700.2	Ccr11	Chemokine (C-C motif) receptor-like 1	1,17

Table 1. continued

RefSeq	Symbol	Description	Fold Up- or Down- regulation
NM_017466.4	Ccr12	Chemokine (C-C motif) receptor-like 2	1,28
NM_008153.3	Cmklr1	Chemokine-like receptor 1	1,29
NM_027022.4	Cmtm2a	CKLF-like MARVEL transmembrane domain containing 2A	1,54
NM_024217.3	Cmtm3	CKLF-like MARVEL transmembrane domain containing 3	1,20
NM_153582.5	Cmtm4	CKLF-like MARVEL transmembrane domain containing 4	-1,04
NM_026066.2	Cmtm5	CKLF-like MARVEL transmembrane domain containing 5	1,03
NM_026036.3	Cmtm6	CKLF-like MARVEL transmembrane domain containing 6	1,11
NM_009142.3	Cx3cl1	Chemokine (C-X3-C motif) ligand 1	-1,06
NM_009987.4	Cx3cr1	Chemokine (C-X3-C) receptor 1	1,19
NM_008176.3	Cxcl1	Chemokine (C-X-C motif) ligand 1	-1,34
NM_021274.2	Cxcl10	Chemokine (C-X-C motif) ligand 10	12,79
NM_019494.1	Cxcl11	Chemokine (C-X-C motif) ligand 11	1,91
NM_001012477.2	Cxcl12	Chemokine (C-X-C motif) ligand 12	-1,00
NM_018866.2	Cxcl13	Chemokine (C-X-C motif) ligand 13	2,42
NM_019568.2	Cxcl14	Chemokine (C-X-C motif) ligand 14	1,34
NM_011339.2	Cxcl15	Chemokine (C-X-C motif) ligand 15	-1,34
NM_023158.6	Cxcl16	Chemokine (C-X-C motif) ligand 16	2,09
NM_009140.2	Cxcl2	Chemokine (C-X-C motif) ligand 2	1,79
NM_203320.2	Cxcl3	Chemokine (C-X-C motif) ligand 3	1,17
NM_009141.2	Cxcl5	Chemokine (C-X-C motif) ligand 5	3,02
NM_008599.4	Cxcl9	Chemokine (C-X-C motif) ligand 9	-1,19
NM_178241.4	Cxcr1	Chemokine (C-X-C motif) receptor 1	-1,29
NM_009909.3	Cxcr2	Chemokine (C-X-C motif) receptor 2	1,22
NM_009910.2	Cxcr3	Chemokine (C-X-C motif) receptor 3	2,90
NM_009911.3	Cxcr4	Chemokine (C-X-C motif) receptor 4	2,12
NM_007551.2	Cxcr5	Chemokine (C-X-C motif) receptor 5	-1,59
NM_030712.4	Cxcr6	Chemokine (C-X-C motif) receptor 6	1,09
NM_001271607.1	Cxcr7	Chemokine (C-X-C motif) receptor 7	1,03
NM_010045.2	Darc	Duffy blood group, chemokine receptor	1,11
NM_013521.2	Fpr1	Formyl peptide receptor 1	-1,11
NM_001025381.2	Gpr17	G protein-coupled receptor 17	-1,15
NM_009909.3	Cxcr2	Chemokine (C-X-C motif) receptor 2	1,22

Table 1. continued

RefSeq	Symbol	Description	Fold Up- or Down- regulation
NM_009910.2	Cxcr3	Chemokine (C-X-C motif) receptor 3	2,90
NM_009911.3	Cxcr4	Chemokine (C-X-C motif) receptor 4	2,12
NM_007551.2	Cxcr5	Chemokine (C-X-C motif) receptor 5	-1,59
NM_030712.4	Cxcr6	Chemokine (C-X-C motif) receptor 6	1,09
NM_001271607.1	Cxcr7	Chemokine (C-X-C motif) receptor 7	1,03
NM_010045.2	Darc	Duffy blood group, chemokine receptor	1,11
NM_013521.2	Fpr1	Formyl peptide receptor 1	-1,11
NM_001025381.2	Gpr17	G protein-coupled receptor 17	-1,15
NM_010431.2	Hif1a	Hypoxia inducible factor 1, alpha subunit	1,03
NM_008337.3	Ifng	Interferon gamma	1,50
NM_010551.3	Il16	Interleukin 16	1,15
NM_008361.3	Il1b	Interleukin 1 beta	2,58
NM_021283.2	Il4	Interleukin 4	-1,37
NM_031168.1	Il6	Interleukin 6	1,19
NM_001082960.1	Itgam	Integrin, alpha M	1,52
NM_008404.4	Itgb2	Integrin beta 2	3,31
NM_001038663.1	Mapk1	Mitogen-activated protein kinase 1	-1,08
NM_001168508.1	Mapk14	Mitogen-activated protein kinase 14	-1,18
NM_019932.4	Pf4	Platelet factor 4	-1,07
NM_023785.2	Ppbp	Pro-platelet basic protein	-2,37
NM_178804.3	Slit2	Slit homolog 2 (Drosophila)	1,01
NM_011577.1	Tgfb1	Transforming growth factor, beta1	1,53
NM_011905.3	Tlr2	Toll-like receptor 2	2,96
NM_021297.2	Tlr4	Toll-like receptor 4	1,91
NM_013693.2	Tnf	Tumor necrosis factor	2,04
NM_138302.1	Tymp	Thymidine phosphorylase	-1,28
NM_008510.1	Xcl1	Chemokine (C motif) ligand 1	1,05
NM_011798.4	Xcr1	Chemokine (C motif) receptor 1	-1,18

Table 2. Down- or upregulated genes at 17 days after HI in comparison to 10 days after HI.

RefSeq	Symbol	Description	Fold Up- or Down-regulation
NM_001173550.1	C5ar1	Complement component 5a receptor 1	1,02
NM_021609.3	Ccbp2	Chemokine binding protein 2	1,33
NM_011329.3	Ccl1	Chemokine (C-C motif) ligand 1	1,01
NM_011330.3	Ccl11	Chemokine (C-C motif) ligand 11	-1,13
NM_011331.2	Ccl12	Chemokine (C-C motif) ligand 12	-4,73
NM_011332.3	Ccl17	Chemokine (C-C motif) ligand 17	-1,77
NM_011888.2	Ccl19	Chemokine (C-C motif) ligand 19	1,06
NM_011333.3	Ccl2	Chemokine (C-C motif) ligand 2	-2,18
NM_001159738.1	Ccl20	Chemokine (C-C motif) ligand 20	-1,16
NM_009137.2	Ccl22	Chemokine (C-C motif) ligand 22	-1,42
NM_019577.4	Ccl24	Chemokine (C-C motif) ligand 24	3,50
NM_009138.3	Ccl25	Chemokine (C-C motif) ligand 25	1,02
NM_001013412.2	Ccl26	Chemokine (C-C motif) ligand 26	1,69
NM_020279.3	Ccl28	Chemokine (C-C motif) ligand 28	2,31
NM_011337.2	Ccl3	Chemokine (C-C motif) ligand 3	-3,39
NM_013652.2	Ccl4	Chemokine (C-C motif) ligand 4	-2,40
NM_013653.3	Ccl5	Chemokine (C-C motif) ligand 5	-3,28
NM_009139.3	Ccl6	Chemokine (C-C motif) ligand 6	-1,91
NM_013654.3	Ccl7	Chemokine (C-C motif) ligand 7	-1,87
NM_021443.3	Ccl8	Chemokine (C-C motif) ligand 8	-1,34
NM_011338.2	Ccl9	Chemokine (C-C motif) ligand 9	1,05
NM_009912.4	Ccr1	Chemokine (C-C motif) receptor 1	-1,38
NM_007721.4	Ccr10	Chemokine (C-C motif) receptor 10	1,02
NM_007718.3	Ccr11	Chemokine (C-C motif) receptor 1-like	2,54
NM_009915.2	Ccr2	Chemokine (C-C motif) receptor 2	-1,92
NM_009914.4	Ccr3	Chemokine (C-C motif) receptor 3	1,07
NM_009916.2	Ccr4	Chemokine (C-C motif) receptor 4	-1,28
NM_009917.5	Ccr5	Chemokine (C-C motif) receptor 5	1,09
NM_001190333.1	Ccr6	Chemokine (C-C motif) receptor 6	1,67
NM_007719.2	Ccr7	Chemokine (C-C motif) receptor 7	-2,74
NM_007720.2	Ccr8	Chemokine (C-C motif) receptor 8	-1,12
NM_001166625.1	Ccr9	Chemokine (C-C motif) receptor 9	-1,03
NM_145700.2	Ccr11	Chemokine (C-C motif) receptor-like 1	1,06

Table 2. continued

RefSeq	Symbol	Description	Fold Up- or Down- regulation
NM_017466.4	Ccr12	Chemokine (C-C motif) receptor-like 2	-1,32
NM_008153.3	Cmklr1	Chemokine-like receptor 1	-1,32
NM_027022.4	Cmtm2a	CKLF-like MARVEL transmembrane domain containing 2A	-1,18
NM_024217.3	Cmtm3	CKLF-like MARVEL transmembrane domain containing 3	-1,48
NM_153582.5	Cmtm4	CKLF-like MARVEL transmembrane domain containing 4	1,09
NM_026066.2	Cmtm5	CKLF-like MARVEL transmembrane domain containing 5	1,15
NM_026036.3	Cmtm6	CKLF-like MARVEL transmembrane domain containing 6	-1,11
NM_009142.3	Cx3cl1	Chemokine (C-X3-C motif) ligand 1	1,10
NM_009987.4	Cx3cr1	Chemokine (C-X3-C) receptor 1	-1,16
NM_008176.3	Cxcl1	Chemokine (C-X-C motif) ligand 1	1,02
NM_021274.2	Cxcl10	Chemokine (C-X-C motif) ligand 10	-5,44
NM_019494.1	Cxcl11	Chemokine (C-X-C motif) ligand 11	-3,47
NM_001012477.2	Cxcl12	Chemokine (C-X-C motif) ligand 12	1,01
NM_018866.2	Cxcl13	Chemokine (C-X-C motif) ligand 13	-1,41
NM_019568.2	Cxcl14	Chemokine (C-X-C motif) ligand 14	1,03
NM_011339.2	Cxcl15	Chemokine (C-X-C motif) ligand 15	1,64
NM_023158.6	Cxcl16	Chemokine (C-X-C motif) ligand 16	-1,73
NM_009140.2	Cxcl2	Chemokine (C-X-C motif) ligand 2	-1,57
NM_203320.2	Cxcl3	Chemokine (C-X-C motif) ligand 3	-1,39
NM_009141.2	Cxcl5	Chemokine (C-X-C motif) ligand 5	1,48
NM_008599.4	Cxcl9	Chemokine (C-X-C motif) ligand 9	1,11
NM_178241.4	Cxcr1	Chemokine (C-X-C motif) receptor 1	1,71
NM_009909.3	Cxcr2	Chemokine (C-X-C motif) receptor 2	3,47
NM_009910.2	Cxcr3	Chemokine (C-X-C motif) receptor 3	-3,15
NM_009911.3	Cxcr4	Chemokine (C-X-C motif) receptor 4	-1,71
NM_007551.2	Cxcr5	Chemokine (C-X-C motif) receptor 5	1,21
NM_030712.4	Cxcr6	Chemokine (C-X-C motif) receptor 6	-1,02
NM_001271607.1	Cxcr7	Chemokine (C-X-C motif) receptor 7	-1,56
NM_010045.2	Darc	Duffy blood group, chemokine receptor	-1,07
NM_013521.2	Fpr1	Formyl peptide receptor 1	-1,07
NM_001025381.2	Gpr17	G protein-coupled receptor 17	-1,30
NM_010431.2	Hif1a	Hypoxia inducible factor 1, alpha subunit	-1,11

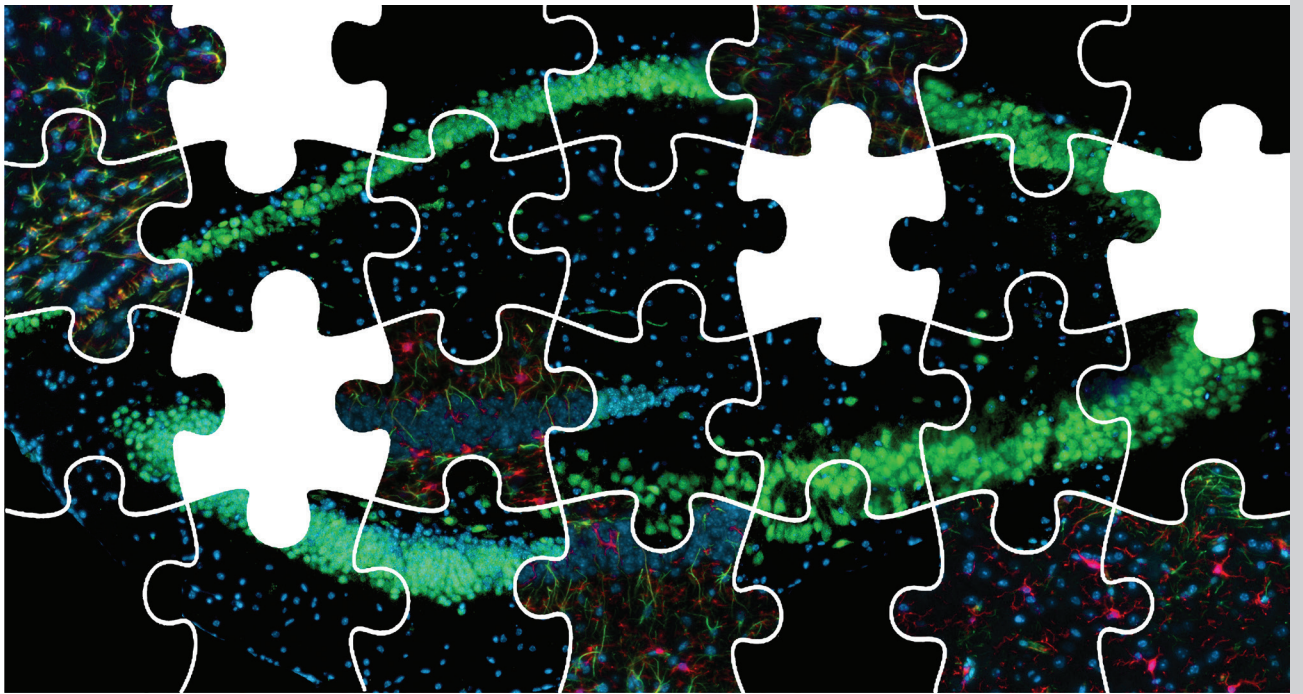
Table 2. continued

RefSeq	Symbol	Description	Fold Up- or Down- regulation
NM_008337.3	Ifng	Interferon gamma	-3,17
NM_010551.3	Il16	Interleukin 16	-1,16
NM_008361.3	Il1b	Interleukin 1 beta	-1,26
NM_021283.2	Il4	Interleukin 4	-1,05
NM_031168.1	Il6	Interleukin 6	1,11
NM_001082960.1	Itgam	Integrin, alpha M	-1,34
NM_008404.4	Itgb2	Integrin beta 2	-2,03
NM_001038663.1	Mapk1	Mitogen-activated protein kinase 1	-1,14
NM_001168508.1	Mapk14	Mitogen-activated protein kinase 14	1,22
NM_019932.4	Pf4	Platelet factor 4	-1,10
NM_023785.2	Ppbp	Pro-platelet basic protein	1,11
NM_178804.3	Slit2	Slit homolog 2 (Drosophila)	-1,01
NM_011577.1	Tgfb1	Transforming growth factor, beta1	-1,44
NM_011905.3	Tlr2	Toll-like receptor 2	-1,79
NM_021297.2	Tlr4	Toll-like receptor 4	-1,53
NM_013693.2	Tnf	Tumor necrosis factor	-2,06
NM_138302.1	Tymp	Thymidine phosphorylase	1,25
NM_008510.1	Xcl1	Chemokine (C motif) ligand 1	1,24
NM_011798.4	Xcr1	Chemokine (C motif) receptor 1	-1,88

References

1. Dammann O, Ferriero D, Gressens P. Neonatal encephalopathy or hypoxic ischemic encephalopathy? Appropriate terminology matters. *Pediatr Res* 2011; 70: 1-2.
2. De Haan M, Wyatt JS, Roth S, et al. Brain and cognitive-behavioural development after asphyxia at term birth. *Dev Sci* 2006; 9: 350-358.
3. Ferriero DM. Neonatal brain injury. *N Engl J Med* 2004; 351: 1985-1995.
4. Graham EM, Ruis KA, Hartman AL, et al. A systematic review of the role of intrapartum hypoxia-ischemia in the causation of neonatal encephalopathy. *Am J Obstet Gynecol* 2008; 199: 587-595.
5. van Handel M, Swaab H, de Vries LS, et al. Long-term cognitive and behavioural consequences of neonatal encephalopathy following perinatal asphyxia: a review. *Eur J Pediatr* 2007; 166: 645-654.
6. Wang CC, Chen CH, Lin WW, et al. Direct intramyocardial injection of mesenchymal stem cell sheet fragments improves cardiac functions after infarction. *Cardiovasc Res* 2008; 77: 515-524.
7. Gonzalo-Daganzo R, Regidor C, Martin-Donaire T, et al. Results of a pilot study on the use of third-party donor mesenchymal stromal cells in cord blood transplantation in adults. *Cytotherapy* 2009; 11: 278-288.
8. Deans RJ, Moseley AB. Mesenchymal stem cells: Biology and potential clinical uses. *Exp Hematol* 2000; 28: 875-884.
9. Zhang R, Liu Y, Yan K, et al. Anti-inflammatory and immunomodulatory mechanisms of mesenchymal stem cell transplantation in experimental traumatic brain injury. *J Neuroinflammation* 2013; 10: 106-118.
10. Salem HK, Thiemermann C. Mesenchymal stromal cells: Current understanding and clinical status. *Stem Cells* 2010; 28: 585-596.
11. Donega V, van Velthoven CT, Nijboer CH, et al. Intranasal mesenchymal stem cell treatment for neonatal brain damage: Long-Term cognitive and sensorimotor improvement. *PLoS ONE* 2013; 8: e51253.
12. Borlongan CV, Weiss MD. Baby STEPS: A giant leap for cell therapy in neonatal brain injury. *Pediatr Res* 2011; 70: 3-9.
13. van Velthoven CT, Kavelaars A, van Bel F, et al. Repeated mesenchymal stem cell treatment after neonatal hypoxia-ischemia has distinct effect on formation and maturation of new neurons and oligodendrocytes leading to restoration of damage, corticospinal motor tract activity, and sensorimotor function. *J Neurosci* 2010; 28: 9603-11.
14. Titomanlio L, Kavelaars A, Dalous J, et al. Stem cell therapy for neonatal brain injury: perspectives and challenges. *Ann Neurol* 2011; 70: 698-712.
15. van Velthoven CT, van de Looij Y, Kavelaars A, et al. Mesenchymal stem cells restore cortical rewiring after neonatal ischemia in mice. *Ann Neurol* 2012; 71: 785-96.
16. Velthoven C, Kavelaars A, van Bel F, et al. Mesenchymal stem cell transplantation changes the gene expression profile of the neonatal ischemic brain. *Brain Behav Immun* 2011; 25: 1342-1348.
17. Yasuhara T, Hara K, Maki M, et al. Intravenous grafts recapitulate the neurorestoration afforded by intracerebrally delivered multipotent adult progenitor cells in neonatal hypoxic-ischemic rats. *J Cereb Blood Flow Metab* 2008; 28: 1804-1810.
18. Tse WT, Pendleton JD, Beyer WM, et al. Suppression of allogeneic T-cell proliferation by human marrow stromal cells: implications in transplantation. *Transplantation* 2003; 75: 389-397.

19. Toyoma K, Honmou O, Harada K, et al. Therapeutic benefits of angiogenetic gene-modified human Mesenchymal stem cells after cerebral ischemia. *Exp Neurol* 2009; 216: 47-55.
20. Liu H, Honmou O, Harada K, et al. Neuroprotection by PIGF gene-modified human mesenchymal stem cells after cerebral ischemia. *Brain* 2006; 129: 2734-2745.
21. Yang B, Xi XP, Aronowski J, et al. Ischemic stroke may activate bone marrow mononuclear cells to enhance recovery after stroke. *Stem Cells Dev* 2012; 21: 3332-3340.
22. Prins HJ, Rozemuller H, Vonk-Griffioen S, et al. Bone forming capacity of mesenchymal stromal cells when cultured in presence of human platelet lysate as substitute for fetal calf serum. *Tissue Eng Part A*
23. Dominici M, Le Blanc K, Mueller I, et al. Minimal criteria for defining multipotent Mesenchymal stromal cells. The international Society for Cellular Therapy. *Cytotherapy* 2006; 8: 315-317.
24. Horwitz EM, Le BK, Dominici M, et al. Clarification of the nomenclature for MSC: The International Society for Cellular Therapy position statement. *Cytotherapy* 2005; 7: 393-395.
25. Van Velthoven CT, Braccioli L, Willems HL, et al. Therapeutic potential of genetically modified mesenchymal stem cells after neonatal hypoxic-ischemic brain damage. *Mol Ther* 2013 [epub ahead of print].
26. Croft A, Przyborski SA. Mesenchymal stem cells expressing neural antigens instruct a neurogenic cell fate on neural stem cells. *Exp Neurol* 2009; 216: 329-341.
27. Hack MA, Sugimori M, Lundberg C, et al. Regionalization and fate specification in neurospheres: the role of Olig2 and Pax6. *Mol Cell Neurosci* 2004; 25: 664-678.
28. Hack MA, Saghatelian A, de Chevigny A, et al. Neuronal fate determinants of adult olfactory bulb neurogenesis. *Nat Neurosci* 2005; 8: 865-872.
29. Lee JA, Kim BI, Jo CH, et al. Mesenchymal stem cell transplantation for hypoxic-ischemic brain injury in neonatal rat model. *Pediatr Res* 2010; 67: 42-46.
30. Silver J, Miller JH. Regeneration beyond the glial scar. *Nat Rev Neurosci* 2004; 5: 146-156.
31. Sofroniew MV. Multiple Roles for astrocytes as effectors of cytokines and inflammatory mediators. *Neuroscientist* 2013 [epub ahead of print].
32. Wake H, Moorhouse AJ, Miyamoto A, et al. Microglia: actively surveying and shaping neuronal circuit structure and function. *Trends Neurosci* 2013; 36: 209-217.
33. Donega V, van Velthoven CT, Nijboer CH, et al. The endogenous regenerative capacity of the newborn brain: Boosting neurogenesis with mesenchymal stem cell treatment. *JCBFM* 2013; 33: 625-634.
34. Ziebell JM, Morganti-Kossmann MC. Involvement of pro-and anti-inflammatory cytokines and chemokines in the pathophysiology of traumatic brain injury. *Neurotherapeutics* 2010; 7: 22-30.
35. Reglero-Real N, Marcos-Ramiro B, Millan J. Endothelial membrane reorganization during leukocyte extravasation. *Cell Mol Life Sci* 2012; 69: 3079-3099.
36. Ransohoff RM, Hamilton TA, Tani M, et al. Astrocyte expression of mRNA encoding cytokines IP-10 and JE/MCP-1 in experimental autoimmune encephalomyelitis. *FASEB J* 1993; 7: 592.
37. Ubogu EE, Cossoy MB, Ransohoff RM. The expression and function of chemokines involved in CNS inflammation. *Trends in Pharmacol Sci* 2006; 27: 48-55.



Chapter 6

Assessment of long-term safety and efficacy of intranasal Mesenchymal Stem Cell treatment for neonatal brain injury

Vanessa Donega¹, Cindy T.J. van Velthoven^{1*}, Cora H. Nijboer^{1*}, Sameh A. Youssef²,
Alain de Bruin², Frank van Bel³, Annemieke Kavelaars⁴ and Cobi J. Heijnen^{1,4}

¹Lab. of Neuroimmunology and Developmental Origins of Disease, University Medical Center Utrecht, Utrecht, The Netherlands, ²Dutch Molecular Pathology Center, Department of Pathobiology, Faculty of Veterinary Medicine, Utrecht University, The Netherlands. ³Dept. of Neonatology, University Medical Center Utrecht. ⁴Dept. of Symptom Research, MD Anderson Cancer Center, Houston TX, USA.

*Authors contributed equally to the manuscript

Submitted to Neurotherapeutics

Abstract

We have previously shown that intranasal MSC treatment significantly improves sensorimotor and cognitive behavior and decreases lesion size at 5 weeks following hypoxia-ischemia (HI) in neonatal mice. For possible clinical translation, we assessed whether intranasal MSC treatment induces neoplasia in the brain or periphery at 14 months after HI. Furthermore, the long-term effects on behavior and lesion volume were determined following MSC administration.

HI was induced in 9 day old mouse pups. Pups received intranasal administration of 0.5×10^6 MSCs or Vehicle at 10 days after HI. Full macroscopical and microscopical pathological analysis on 39 organs per mouse was performed by two board-certified veterinary pathologists. Sensorimotor behavior was assessed in the CRT at 10 days, 28 days, 6 and 9 months. Cognition was measured with the NORT at 3 and 14 months post-HI. Lesion volume was determined by analyzing MAP2 and MBP area loss at 5 weeks and 14 months.

At 14 months following HI we did not observe any significant lesion or neoplasia in the nasal turbinates, brain or other peripheral organs of HI-mice treated with MSCs in comparison to controls. Furthermore, our results show that MSC induced improvement of sensorimotor and cognitive function are maintained for at least 9 and 14 months, respectively. In contrast, HI-Vehicle mice showed severe behavioral impairment. Recovery of MAP2 and MBP area lasted up to 14 months following MSC treatment.

Our results provide strong evidence of the long-term safety and positive effects of MSC treatment following neonatal HI in mice. This work is an important step towards translation to the clinic.

Introduction

Neonatal encephalopathy due to hypoxia-ischemia (HI) remains a major health issue worldwide. A HI-insult results in brain damage with subsequent development of motor and cognitive impairments like cerebral palsy and mental retardation¹⁻⁵. Currently, hypothermia is the only available treatment, but is only moderately neuroprotective and solely effective in babies born at term if applied within 6h following HI. Hence, there is a strong need for novel treatment strategies¹⁻⁵.

Over the past years mesenchymal stem cells (MSCs) have become a potentially attractive therapeutic option for several diseases^{6,7}. The growing interest in MSC therapy is partially due to the immunosuppressive capacities of MSCs. Furthermore, MSCs can be easily and effectively obtained from *e.g.* bone marrow or Wharton's Jelly and are hardly immunogenic as they do not express MHC class II antigens or co-stimulatory proteins (*e.g.* CD40, CD80 and CD86)⁸⁻⁹.

We have recently demonstrated that intranasal MSC treatment significantly improves cognitive and motor behavior and declines lesion volume following neonatal HI brain injury in the mouse¹⁰. Furthermore, we showed that MSC treatment has a long therapeutic window of 10 days. We demonstrated that intranasally administered MSCs reach the lesion site within 24h after application to both nostrils¹¹. Moreover, previous studies from our group showed that intracranial MSC treatment increases gene expression of several neurotrophic and anti-inflammatory factors in the brain^{12,13}. Therefore, intranasal MSC administration holds strong potential as a non-invasive therapeutic strategy to repair neonatal HI brain injury.

However, the long-term safety of MSC administration remains under debate. Therefore, we investigated in depth whether MSC treatment is associated with malignancies in the brain or other organs after intranasal MSC treatment at 14 months after HI. To this end, mice were submitted to thorough histopathological analysis performed by board-certified mouse pathologists. Furthermore, we determined at 14 months following HI whether MSC treatment has effects on sensorimotor and cognitive behavior, and lesion size.

Material and Methods

Ethics statement

Experiments were approved by the Experimental Animal Committee Utrecht (DEC-ABC, University Utrecht, Utrecht, Netherlands) and performed according to international guidelines.

HI induction and intranasal MSC administration

An unilateral HI brain lesion was induced in 9 day old C57BL/6 mouse pups (Harlan Laboratories, The Netherlands) under isoflurane anesthesia (5% induction, 1,5% maintenance in O₂: air; 1:1) by permanently occluding the right common carotid artery, followed by hypoxia for 45min at 10% oxygen. Control mouse pups, *i.e.* sham-operated, underwent anesthesia and incision only. The HI procedure resulted in a mortality rate of 10%. At 10 days after HI, 3 µl of PBS diluted hyaluronidase (100 U, Sigma-Aldrich, St. Louis, MO) was administered twice to each nostril to increase the permeability of the nasal mucosa. After thirty minutes, mice received either 0.5x10⁶ C57BL/6 mice bone marrow-derived MSCs or PBS (HI-Vehicle group). 3 µL of cell suspension was administered twice to each nostril making an end volume of 12 µL.

Animals were randomly assigned to each experimental group. Occasionally some animals did not perform on the behavioral tests due to a lack in motivation. Therefore, these animals were not included to the analyses. Furthermore, 3 sham-operated animals died before the end of the study.

MSCs

MSCs were purchased from Invitrogen (GIBCO mouse C57BL/6 MSCs, Life Technologies, UK) and cultured according to the manufacturer's instructions. Characterization of cell specific antigens has been described previously by us¹³.

Sensorimotor and cognitive function

Unilateral sensorimotor impairment was assessed in the cylinder rearing test (CRT). Weight-bearing left (impaired), right (unimpaired) or both paw(s) contacting the wall during full rear were scored. Paw preference was calculated as $((\text{right} - \text{left}) / (\text{right} + \text{left} + \text{both})) \times 100\%$.

Cognitive function was assessed with the novel object recognition test (NORT). Briefly, habituation to the test environment was performed the day before the actual experiment, in an empty cage for 10 min. At the day of the test, two similar objects were first placed in the cage and the mouse was allowed to explore for 10 min. The mouse was then removed from the test cage and returned to its home cage for 5 min. In the second phase, one of the explored objects was replaced by a novel object. We measured the time that the mouse spends exploring the familiar and novel object during 5 min. Time spent with the novel object was calculated as $((\text{interaction time novel object}) / (\text{total interaction time}) \times 100\%)$.

Pathological assessment

Sham-operated (n=13), HI-Vehicle (n=17) and HI-MSC (n=17) mice were submitted to the Dutch Molecular Pathology Center (DMPC), Utrecht University for post-mortem examination at 14 months after HI. Mice were euthanized by an overdose of pentobarbital and subsequently examined for external and internal lesions. Significant lesions were recorded, scored and photographed. Representative specimens were collected from 39 organs (Table 2) from every mouse and fixed in 10% neutral buffered formalin. After fixation the organs were trimmed according to the DMPC standard protocol, embedded in paraffin and sectioned. The presence of histopathological lesions was examined microscopically on Hematoxylin-Eosin (HE) stained sections.

The brains from 30 mice (n=10 per group) were analyzed for pathological lesions. The skull was decalcified and sliced transversely at the level of the nasal turbinates. The sections were processed for histopathology as described above. Five brain sections and three sections from the nasal turbinates were examined for each mouse.

Histological assessment of lesion volume

Histological assessment of brain lesion volume was determined from the remaining mice (Sham-operated n=3; HI-Vehicle n=7; HI-MSC n=7). Briefly, mice were perfused intracardially with 4% paraformaldehyde (PFA) and brains were removed and embedded in paraffin. 8 μm coronal brain sections were incubated with mouse-anti-myelin basic protein (MBP) (Sternberger Monoclonals, Lutherville, MD,) or mouse-anti-microtubule-associated protein 2 (MAP2) (Sigma-Aldrich) followed by biotinylated horse-anti-mouse antibody (Vector Laboratories, Burlingame, CA). Binding was visualized with Vectastain ABC kit (Vector Laboratories) and diaminobenzamidine.

Statistical analysis

Analyzes were performed in a blinded set-up. Quantification of ipsilateral MAP2 or MBP area loss was determined by Adobe Photoshop CS5 and ImageJ software (<http://rsb.info.nih.gov/ij/>), respectively. Data are presented as mean \pm SEM. Statistical significance was determined by using Two-way ANOVA followed by Bonferroni post-hoc tests for all analyzes except the NORT, where statistical significance was assessed by one-sample T-test (Two-tailed). $p < 0.05$ was considered statistically significant. Outliers were detected with the Grubbs (Q=5%) and ROUT (Q=5%) tests. Removed outliers: In the NORT 3 months; 1 outlier (sham-operated), in the CRT 6 months; 3 outliers (MSC-treated), in the CRT 9 months; 2 outliers (sham-operated and MSC-treated), in the MPB 5 weeks; 1 outlier (MSC-treated).

Results

MSC administration induces long-term motor and cognitive improvement after HI

To investigate the long-term effects of intranasal MSC treatment on motor performance, we assessed sensorimotor behavior in the cylinder rearing test (CRT), which measures the preference to use the unimpaired forepaw. CRT was measured at 10 and 28 days and at 6 and 9 months following sham-operation or HI induction. All mice show similar motor impairment at 10 days following HI. Our results show that motor impairment in HI-Vehicle mice further deteriorated over time. In contrast, MSC treatment at 10 days following HI induces long-term improvement of sensorimotor behavior (Fig 1). Our results show a significant decrease in the preference to use the unimpaired forepaw in HI-MSC mice at 28 days following the insult. At 9 months following HI, motor performance of HI-MSC mice had improved even further and impairment had decreased another 79% reaching sham level.

We used the novel object recognition test (NORT) to assess cognitive behavior at 3 and 14 months after HI. As expected, sham-operated animals showed a significant preference for the novel object. HI-Vehicle mice had no preference for either the novel or the known object (Fig 2). However, MSC treatment significantly restored cognitive performance as our results demonstrate that HI-MSC mice have a significant preference to explore the novel object at 3 and 14 months following HI.

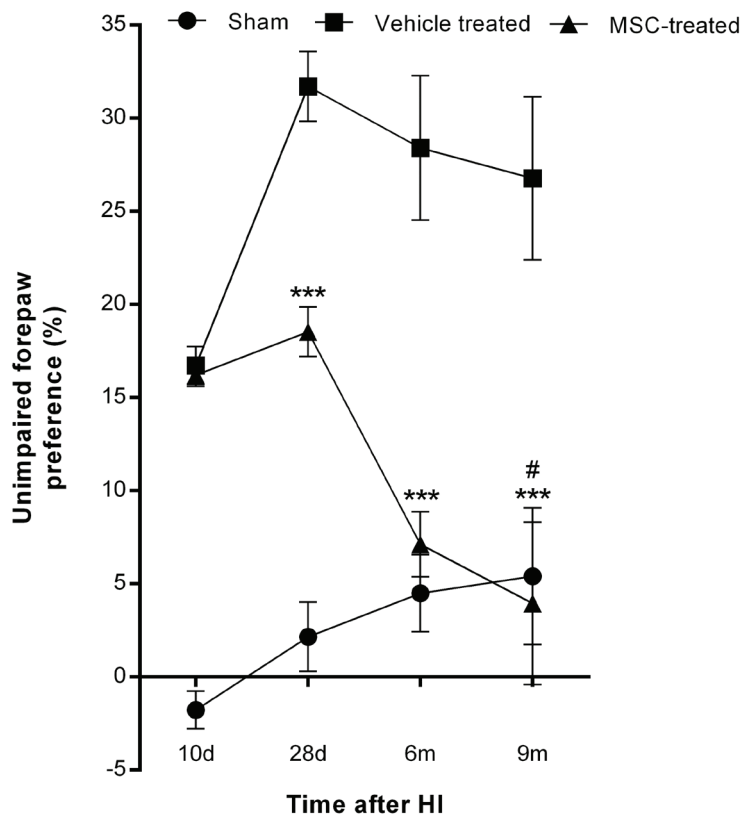


Figure 1. Long-term effect of MSC-treatment on sensorimotor behavior over time. Mice received either 0.5×10^6 MSCs or Vehicle intranasally at 10 days after HI. Performance in the CRT was assessed at 10 days (*i.e.* before treatment) and 28 days and at 6 and 9 months post-HI-induction or sham-operation. The results show that MSC administration improves performance in the CRT up to 9 months post-HI. *** $p < 0.001$; # $p < 0.001$ (HI-MSC 28d vs HI-MSC 9 months) with Two-way ANOVA and Bonferroni post-hoc test. 10 days Sham $n=16$; HI-Vehicle/HI-MSC $n=17$; 28 days Sham $n=15$; HI-Vehicle/HI-MSC $n=17$ per group; 6 months Sham $n=15$; HI-Vehicle $n=17$; HI-MSC $n=14$; 9 months Sham $n=13$; HI-Vehicle $n=16$; HI-MSC $n=13$

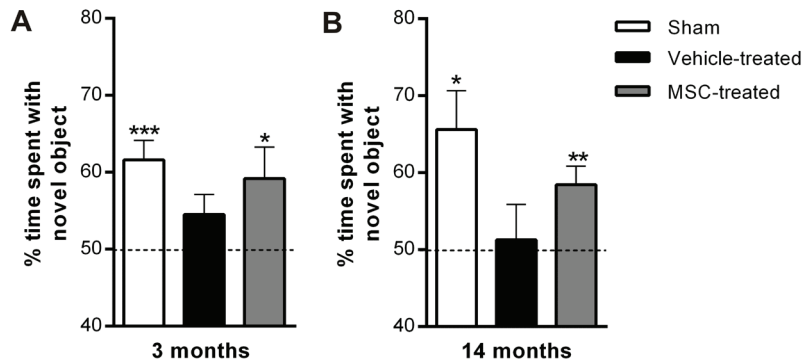


Figure 2. Long-term effect of MSC-treatment on cognitive behavior over time. Cognitive performance in the NORT was assessed at 3 and 14 months after HI induction or sham-operation. Intranasal MSC administration at 10 days following HI significantly improves performance in the NORT up to 14 months after HI. * $p < 0.05$; ** $p < 0.01$; *** $p < 0.001$ with one sample T-test (two-tailed) vs. 50% interaction time. 3 months Sham $n = 13$; HI-Vehicle $n = 15$; HI-MSc $n = 16$; 14 months Sham $n = 8$; HI-Vehicle $n = 10$; HI-MSc $n = 11$.

Changes in lesion volume over time

To assess long-term effects of MSC treatment on lesion volume we sacrificed mice at 5 weeks and 14 months after HI or sham-operation and analyzed brain sections for MAP2 and MBP staining as a measure of gray- and white-matter injury volume, respectively. Our results show that at 5 weeks following HI the entire hippocampus and part of the sensorimotor cortex were absent following vehicle administration. MSC treatment, however, significantly decreased both gray- and white-matter damage at 5 weeks after HI. The sensorimotor cortex was completely restored and part of the hippocampal structure could be distinguished. The effect of MSCs on neuronal and white matter damage remained constant over time between 5 weeks and 14 months (Fig 3A, B). Moreover, the sensorimotor cortex remained intact over time. In HI-Vehicle mice, MAP2 area loss decreased non-significantly from 5 weeks to 14 months (Fig 3A, B). In HI-Vehicle mice MBP area loss did not change significantly over time either.

MSCs do not induce neoplasia in the brain and nasal turbinates in the long-term

To determine whether MSC treatment has any adverse long-term effects in the brain or nasal turbinates, HE stained sections from sham-operated, HI-Vehicle and HI-MSc mouse brains were examined for histopathological changes at 14 months. Importantly,

our results show no evidence of neoplasia in the brain or nasal turbinates in any of the examined mice (n=10 per group) (Fig 4). Several mice had mild nasal mucosal degeneration and necrosis with presence of intracellular eosinophilic hyalinized materials typical of murine nasal mucosal epithelial hyalinosis, but there were no differences between the experimental groups (Sham: 2/13; HI-Vehicle: 5/17; HI-MSC: 5/17).

No significant increase in systemic pathological lesions after MSC treatment

Next, we determined whether intranasal MSC treatment had any adverse effects on other peripheral organs and tissues at 14 months after HI induction. To this end, 38 organs were analyzed for macroscopic and/or microscopic lesions. Multisystemic lymphosarcoma affecting the lymph nodes, uterus and salivary glands was found in two mice; one HI-Vehicle (out of 17 mice) and one HI-MSC (out of 16 mice) (Table 1 and 2). One HI-MSC mouse (out of 10 mice) had a poorly differentiated focal uterine sarcoma that was compatible with a leiomyosarcoma. No other significant lesions were found in any of the examined mice.

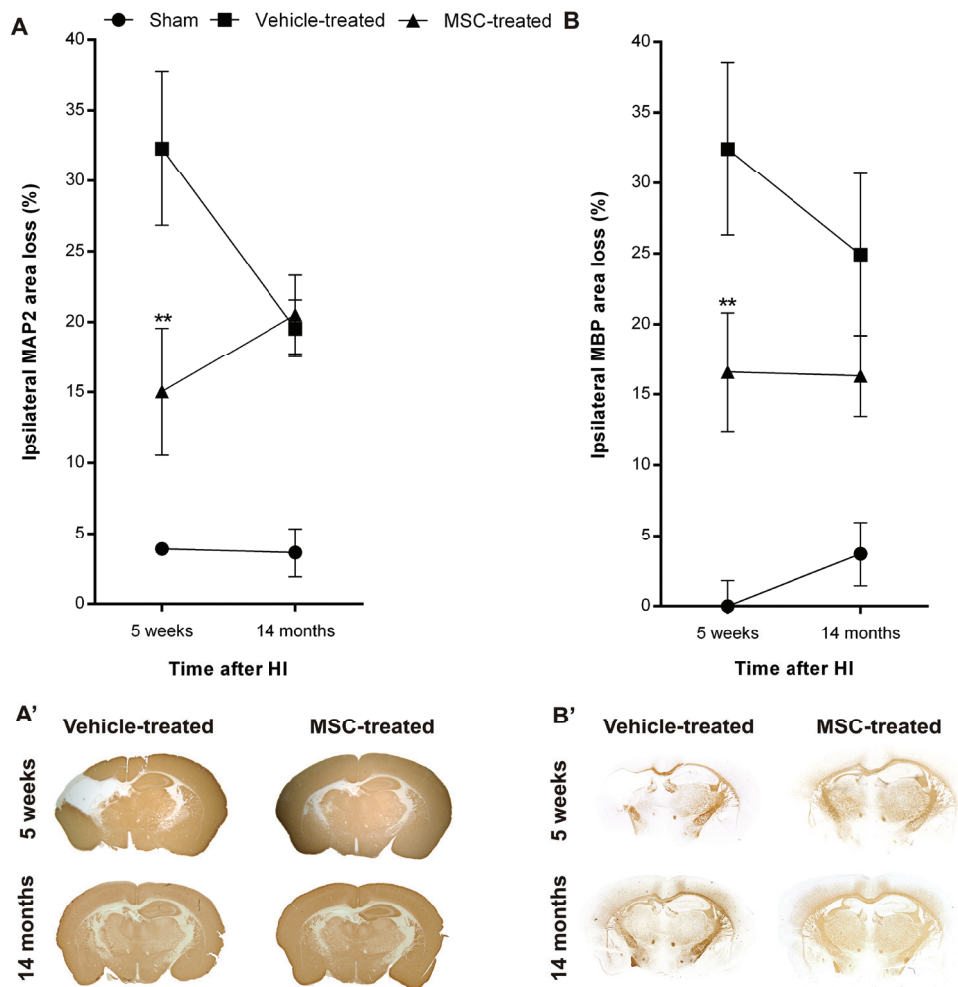


Figure 3. Long-term effect of MSCs on gray and white matter injury over time. Ipsilateral loss of MAP2 and MBP at 5 weeks and 14 months following HI. (A) MSC treatment significantly decreases MAP2 area loss at 5 weeks after HI. (A') Representative sections of MAP2 staining. (B) MSC treatment decreases MBP area loss at 5 weeks after HI. (B') Representative sections of MBP staining. ** $p < 0.01$ with Two-way ANOVA and Bonferroni post-hoc test. MAP2 Sham $n = 3$; HI-Vehicle 5 weeks $n = 9$; HI-Vehicle 14 months $n = 8$; HI-MSC 5 weeks $n = 10$; HI-MSC 14 months $n = 8$. MBP Sham 5 weeks $n = 3$; Sham 14 months $n = 4$; HI-Vehicle 5 weeks $n = 10$; HI-Vehicle 14 months $n = 7$; HI-MSC 5 weeks $n = 9$; HI-MSC 14 months $n = 6$.

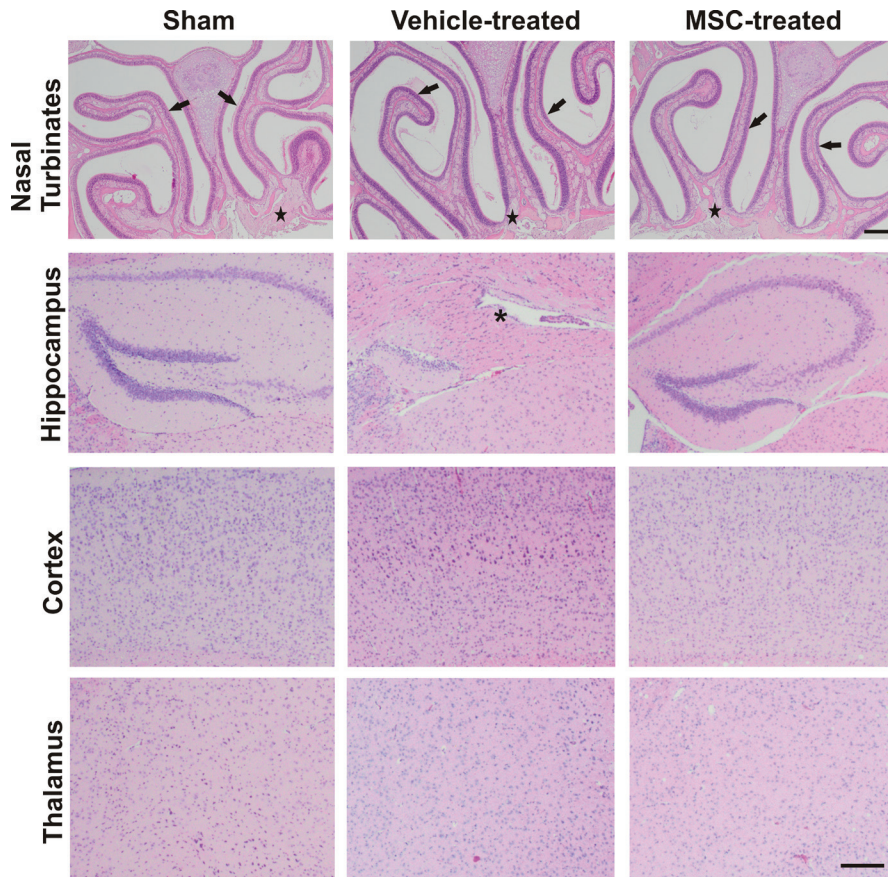


Figure 4. No malignancies are induced in the nasal turbinates or brain after intranasal MSC treatment. HE staining of brain and nasal turbinates sections from Sham-operated, HI-Vehicle and HI-MSc mice at 14 months following HI. No neoplasia or lesion was observed. Examples of the nasal turbinates and cortical, hippocampal and thalamic brain regions. n=10 per group; arrows=nasal/olfactory mucosa; star=olfactory nerve; asterisk=damaged hippocampus; Scale bar=200µm.

Discussion

Previous work by our group has demonstrated the strong therapeutic potential of intranasal MSC administration for repair of neonatal ischemic brain damage using the mouse model. Intranasal MSC treatment significantly improves motor and cognitive behavior and decreases lesion volume at 5 weeks after HI. However, for translation to

the clinic it is absolutely essential to determine whether MSCs may have any adverse effects, especially during aging. Another important question is how long the positive effects of MSC-induced brain repair last. To our knowledge this is the first study to investigate whether intranasally administered MSCs applied early in life induce tumor formation or any other microscopic or macroscopic lesions later in life. We followed the mice for a considerable period of time, as C57BL/6 mice have a normal life span of about 18-24 months. The mice examined in our study were 14 months old when pathological assessment was carried out. Detailed pathological analysis was performed by unbiased assessment at a pathological center. Our findings show that intranasal MSC administration does not induce any macroscopic or microscopic lesions in the brain or in any peripheral organ in the long-term.

We assessed 47 mice (Sham-operated (n = 13), HI-Vehicle (n = 17) and HI-MS (n = 17) mice) for macroscopic or microscopic lesions in the brain, nasal turbinates and also in 38 other organs (Table 1 and 2). All analyses were performed without prior knowledge of the mouse identification code. Our data shows no evidence of tumor formation or other significant lesions in the brain of any of the examined mice (Fig 4). No tumor formation was observed in the brain or the nasal turbinates following MSC-treatment. Lymphosarcoma and the other non-cerebral lesions (*e.g.* nasal hyalinosis, lymphocytic sialoadenitis) are common findings in aged mice and are considered spontaneous lesions that are not related to intranasal MSC treatment¹⁴. We observed lymphosarcoma following both Vehicle and MSC treatment. Incidence of lymphosarcoma in B6C3F1 mice (*i.e.* C57BL/6 and C3HJ/HeJ hybrids) has been reported to be 8.3% in males and 16.8% in females at the age of 22-28 months^{15,16}. The uterine sarcoma observed in one HI-MS mouse (out of 7 mice) is likely a primary uterine tumor that originated from the uterine smooth muscle (*i.e.* leiomyosarcoma) or from the uterine mesenchyme (*i.e.* fibrosarcoma). The finding that MSCs do not induce tumor formation or any other lesion in the brain or nasal turbinates has significant implications for the clinic.

One possible explanation as to why MSC administration has no adverse effects in the long-term is that MSCs actually do not engraft in the brain following administration. We have previously demonstrated that the number of MSC decreased drastically to <1% at 18 days after intracranial administration¹³. On the basis of these data we proposed that MSCs do not differentiate into neurons or astrocytes themselves but

rather stimulate endogenous neural stem cells via secretion of neurotrophic factors promoting proliferation and differentiation into functional neurons^{13,17}. Indeed, we have shown that MSC treatment induces functional cortical rewiring following HI¹⁸. Another important factor is that we administered MSCs intranasally and not systemically in our HI model, which may significantly reduce the chance of MSCs reaching peripheral tissues with possible systemic adverse effects. Taken together, these data indicate that intranasal MSC administration early in life does not lead to negative adverse effects with respect to the induction of microscopic or macroscopic lesions during the life time of the animal.

As discussed before, MSCs are hardly immunogenic and have been found to possess immunosuppressive and immunomodulating capacities. For instance, MSCs secrete anti-inflammatory cytokines such as IL-10 and TGF β and suppress expansion of T cells and activation of NK cells^{19,20,21}. On the basis of these cellular characteristics a growing number of clinical trials (www.clinicaltrials.gov) are assessing efficacy and safety to use MSCs as a therapeutic strategy for various pathologies ranging from cardiovascular to auto-immune diseases.

In the present work we show that the positive effects of intranasal MSC-treatment both on sensorimotor and cognitive behavior last up to 9 and 14 months of age in neonatal mice treated with MSCs at 10 days following HI. The latter is important with respect to clinical application. Our data show that the MSC-induced neurogenesis results in functional neurons as HI-MSC mice still showed improved cognitive and sensorimotor performance at 9 and 14 months post-HI induction. Furthermore, based on our results, it does not seem likely that long-term functional impairments due to potential cellular aberrations in the endogenous neural precursors occur.

The lesion volume in HI-MSC and HI-Vehicle mice did not change significantly over time, which suggests that once the lesion is formed, it does not deteriorate any further. The data in Figure 3 indicate that some endogenous repair may also take place in HI animals as lesion size decreases (although not significantly) over time. However, we suggest on the basis of our data that in HI-Vehicle mice the lesion is not repopulated by functionally integrated neurons, since we did not observe cognitive or sensorimotor improvement over time, whereas MSC treatment apparently restores functional neuronal repopulation following a HI event. Hence, our results demonstrate that MSC treatment is essential for long-term neuroregeneration and recovery of motor and cognitive behavior.

Conclusions

We show here for the first time that intranasal MSC treatment after neonatal HI does not induce any malignancies or other pathological abnormalities in the brain, nasal turbinates or any peripheral tissues as shown by the unbiased and thorough assessment performed by an independent pathological center. This study also highlights the lifelong effects of intranasal MSC treatment on both cognitive and sensorimotor behavior and lesion size following neonatal HI injury in the mouse. This work may have important impact for effective and safe translation of intranasal MSC treatment to the clinic and strongly supports intranasal MSC administration as a realistic therapeutic neuroregenerative option for neonatal encephalopathy.

Acknowledgments

The authors are greatly indebted to Miss. Sabine Versteeg, Miss. Elsbeth van Liere, Miss. Saskia van Essen-van Dorresteyn and Miss. Mirjam Koster for excellent technical assistance. This study was supported by the ZorgOnderzoek Nederland-Medische Wetenschappen (Zon-MW) Project (no 116002003).

References

1. Dammann O, Ferriero D, Gressens P. Neonatal encephalopathy or hypoxic ischemic encephalopathy? Appropriate terminology matters. *Pediatr Res* 2011; 70: 1-2.
2. De Haan M, Wyatt JS, Roth S, et al. Brain and cognitive-behavioural development after asphyxia at term birth. *Dev Sci* 2006; 9: 350-358.
3. Ferriero DM. Neonatal brain injury. *N Engl J Med* 2004; 351: 1985-1995.
4. Graham EM, Ruis KA, Hartman AL, et al. A systematic review of the role of intrapartum hypoxia-ischemia in the causation of neonatal encephalopathy. *Am J Obstet Gynecol* 2008; 199: 587-595.
5. van Handel M, Swaab H, de Vries LS, et al. Long-term cognitive and behavioural consequences of neonatal encephalopathy following perinatal asphyxia: a review. *Eur J Pediatr* 2007; 166: 645-654.
6. Wang CC, Chen CH, Lin WW, et al. Direct intramyocardial injection of mesenchymal stem cell sheet fragments improves cardiac functions after infarction. *Cardiovasc Res* 2008; 77: 515-524.
7. Gonzalo-Daganzo R, Regidor C, Martin-Donaire T, et al. Results of a pilot study on the use of third-party donor mesenchymal stromal cells in cord blood transplantation in adults. *Cytotherapy* 2009; 11: 278-288.
8. Deans RJ, Moseley AB. Mesenchymal stem cells: Biology and potential clinical uses. *Exp Hematol* 2000; 28: 875-884.
9. Zhang R, Liu Y, Yan K, et al. Anti-inflammatory and immunomodulatory mechanisms of mesenchymal stem cell transplantation in experimental traumatic brain injury. *J Neuroinflammation* 2013; 10: 106-118.
10. Salem HK, Thiemermann C. Mesenchymal stromal cells: Current understanding and clinical status. *Stem Cells* 2010; 28: 585-596.
11. Donega V, van Velthoven CT, Nijboer CH, et al. Intranasal Mesenchymal Stem Cell Treatment for Neonatal Brain Damage: Long-Term Cognitive and Sensorimotor Improvement. *PLoS ONE* 2013; 8: e51253.
12. van Velthoven CT, van de Looij Y, Kavelaars A, et al. Mesenchymal stem cells restore cortical rewiring after neonatal ischemia in mice. *Ann Neurol* 2012; 71: 785-96.
13. van Velthoven CT, Kavelaars A, van Bel F, et al. Mesenchymal stem cell transplantation changes the gene expression profile of the neonatal ischemic brain. *Brain Behav Immun* 2011; 25: 1342-1348.
14. Taylor I. Mouse. McInnes EF, eds. *Background lesions in laboratory animals*. 1st Ed. Edinburgh, UK: Saunders Elsevier; 2012: 45-72.
15. Ward JM, Goodman DG, Squire RA, et al. Neoplastic and nonneoplastic lesions in aging (C57BL/6N x C3H/HeN)_F₁ (B6C3F₁) mice. *J Natl Cancer Inst* 1979; 63: 849-854.
16. Tarone RE, Chu KC, Ward JM. Variability in the rates of some common naturally occurring tumors in Fischer 344 rats and (C57BL/6N x C3H/HeN)_F₁ (B6C3F₁) mice. *J Natl Cancer Inst* 1981; 66: 1175-1181.
17. van Velthoven CT, Kavelaars A, van Bel F, et al. Repeated mesenchymal stem cell treatment after neonatal hypoxia-ischemia has distinct effects on formation and maturation of new neurons and oligodendrocytes leading to restoration of damage,

- corticospinal motor tract activity, and sensorimotor function. *J Neurosci* 2010; 30: 9603-9611.
18. van Velthoven CT, van de Looij Y, Kavelaars A, et al. Mesenchymal stem cells restore cortical rewiring after neonatal ischemia in mice. *Ann Neurol* 2012; 71: 785-796.
 19. Giuliani M, Fleury M, Vernochet A, et al. Long-lasting inhibitory effects of fetal liver Mesenchymal stem cells on T-lymphocyte proliferation. *PLoS One* 2011; e19988.
 20. Zhang R, Liu Y, Yan K, et al. Anti-inflammatory and immunomodulatory mechanisms of mesenchymal stem cell transplantation in experimental traumatic brain injury. *J Neuroinflammation* 2013; 10: 106-118.
 21. Pluchino S, Cossetti C. How stem cells speak with host immune cells in inflammatory brain diseases. *Glia* 2013; 61: 1379-1401.

Tables

Table 1. Necropsy findings per animal. Sham-operated n=13; Vehicle-treated n=17; MSC-treated n=17.

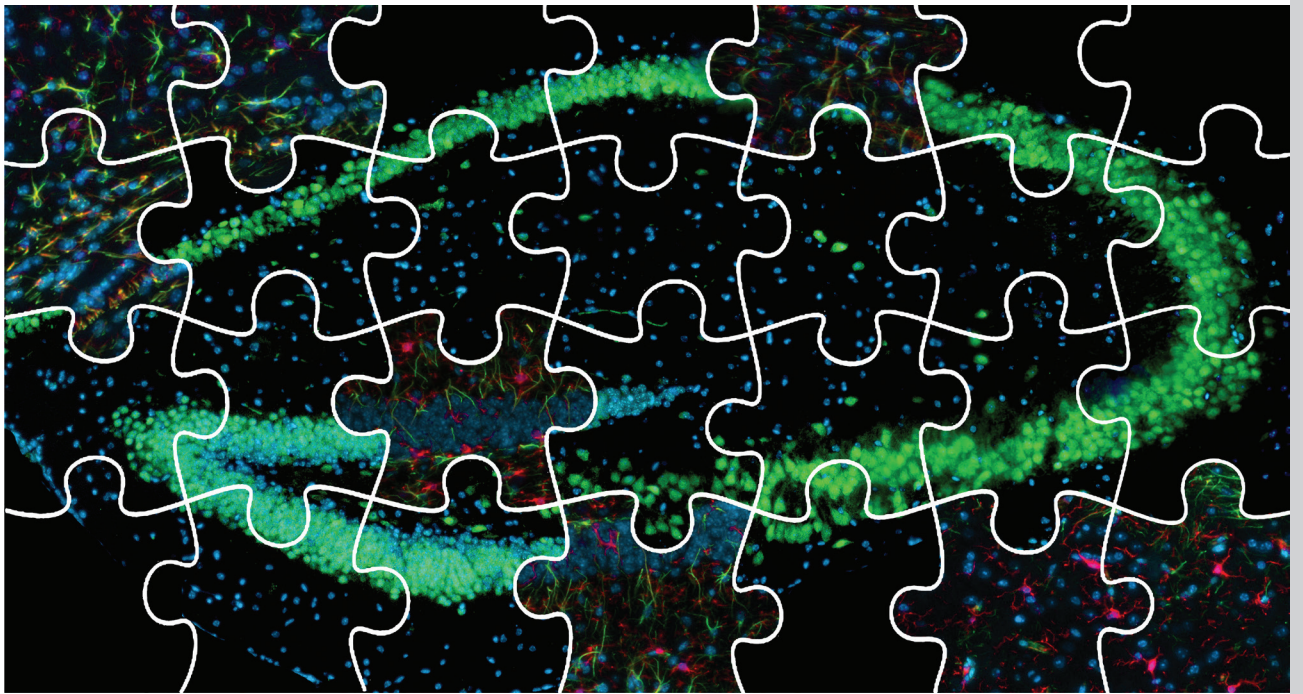
Sham-operated	Vehicle-treated	MSC-treated
Mild right corneal opacity (n=1/13)	Mesenteric left node has lymphoma (n=1/17)	Multisystemic lymphoma in nodes, uterus and intestines (n=1/17)
Right uterine mucometra/hydrometra (n=1/13)	Acute hemorrhage: Left lung lobe (n=1/17)	Severe cerebellar atrophy (n=1/17)
	Olfactory lobe appeared smaller (n=1/17)	Both olfactory lobes appeared atrophied (n=1/17)
	Right corneal opacity (n=1/17)	Spleen is firmer and smaller (n=1/17)
	Acute linear hemorrhage in liver (could be traumatic) (n=1/17)	
	Liver is pale and atrophied (n=1/17)	

Table 2. Full report of histopathological findings. Sham-operated n=13; Vehicle-treated n=17; MSC-treated n=17. NSL=non-significant lesion.

Organs	Sham-operated	Vehicle-treated	MSC-treated
Trachea	NSL	NSL	Mild mucosal atrophy (n=2/17)
Larynx	NSL	NSL	NSL
Oesophagus	NSL	NSL	NSL
Thymus	NSL	Early lymphoma (n=1/17)	NSL
Nasal turbinates (nasal mucosa, olfactory mucosa and nerves)	Mild mucosal hyalinosis (2/13)	Mild mucosal hyalinosis (5/17)	Mild mucosal hyalinosis (5/17)
Eye, Harderian gland	NSL	NSL	NSL
Mammary gland	NSL	NSL	NSL
Spinal cord, sciatic nerve	NSL	NSL	Mild gliosis in the cord (2/17)
Femur (bone and joint)	NSL	NSL	NSL
Vertebra	NSL	Minimal cartilaginous degeneration (n=2/17)	Minimal cartilaginous degeneration (n=2/17)
Bone marrow	NSL	NSL	NSL
Adrenal glands	Mild cortical atrophy (n=1/13)	Mild cortical atrophy (n=1/17)	Mild cortical atrophy (n=1/17)
Axillary, mesenteric and mammary lymph nodes	Mild Lymphoid hyperplasia (n=1/13)	Early lymphoma (n=1/17)	Lymphoma (n=1/17)
Aorta	NSL	Mild lymphocytic and neutrophilic panniculitis (n=1/17)	NSL
Heart	NSL	Moderate lymphocytic inflammation (n=1/17)	NSL
Salivary glands	Mild lymphocytic inflammation (n=8/13)	Mild lymphocytic inflammation (n=5/17) Early lymphoma (n=1/17)	Mild lymphocytic inflammation (n=5/17)
Tongue	NSL	Mild granulomatous inflammation (n=1/17) (likely foreign body granuloma)	NSL

Table 2. continued

Organs	Sham-operated	Vehicle-treated	MSC-treated
Thyroid/ parathyroid	NSL	NSL	NSL
Pituitary	NSL	NSL	NSL
Spleen	NSL	NSL	Severe extramedul- lary hematopoiesis (n=1/17)
Kidneys	Mild polyarteritis nodosa (n=1/13)	Mild membranous glomerulonephritis (n=1/17)	Minimal glomerulonephritis (n=1/17)
Urine bladder	Mild hyalinosis of bladder mucosa (n=1/13)	Mild lipidosis (n=1/17)	Mild hyalinosis of bladder mucosa (n=1/17)
Liver	Mild biliary cystic hyperplasia (n=1/13) Mild to moderate hepatic lipidosis (n=1/13)	Mild lipidosis (n=1/17) Mild fatty change (n=1/17) Mild atrophy (n=1/17)	Mild necrosis and inflammation (n=1/17)
Pancreas	Mild islets hyperplasia (n=1/13)	NSL	NSL
Gastrointestinal tract	NSL	NSL	Mild polyarteritis nodosa (n=1/17)
Testis, epididymis	Mild degeneration with mild Leydig cell hyper- plasia (n=1/8)	NSL	NSL
Male sex glands	NSL	NSL	NSL
Mammary Gland	NSL	NSL	NSL
Ovary	NSL	Mild to Moderate atrophy (n=2/10)	NSL
Uterus	Moderate pleocellular inflammation (n=1/6)	Moderate cystic hyperplasia (n=1/10)	Solitary leiomyosarcoma (n=1/7)
Lung	NSL	Early crystal pneumonia (n=1/17)	Mild crystal acidophilic pneumonia (n=1/17)
Skin	Mild lymphocytic panniculitis (n=2/13)	Small trichogranuloma (n=1/17) Mild lymphocytic and neutrophilic panniculitis (n=1/17)	NSL
Skeletal Muscle	NSL	Focal necrosis with pleocellular inflammation (n=1/17)	Focal area of acute skeletal necrosis with suppurative inflammation (n=1/17)



Chapter 7

Summary and General Discussion

Summary and General Discussion

The work described in this thesis demonstrates the potential of MSCs to repair hypoxic-ischemic (HI) brain injury in our mouse model of neonatal HI. The key findings of this thesis will be discussed in this chapter and I will conclude by deliberating on the main question whether intranasal MSC administration has a future as a therapeutic strategy for human infants suffering from neonatal encephalopathy.

MSCs en route to the lesion site

The intranasal administration route was first explored in the 70's as a technique to deliver oxytocin to the periphery to induce labor in pregnant women¹. Subsequent studies assessed the efficacy of the intranasal route to administer a variety of drugs ranging from insulin² to vaccines³. It was only much later, in the beginning of the 21st century that the intranasal delivery route was explored as a way to deliver neurotrophic factors to the brain. In 2009, Danielyan *et al.* described for the first time the intranasal delivery of stem cells to the intact brain. Ever since, a growing number of studies have investigated the efficiency of delivering neurotrophic factors and cells to the brain⁵⁻¹⁰. To the best of our knowledge we are the first who have used the intranasal route to deliver MSCs to the damaged brain as a possible therapeutic strategy^{10,11}.

However, the question how biologics and cells delivered via the nose reach the brain remained unanswered. Studies by Thorne *et al.* demonstrated that biologics may diffuse from the nose to the brain tissue along olfactory and trigeminal nerve components. Another route may be through or alongside blood vessels and lymphatic vessels in the olfactory epithelium or via the cerebral spinal fluid (CSF) to the subarachnoid space¹².

Our studies show that MSCs migrate specifically towards the lesion site within just 2h following intranasal administration (**chapter 4**). If MSCs would migrate through brain tissue with a similar speed as neuroblasts, which migrate at 60 μm per hour, it would take several days for the MSCs to reach the lesion site. Importantly, our data show that intranasally administered MSCs reach the lesion site within 2h after administration, and therefore, suggest that MSCs reach the lesion site by migrating through cerebral blood vessels (**chapter 4**). Furthermore, MSCs migrate specifically towards the site of injury but do not remain in the contralateral side even though MSCs are administered to both nostrils. This strongly suggests that chemotactic

factors expressed by *e.g.* glial cells at the lesion site, attract MSCs towards the lesion in a very accurate way. Moreover, migration and homing of MSCs to the damaged region may be facilitated by the increased permeability of the blood brain barrier (BBB) following HI¹³. The expression of adhesion molecules on the endothelial cells at the site of injury may have been up-regulated, thereby facilitating migration to the lesion site. Nevertheless, it will be important to determine in future studies the percentage of the administered MSCs that actually reach the lesion. The question whether intranasally administered MSCs also reach organs in the periphery also has to be addressed.

Homing and engraftment of MSCs to the ischemic myocardium following intracardial administration has been shown to be regulated by the expression of P-selectin, VLA-4/VCAM and Itgb2/ICAM-1. These receptors mediate rolling and adhesion of cells to the endothelial cell lining of blood vessels^{14,15}. Extravasation into the brain tissue may be regulated by CCR2/MCP-1, VLA-4/VCAM and matrix metalloproteinase (MMP)-2¹⁶⁻¹⁸. The chemokine CX3CL1 (alias fractalkine) seems to play a role in MSC migration following systemic intravenous administration in rats with hypoglossal nerve injury or Middle Cerebral Artery Occlusion (MCAO)^{19,20}. In **chapter 4**, we provide evidence that the chemotactic factor CXCL10 (alias IP-10) may be a strong attractant for intranasally administered MSCs in the neonatal HI model. Our PCR-array for chemotactic factors demonstrates that CXCL10 is the strongest upregulated factor at 10 days following HI, but has returned to sham level at 17 days after HI. As a consequence intranasally administered MSCs no longer reach the lesion site (**chapter 3**). Increasing CXCL10 expression at 17 days after HI in the lesion by intracranial injection may restore MSC migration although the neurotrophic signaling at the lesion site may not be enough to foster further endogenous stimulation of neurogenic stem cells. Furthermore, we found that the expression of the CXCL10 receptor, *i.e.* CXCR3, increases both on murine and human MSCs after co-culture with HI brain extracts. It would be interesting to investigate whether CXCR3 expression on MSCs is crucial for trafficking. This could be done by administrating MSCs that do not express CXCR3 as a proof of principle that the CXCR3-CXCL10 axis mediates MSC migration towards the lesion after HI. Together, these data suggest that CXCL10 may play an important role in mediating MSC migration towards the lesion following intranasal application.

These results are very important as they demonstrate that administration of MSCs through the nose will target the injury site very specifically and efficiently. Evidence that MSCs reach the lesion through blood vessels, increases the likelihood of

intranasal MSC application being an effective administration route in humans despite the greater distance between the olfactory bulb and nasal cavity in humans. The data presented in **chapter 3** and **4** of this thesis strongly advocate in favor of the potential to deliver MSCs to the injured human brain through intranasal administration.

MSC-induced lesion repair: Regeneration versus neuroprotection

In **chapter 3**, we show that intranasal MSC administration at 10 days after HI significantly improved sensorimotor and cognitive behavior and decreased lesion volume at 25 days following MSC treatment. However, the mechanisms underlying MSC-mediated lesion repair have yet to be clarified. Therefore, in **chapter 4**, we investigated the early effects of MSCs on lesion repair. Importantly, our work provides strong evidence that MSCs promote *repair* and do not induce *neuroprotection*, as at 10 days after HI, the moment when MSCs are given intranasally, the HI lesion is fully developed and does not progress any further over time²¹. Indeed, at 10 days after HI the entire hippocampus and part of the somatosensory cortex have been replaced by a cystic lesion, which remains up to 14 months after HI induction. The capacity of the MSCs to repair this extensive lesion further emphasizes the strong therapeutic potential of these cells.

Over the past years, a number of studies have been investigating how stem cells repair brain injury. For instance, studies by Phinney *et al.*²¹⁻²³ show evidence of MSC engraftment in the neonatal and adult brain following intracranial administration. The authors showed that MSCs engraft and differentiate into GFAP⁺ cells in the striatum, SVZ and cerebellum at 12 days after intracranial injection in 3 day old mouse pups without brain damage²⁴. These results indicate that MSCs may induce lesion repair by differentiating into new neurons, astrocytes or oligodendrocytes themselves. Our work, however, challenges the general validity of this idea, as our results demonstrate that the number of MSCs decreases sharply over time. We found that PKH-26⁺-MSC signal decreases by 86% at 72 hours after administration (**chapter 4**) and previous work by our group show that only 1% of GFP⁺-MSC signal remains at 18 days following administration²⁵. Importantly, in **chapter 4** we demonstrate that lesion repair after MSC administration results from stimulation of *endogenous* regenerative processes rather than from the differentiation of MSCs into neurons or astrocytes.

These findings raise the interesting question as to the source of the newborn neurons in our model. In **chapter 4** we provide evidence that MSCs increase the

number of doublecortin (DCX) positive cells, that is, young migrating neurons in the subventricular zone (SVZ) at 1 and 3 days after administration and at the lesion site at 3 days following application. Interestingly, at 5 days after MSC administration we observed a significant increase in NeuN⁺ cells at the lesion, suggesting that MSCs promote maturation of young migrating DCX⁺ neuronal cells. Indeed, our results demonstrate a dramatic repair of the somatosensory cortex and hippocampal region within just 5 days following intranasal administration of MSCs (Fig 1). Cell fate mapping studies should investigate which neuronal populations are formed following MSC treatment. Our finding that MSC-treated mice still show improved behavior at 14 months following HI, suggests that these newborn neuronal cells are functional neurons. Future studies should also address whether these newborn neurons functionally integrate into the local network by performing electrophysiological assessments.

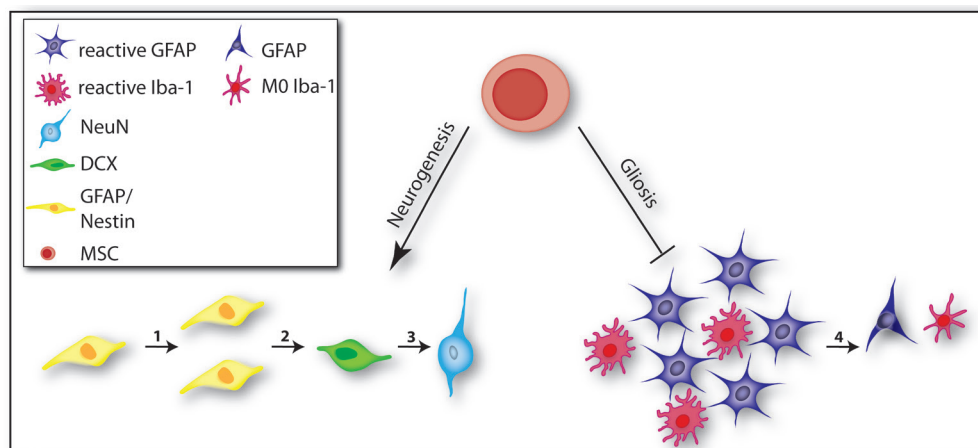


Figure 1. Schematic overview of the effects of MSCs on neurogenesis (left) and gliosis (right) that are likely to play a role in MSC-induced brain repair. MSCs may affect the HI brain environment through paracrine or juxtacrine signaling. These MSC derived factors will stimulate (1) proliferation of endogenous neural stem cells (GFAP⁺/Nestin⁺) and (2) differentiation towards neuroblast (DCX⁺) and (3) more mature neuronal cells (NeuN⁺). Concomitantly, MSC signaling will (4) inhibit and resolve the glial scar (*i.e.* gliosis) by inducing reactive astrocytes and activated microglia to revert into a “resting” state.

We know from our behavioral studies that at 11 days after MSC treatment, the preference to use the unimpaired forepaw decreases, while HI-Vehicle mice develop

severe motor deficits. Furthermore, we have also shown that cognitive performance in social discrimination test and the Novel Object Recognition test (NORT) improves following treatment with MSCs (**chapter 3** and **5**). These tests suggest that short-term memory recovers following treatment with MSCs, which may be explained by improved connectivity between olfactory and visual stimuli to cortical regions involved in short-term memory storage. Other hippocampal-dependent tasks, such as the Morris Water maze, may be used to assess spatial learning and memory. This would be interesting to study as one could determine whether full functional recovery takes place, despite partial recovery of hippocampal volume.

Another important question that remains to be answered is how MSCs stimulate the endogenous neural stem cells to differentiate and repopulate the lost brain regions. As mentioned before, **chapter 3** of this thesis shows that MSCs migrate specifically to the injury site. **Chapter 4** demonstrates that MSC treatment increases the number of DCX⁺ cells in the SVZ. This suggests that MSCs in the lesion sense the environment and induce differentiation of endogenous NSCs through paracrine signaling. Indeed, a growing number of studies demonstrate that MSCs have a remarkable capacity to sense the local brain environment and act accordingly^{26,27}. MSCs have been shown to regulate endogenous cells by juxtacrine or paracrine signaling^{28,29}. For instance, transplanted MSCs secrete neurotrophic factors such as BDNF and NGF³⁰, which are involved in neurogenesis (**chapter 4**). In **chapter 5**, we showed that co-culture of hMSCs with mouse NSCs induces differentiation of mouse NSCs towards neuronal and glial cell fate. This demonstrates the paracrine effects that MSCs can have on their local environment. Furthermore, secretion of anti-inflammatory factors such as IL-10²⁵ may inhibit microglia and thereby inflammatory processes at the lesion site. Indeed, in **chapter 4** and **chapter 5** we demonstrate that MSCs induce glial scar resolution and that reverting the astrocytic scar is likely pivotal for regeneration to occur.

MSCs: Cells with a therapeutic potential?

In **chapter 6** we show that the positive effects of MSC treatment on sensorimotor and cognitive behavior, and lesion volume are long-lasting. Thorough investigation of possible pathological side-effects of intranasal MSC treatment revealed no evidence of any malignancy in the nasal turbinates or brain or any other organ. Besides, as discussed in the previous section, we found no indication of MSC engraftment following intranasal or intracranial administration.

In the last few years, studies have shown that neurogenesis takes place in the SVZ, hippocampus and striatum of the neonatal and adult *human brain*^{31,32}. This means that like other mammalian species, the human brain maintains a certain neurogenic potential throughout life. Future studies will tell the extent of this neurogenic capacity. Nevertheless, this recent groundbreaking work on the neurogenic potential of the human brain paves the way for the development of therapeutic strategies for neurodegenerative diseases and other brain injuries, as it could serve as a tool to regenerate lost or damaged tissue. Animal studies show that following HI injury, a shift occurs from neurogenesis to gliogenesis, thus favoring an astrocytic cell fate for newborn cells (**chapter 2**).

We show in this thesis that intranasal MSC administration is an efficient route to deliver MSCs to the brain. Another advantage of MSCs is that they are relatively easy to obtain and to maintain in *in vitro* settings. However, before efficient translation to the clinic is possible, the optimal dose and time of administration should be carefully determined. We showed in **chapter 3** and **5** that the effect of MSCs is dose dependent, as the lowest dose of mMSCs and hMSCs did not decrease lesion volume. Therefore, determining the optimal dose will be pivotal for treatment efficiency. Another important aspect to keep in mind is the optimal time-point to start MSC administration in the human neonate. The treatment may not be efficient if MSCs are given too late, that is, past the period when the brain environment expresses the necessary factors to attract the MSCs to the lesion and stimulate the transplanted cells to induce neurogenesis and ultimately lead to brain repair. We did not determine whether there is a limit in how early one can start with MSC treatment. The earliest time-point we determined is 3 days following HI induction (**chapter 3**). Therefore, we cannot exclude the possibility that MSC treatment before 3 days may not be effective due to the detrimental (inflammatory) environment in the brain following HI. Unfortunately, accurate translation of the therapeutic window directly from mice to humans is not possible. Furthermore, we know exactly when the HI insult occurred in our HI mouse model, which is not always the case in the clinical setting. This has also to be taken into account when determining the optimal therapeutic window. As our results clearly show a time-point when MSCs no longer reach the lesion site and thus, have no effect on the lesion, it would be safest to treat neonatal encephalopathy as soon as possible. Therefore, one approach would be to administer MSCs as soon as encephalopathy has been diagnosed (within 24-72 hours) by electroencephalogram

(aEEG), magnetic resonance imaging (MRI) or near infrared spectroscopy (NIRS). This would mean that babies with encephalopathy could be treated within the first week after birth.

In conclusion, this thesis shows the potential of intranasal MSCs to become a safe and efficient therapeutic strategy for neonatal HI. Moreover, it also underlines the prospect to effectively use MSCs intranasally to treat other diseases of the central nervous system. Critical assessment of clinical trials will be crucial to evaluate efficacy in the clinic and its future as a treatment.

References

1. Stander RW, Thompson JF, Gibbs CP. Evaluation of intranasal oxytocin by amniotic fluid pressure recordings. *Am J Obstet Gynecol* 1963; 85: 193-9.
2. Schade DS, Eaton RP. Insulin delivery: how, when, and where. *N Engl J Med* 1985; 312: 1120-1121.
3. Bowen JC, Alpar HO, Phillipotts R, et al. Mucosal delivery of herpes simplex virus vaccine. *Res Virol* 1992; 143: 269-278.
4. Danielyan L, Schafer R, von Ameln-Mayerhofer A, et al. Intranasal delivery of cells to the brain. *Eur J Cell Biol* 2009; 88: 315-324.
5. Liu XF, Fawcett JR, Thorne RG, et al. Non-invasive intranasal insulin-like growth factor-1 reduces infarct volume and improves neurologic function in rats following middle cerebral artery occlusion. *Neurosci Lett* 2001; 308: 91-94.
6. De Rosa R, Garcia AA, Braschi C, et al. Intranasal administration of nerve growth factor (NGF) rescues recognition memory deficits in AD11 anti-NGF transgenic mice. *Proc Natl Acad Sci USA* 2005; 102: 3811-3816.
7. Ma M, Ma Y, Yi X, et al. Intranasal delivery of transforming growth factor-beta1 in mice after stroke reduces infarct volume and increases neurogenesis in the subventricular zone. *BMC Neurosci* 2008; 9: 117.
8. Danielyan L, Schafer R, von Ameln-Mayerhofer A, et al. Therapeutic efficacy of intranasally delivered mesenchymal stem cells in a rat model of Parkinson disease. *Rejuvenation Res* 2011; 14: 3-16.
9. Reitz M, Demestre M, Sedlacik J, et al. Intranasal delivery of neural stem/progenitor cells: a noninvasive passage to target intracerebral glioma. *Stem Cells Transl Med* 2012; 12: 866-873.
10. Donega V, van Velthoven CT, Nijboer CH, et al. Intranasal Mesenchymal Stem Cell Treatment for Neonatal Brain Damage: Long-Term Cognitive and Sensorimotor Improvement. *PLoS ONE* 2013a; 8: e51253.
11. van Velthoven CT, Kavelaars A, van Bel F, et al. Nasal administration of stem cells: a promising novel route to treat neonatal ischemic brain damage. *Pediatr Res* 2010; 68: 419-422.
12. Lochhead JJ, Thorne RG. Intranasal delivery of biologics to the central nervous system. *Adv Drug Deliv Rev* 2012; 64: 614-628.
13. Alvarez-Diaz A, Hilario E, Goni de Cerio F, et al. Hypoxic-ischemic injury in the immature brain- Key vascular and cellular players. *Neonatology* 2007; 92: 227-235.
14. Ruster B, Gottig S, Ludwig RJ, et al. Mesenchymal Stem Cells display coordinated rolling and adhesion behavior on endothelial cells. *Blood* 2006; 108: 3938-3944.
15. Karp JM, Leng Teo GS. Mesenchymal stem cell homing: the devil is in the details. *Cell Stem Cell* 2009; 4: 206-216.
16. Belema-Bedada F, Uchida S, Martire A, et al. Efficient homing of multipotent adult Mesenchymal stem cells depends on FROUNT-mediated clustering of CCR2. *Cell Stem Cell* 2008; 6: 566-575.
17. Ries C, Egea V, Karow M, et al. MMP-2, MT1-MMP, and TIMP-2 are essential for the invasive capacity of human Mesenchymal stem cells: differential regulation by inflammatory cytokines. *Blood* 2007; 9: 4055-4063.

18. De Becker A, Van Hummelen P, Bakkus M, et al. Migration of culture-expanded human mesenchymal stem cells through bone marrow endothelium is regulated by matrix metalloproteinase-2 and tissue inhibitor of metalloproteinase-3. *Haematologica* 2007; 92: 440-449.
19. Ji JF, He BP, Dheen ST, et al. Expression of chemokine receptors CXCR4, CCR2, CCR5 and CX3CR1 in neural progenitor cells isolated from the subventricular zone of the adult rat brain. *Neurosci Lett* 2004; 355: 236-240.
20. Zhu J, Zhou Z, Liu Y, et al. Fractalkine and CX3CR1 are involved in the migration of intravenously grafted human bone marrow stromal cells toward ischemic brain lesion in rats. *Brain Res* 2009; 1287: 173-183.
21. Bonestroo HJC, Heijnen CJ, Groenendaal F, et al. Kinetics of cerebral gray and white matter injury and cerebral inflammation after inflammatory perinatal asphyxia. submitted to *Neurobiol Dis* 2014.
22. Isakova IA, Lanclos C, Bruhn J, et al. Allo-reactivity of mesenchymal stem cells in rhesus macaques is dose and haplotype dependent and limits durable cell engraftment in vivo. *PLOS One* 2014; 9: e87238.
23. Isakova IA, Baker K, Dufour J, et al. Preclinical evaluation of adult stem cell engraftment and toxicity in the CNS of Rhesus Macaques. *Mol Therapy* 2006; 13: 1173-1184.
24. Phinney DG, Baddoo M, Dutreil M, et al. Murine Mesenchymal stem cells transplanted to the central nervous system of neonatal versus adult mice exhibit distinct engraftment kinetics and express receptors that guide neuronal cell migration. *Stem Cells and Develop* 2006; 15: 437-447.
25. Kopen GC, Prockop DJ, Phinney DG. Marrow stromal cells migrate throughout forebrain and cerebellum, and they differentiate into astrocytes after injection into neonatal mouse brains. *Proc Natl Acad Sci USA* 1999; 96: 10711-10716.
26. Van Velthoven CT, Kavelaars A, van Bel F, et al. Mesenchymal stem cell transplantation changes the gene expression profile of the neonatal ischemic brain. *Brain Behav Immun* 2011; 25: 1342-1350.
27. Pluchino S, Cossetti C. How stem cells speak with host immune cells in inflammatory brain diseases. *Glia* 2013; 61: 1379-1401.
28. Pevsner-Fischer M, Morad V, Cohen-Sfady M, et al. Toll-like receptors and their ligands control mesenchymal stem cell functions. *Blood* 2007; 109: 1422-1432.
29. Akiyama K, Chen C, Wang D, et al. Mesenchymal stem cell induced immunoregulation involves FAS-ligand-/FAS-mediated T cell apoptosis. *Cell Stem Cell* 2012; 10: 544-555.
30. Knight JC, Scharf EL, Mao-Draayer Y. Fas activation increases neural progenitor cell survival. *J Neurosci Res* 2010; 88: 746-757.
31. Crigler L, Robey RC, Asawachaicharn A, et al. Human Mesenchymal stem cell subpopulations express a variety of neuro-regulatory molecules and promote neuronal cell survival and neuritogenesis. *Exp Neurol* 2006; 198: 54-64.
32. Spalding KL, Bergmann O, Alkass K, et al. Dynamics of hippocampal neurogenesis in adult humans. *Cell* 2013; 153: 1219-1227.
33. Ernst A, Alkass K, Bernard S, et al. Neurogenesis in the striatum of the adult human brain. *Cell* 2014; 156: 1072-1083.

Chapter 8

Nederlandse Samenvatting

(Summary in Dutch)

Nederlandse Samenvatting

Neonatale encefalopathie veroorzaakt door hypoxie-ischemie (HI) is een belangrijke oorzaak van mortaliteit en hersenschade bij pasgeboren baby's. HI wordt veroorzaakt door een tekort aan zuurstof en bloedtoevoer in het neonatale brein. Wereldwijd worden er 1-6 per 1000 baby's geboren die HI hersenschade ontwikkelen. Door het tekort aan zuurstof en glucose ontstaan er vrije zuurstof radicalen (*i.e.* schadelijke moleculen) die onder andere het celmembraan en de celkern van de hersencellen beschadigen waardoor de hersencellen sterven en er hersenschade ontstaat. Hoe meer hersencellen dood gaan, hoe ernstiger de schade is. HI hersenschade kan ernstige levenslange gevolgen hebben voor het kind door het veroorzaken van ernstige neurologische aandoeningen, zoals epilepsie, motorische afwijkingen en mentale retardatie. Dit eist veel van hun familie en de samenleving. De therapeutische mogelijkheden die momenteel voor handen zijn, zijn niet bij alle baby's met HI hersenschade effectief. Daarom is onderzoek naar nieuwe behandelingsmethoden van cruciaal belang.

Mesenchymale stam cellen (MSC) zijn stam cellen die bijvoorbeeld uit het beenmerg of vetweefsel kunnen worden geïsoleerd. Deze stam cellen zijn multipotente stam cellen, dat wil zeggen dat ze verschillende soorten cellen kunnen worden uit een type weefsel (in dit geval mesenchym). Uit deze mesenchymale stam cellen kunnen vet cellen, bot cellen en kraakbeen cellen ontstaan. Recent heeft onze onderzoeksgroep laten zien dat het toedienen van mesenchymale stam cellen (MSC) via de neus van neonatale muizen met HI hersenschade de motoriek herstelt en het laesie volume vermindert na HI. Studies uit andere onderzoeksgroepen hebben aangetoond dat MSC ook effectief zijn als behandeling voor verschillende (hersenen)aandoeningen zoals beroerte en de ziekte van Parkinson. Op het moment lopen er wereldwijd meer dan 300 clinical trials om de veiligheid en effectiviteit van MSC behandeling bij mensen te onderzoeken.

Om het effect van MSC op neonatale HI hersenschade te kunnen onderzoeken, hebben we HI nagebootst in een muis model. In dit muis model ontstaat er een cyste in de rechter hersenhemisfeer, dit wil zeggen dat in bepaalde gebieden de hersencellen vervangen worden door hersenvloeistof. Deze muizen met HI hersenschade ontwikkelen langdurig motorische en cognitieve beperkingen, welke met gedragstesten zoals de 'cilinder rearing test' en de 'sociale discriminatie test' meetbaar zijn.

In **hoofdstuk 2** van dit proefschrift bespreek ik de capaciteit van het neonatale muisbrein om te herstellen, door de aanmaak van nieuwe neuronen te verhogen. Tijdens dit proces, genaamd neurogenese, worden nieuwe neuronen gemaakt vanuit neurale stam cellen, dat wil zeggen stam cellen die alleen neuronen (grijze stof cellen), oligodendrocyten (witte stof cellen) en astrocyten (belangrijke cellen die een rol spelen in verschillende processen zoals metabolisme, inflammatie en activiteit van neuronen) kunnen worden. Ik concludeer dat hoewel er nieuwe neuronen worden aangemaakt deze niet uitrijpen tot functionele neuronen. Dit betekent dat het brein van muizen pups met HI hersenschade niet in staat is om te herstellen zonder behandeling. Een nog belangrijker conclusie is dat het brein wel de capaciteit heeft om te herstellen als we deze kunnen boosten door middel van bijvoorbeeld MSC toediening.

In **hoofdstuk 3** van dit proefschrift hebben we het effect van MSC op motoriek, cognitie en laesie volume na HI onderzocht. Muizenpups zijn op 10 dagen na HI behandeld met MSC of saline via de neus. Onze resultaten laten zien dat behandeling met MSC via de neus, de motoriek en cognitie van muizenpups met HI hersenschade sterk verbetert en dat het laesie volume in de hersenen significant vermindert. Ook van belang is dat we laten zien dat de MSC specifiek naar het laesie gebied migreren en clusters van cellen vormen rondom de cyste. We zien dat MSC die op 17 dagen na HI intranasaal zijn toegediend niet in het laesie gebied aankomen en als gevolg daarvan, dat de behandeling dus ook geen effect heeft op motoriek of laesie volume na HI.

In **hoofdstuk 4** hebben we eerst bepaald hoe snel de MSC in het schade gebied terechtkomen. We laten zien dat de MSC al binnen twee uur na intranasale toediening specifiek naar het laesie gebied in de hersenen migreren. Dit is erg snel als je je voorstelt dat endogene stam cellen met een snelheid van 60 μm per uur door het brein migreren en de afstand van de neus tot het schade gebied meer dan 2000 μm bedraagt. Deze bevinding suggereert dat de MSC niet via het brein migreren, maar door de bloedvaten of meningeale circulatie. Onze resultaten laten ook zien dat de MSC niet lang in het brein aanwezig blijven. Dit blijkt uit onze data die laten zien dat het aantal toegediende MSC op 12 uur na toediening piekt in de hersenen en al significant verlaagd is op 72 uur na toediening.

We weten uit **hoofdstuk 3** dat MSC een sterk herstellend effect hebben op HI hersenschade. In **hoofdstuk 4** hebben we onderzocht hoe de MSC dit effect bereiken. Onze resultaten laten zien dat de MSC binnen 5 dagen het laesie gebied kunnen herstellen. We zien dat nieuwe neuronen ontstaan die de hersenstructuren her-

opbouwen. Een belangrijke bevinding is dat de MSC niet zelf in de hersenen worden ingebouwd, met andere woorden zelf geen nieuwe hersencellen, zoals neuronen of astrocyten, vormen. We hebben aangetoond dat MSC *herstel* van het brein *bevorderen* door endogene stam cellen te stimuleren tot proliferatie en de uitrijping van nieuwe neuronen tot functionele neuronen te bevorderen, ofwel neurogenese stimuleren. Bovendien stimuleert MSC behandeling het herstel van het brein door de schadelijk inflammatoire omgeving te dempen, waardoor het ontstaan van nieuwe neuronen wordt ondersteund. We hebben aangetoond dat MSC direct betrokken zijn bij herstel mechanismen aangezien de stam cellen, na het kweken in een HI hersenextract milieu, factoren produceren die zeer belangrijk zijn voor het ontstaan van nieuwe neuronen.

In **hoofdstuk 5** hebben we onderzocht of *humane* MSC ook een positieve effect kunnen hebben op HI hersenschade. Dit onderzoek is in samenwerking met de Stam Cel Faciliteit van het UMC Utrecht uitgevoerd. De *humane* MSC die wij hebben gebruikt worden al in de kliniek gebruikt om andere ziektebeelden te behandelen. We laten zien dat *humane* MSC, neuronale stam cellen van muis origine kunnen aanzetten tot uitrijping naar neuronen en astrocyten. Ook hebben we gevonden dat *humane* MSC naar het laesie gebied kunnen migreren in muizen hersenen met een HI insult. Van groot klinisch belang is dat onze resultaten laten zien dat *humane* MSC ook in staat zijn om HI hersenschade in de muis significant te verminderen en de motoriek van de muizen te verbeteren. Een andere hoogtepunt uit mijn onderzoek, welke we in **hoofdstuk 6** bespreken, is dat intranasale MSC toediening geen nadelige bijwerkingen heeft. We hebben dit onderzocht door muizen met een HI insult, geïnduceerd op neonatale leeftijd, tot 14 maanden na MSC behandeling te volgen. Dit is een aanzienlijk lange periode aangezien muizen maximaal 1.5 tot 2 jaar kunnen leven. We hebben geen evidentie gevonden voor tumor vorming in het brein of neus epithelium na methodologisch onderzoek door het Dutch Molecular Pathology Center van de Universiteit Utrecht. We laten ook zien dat de motoriek en cognitie van de muizen behandeld met MSC nog steeds verbeterd is op 14 maanden na behandeling en dus dat de effecten van MSC behandeling langdurig zijn. Dit is van groot belang voor de kliniek.

In dit proefschrift laten we zien dat het mogelijk is om het door HI beschadigde neonatale brein te *herstellen/repareren* door intranasale MSC behandeling. De effecten van deze MSC behandeling zijn langdurig en MSC behandeling induceert geen nadelige bijwerkingen in de muis. Ter conclusie, intranasale MSC behandeling is een zeer potente, toekomstige, therapeutische mogelijkheid om ne

Dankwoord (Acknowledgments)

This should be the easiest chapter to write, but I find it quite difficult, because after I finish writing it, my thesis will be complete and this journey will be almost at its end. After all the hard work of these past 4,5 years I have reached my destination! I have learned a lot during this journey, and, therefore, I would like to thank everyone who has helped me along the way or have contributed in some way to the work described in this thesis.

Geachte Prof. Heijnen, beste Cobi, bedankt dat je mij de kans hebt gegeven om bij het NIDOD lab te promoveren. Dank je wel voor al je hulp en betrokkenheid in de afgelopen jaren! Ik heb veel geleerd van alle werkbeprekingen en ik zal onze live (en skype) werkbeprekingen erg missen! Bedankt dat je mij de ruimte hebt gegeven om met mijn eigen ideeën en interpretaties te komen. Veel dank dat je ondanks dat je 2 drukke banen hebt, mijn manuscripten zo snel hebt kunnen nakijken, zodat ik mijn deadline kon halen.

Geachte Prof. Kavelaars, beste Annemieke, ik heb veel van je geleerd. Dank je wel voor je begeleiding, voor je kritische blik en dat je deur altijd open stond als ik vragen had! Ik heb van je geleerd om je onderzoeksvragen vooraf heel goed te formuleren om zo de juiste experimenten op te zetten en uit te voeren.

Geachte Prof. van Bel, beste Frank, dank je wel dat ik altijd bij je kon komen met klinische vragen en dat je altijd heel snel mijn manuscripten nakeek.

Dr. Nijboer, lieve Cora, waar zal ik beginnen? Bedankt voor je betrokkenheid en al je hulp de afgelopen jaren! Ik ben erg blij dat ik jou als copromotor heb gehad! Dank je wel dat ik altijd bij je terecht kon. Ik heb veel van je geleerd op het lab. Ik hoop dat ik jouw methodisch aanpak van opzetten en uitvoeren van experimenten heb geërfd 😊.

Prof. dr. R. J. Pasterkamp, Prof. dr. A. de Bruin, Prof. dr. P. Coffe, Prof. dr. L. de Vries and Prof. dr. M. van der Knaap thank you for taking part in my PhD committee.

Beste Dr. Kas en Dr Laarakker, veel dank voor de samenwerking en voor jullie inzicht in cognitieve gedragtesten, het heeft tot een mooie publicatie geleidt.

Beste Prof. Dijkhuizen en Dr. van Tilborg, veel dank voor de samenwerking! Hoewel we niet onze primaire vraag mee konden beantwoorden hebben we alsnog een mooi figuur voor het artikel kunnen maken!

Beste Dr. Slaper-Cortenbach, Marcelle van Gelder en Kasper Westinga, dank jullie voor de samenwerking en voor jullie hulp met de humane stam cellen! Ineke bedankt dat ik altijd bij terecht kon met stam cel gerelateerde vragen.

Dear Prof. de Bruin en Dr. Youssef, thank you for the collaboration on the histopathology paper. It was a humongous task, but it led to a very nice paper, which hopefully, will soon be accepted for publication.

Beste Elsbeth, Saskia en Mirjam, dank je wel voor jullie inzet om al die samples te snijden en kleuren voor de lange-termijn proef!

Ik wil graag Anja, Helma, Paul, Romy, Roon, Kees, Jan en iedereen van het GDL bedanken voor het verzorgen van mijn dieren, voor het verwisselen van gasflessen en bestellingen. Veel dank dat jullie altijd bereidt waren om te helpen.

Lieve (ex)-collega's van het NIDOD lab, dank jullie wel voor de gezelligheid! De labuitjes, diners en borrels waren altijd erg gezellig! Ik heb echt geluk dat ik zulke aardige en betrokken collega's heb gehad! Ik zal jullie missen!

Jitske, ik vond het heel jammer toen je met pensioen ging. Dank je wel dat ik altijd bij je terecht kon met lab vragen en IHC vragen. Bedankt voor je hulp met de kleuringen en snijwerk!

Karima, dank je wel voor je hulp op het lab! Bedankt voor al die qPCR's en al die blokjes die je hebt gesneden.

Marijke, je hebt altijd een luisterend oor! Veel dank voor je hulp op het lab, vooral met de sociale discriminatie test!

Mirjam, bedankt voor je hulp met inzetten van een groot in vitro proef!

Sabine, ik vind het erg leuk dat ik je als collega kan bedanken voor al je hulp! Bedankt dat je mij zelf in het weekend kwam helpen met de NORT! Het was met jou altijd gezellig op het GDL! Ongeacht hoe gestrest ik was, sushi maakte het altijd goed ☺.

Ilona, ik vond het erg jammer toen je weg ging. Je was altijd klaar om mij te helpen en daar ben ik je erg dankbaar voor!

Lubna, Roos en Nour. Jullie zijn even studenten bij ons geweest en hebben veel geholpen met snijden en kleuren. Dank daarvoor!

Hanneke en Niels, bij jullie kon ik altijd langs als ik praktische vragen had, veel dank hiervoor!

Elke, je was altijd een gezellige en aardige buurvrouw in de AIO kamer en in het lab! Het was erg gezellig (en druk) op het congres in Washington D.C.! Succes met de laatste weekjes ☺, je bent er bijna!

Hilde, het werd een beetje ongezellig met die kast in de AIO kamer, we moesten even wennen om tegen de “kast” te praten, en soms heb ik tegen je zitten te praten terwijl jij er niet was. Succes nog met de laatste weekjes!

Emiel, succes nog met de laatste maanden en veel plezier alvast in NYC!

Erik and Luca, good luck with your PhD! I am sure you will get lots of nice results!

Dear Hui-Jing, I am very happy to have made a friend like you! We were neighbours in the PhD room for 3 years. I could always ask you questions about IHC. You left an empty space in the PhD room! Thank you for the good time we had, having good Chinese food, real Chinese tea and learning some Chinese (I am afraid I forgot most of the words ☺). I really enjoyed our conversations. Thank you for “listening” and for your support all this time! I am privileged to have you as a friend!

Dear friends, thank you for the support these past years! Thanks for the trips, dinners and concerts when I could relax!

Lieve paranimfen, Carmen en Amila, we kennen elkaar al lang, eerst als bachelorstudenten en daarna als master-studenten. Met jullie kon ik altijd de piek (en dalen) van het promoveren delen. Bedankt voor de gezelligheid van de afgelopen jaren en voor de gezellige lunches aan de overkant. Ik ben daarom ook erg blij dat jullie mij tijdens mijn verdediging willen bijstaan! Succes met het afronden van jullie promotie! Ik weet zeker dat het goed gaat komen!

Lieve mam en pap. Jullie zijn de laatste, maar zeker de belangrijkste. Dank jullie wel dat jullie altijd in mij hebben geloofd en dat jullie er altijd voor me zijn! Bedankt dat jullie mij een omgeving hebben gegeven waar ik mijn dromen kon volgen. Pap, het was/is altijd leuk om (neuro)wetenschappen met jou te bespreken. Ik heb veel van je geleerd. Door jullie kon ik mijn passie voor de neurowetenschappen volgen. Jullie hebben dit traject leuk gemaakt! Zonder jullie steun was ik nooit zo ver gekomen!

List of Publications and Presentations

Publications

Donega V, van Velthoven CT, Nijboer CH, Kavelaars A, Heijnen CJ. The endogenous regenerative capacity of the damaged newborn brain: boosting neurogenesis with mesenchymal stem cell treatment. *J Cereb Blood Flow Metab* (2013); **33(5)**:625-34; doi:10.1038/jcbfm.2013.3

Donega V, Nijboer CH, van Velthoven CT, van Bel F, Kas MJ, Kavelaars A, Heijnen CJ. Intranasal Mesenchymal Stem Cell Treatment for Neonatal Brain Damage: Long-Term Cognitive and Sensorimotor Improvement. *PLoS ONE* (2013); **8(1)**: e51253; doi: 10.1371/journal.pone.0051253.

Donega V, Nijboer CH, van Tilborg G, Dijkhuizen R, Kavelaars A, Heijnen CJ. Intranasally administered mesenchymal stem cells promote a regenerative niche for repair of neonatal ischemic brain injury. (Under review *Experimental Neurology*)

Donega V, Nijboer CH, Slaper-Cortenbach I, Braccioli L, Kavelaars A, van Bel F, Heijnen CJ. Intranasal administration of human MSC for ischemic brain injury in the mouse: In vitro and in vivo neuroregenerative functions. (Under review *Plos One*)

Donega V, Velthoven C, Nijboer CH, Hassan S, de Bruin A, van Bel F, Kavelaars A, Heijnen CJ. Assessment of long-term safety and efficacy of intranasal Mesenchymal Stem Cell treatment for neonatal brain injury. (Under review *Stroke*)

Conferences and meetings

9th FENS Forum of Neuroscience, Milan, Italy, July 8, 2014. Poster Presentation. **Donega V.**, Nijboer CH, Kavelaars A, Heijnen CJ. “*Intranasal MSC administration boosts the regenerative capacity of the neonatal brain following hypoxia-ischemia*”.

Research Meeting Neonatology, University Medical Center Utrecht, Utrecht, The Netherlands, June 26, 2014. Oral Presentation. **Donega V.**, “*Nasal MSC treatment: Boosting the regenerative capacity of the neonatal mouse brain after injury*”.

X, Stem Cell and Brain Research Institute, Lyon, France, April 25, 2014. Oral Presentation. Donega V., *“Nasal MSC treatment: Boosting the regenerative capacity of the neonatal mouse brain after injury”*.

Regenerative Medicine & Stem Cells Day, Utrecht, Netherlands, March 6, 2014. Poster Presentation. Donega V., Nijboer CH, van Tilborg G, Dijckhuizen R, van Bel F, Kavelaars A, Heijnen CJ; *“Intranasal mesenchymal stem cell delivery: Orchestrating regeneration following hypoxic-ischemic brain injury”*.

FENS Featured Regional Meeting Prague 2013, Prague, Czech Republic, September 11-14, 2013. Poster Presentation. Donega V., Nijboer CH, van Tilborg G, Dijckhuizen R, van Bel F, Kavelaars A, Heijnen CJ; *“Intranasal mesenchymal stem cell delivery: Orchestrating regeneration following hypoxia-ischemia”*.

Research Meeting Neonatology, University Medical Center Utrecht, Utrecht, The Netherlands, May 16, 2013. Oral Presentation. Donega V., *“Long-term effects of nasal Mesenchymal stem cell treatment after neonatal hypoxic-ischemic brain damage”*.

RMI Symposium 2011, Utrecht, The Netherlands, December, 2011. Poster presentation. Donega V., van Velthoven CJ, Nijboer CH, Kas MJ, van Bel F, Kavelaars A, Heijnen CJ. *“Nasal mesenchymal stem cell treatment after neonatal hypoxic-ischemic brain damage improves motor and cognitive function”*.

Neuroscience 2011, Washington DC, USA, November 14, 2011. Poster presentation. Donega V.; van Velthoven CJ, Nijboer CH, Kas MJ, van Bel F, Kavelaars A, Heijnen CJ. *“Nasal mesenchymal stem cell treatment after neonatal hypoxic-ischemic brain damage improves motor and cognitive function”*.

‘Mind the Brain’ Symposium, Utrecht, Netherlands, April 23, 2008. Poster presentation. Donega V., Zhou Y, Pasterkamp RJ. *“A structure-function analysis of MICAL-1 in a heterologous model for growth cone collapse”*.

10th Student Science Day UMC Utrecht, Netherlands, March 06, 2008. Poster presentation. Donega V., van der Zwaag B, Burbach JPH. *“A Molecular Interaction Model for Autism Spectrum Disorder”*.

Curriculum Vitae

Vanessa Donega was born on September 6th 1985, in Sao Paulo, Brazil. In July 2004 she finished high school (VWO) at the De Bruijne Lyceum in Utrecht, The Netherlands and initiated her studies on Biomedical Sciences at Utrecht University. In July 2007 she obtained her Bachelor's degree and entered the "prestige master Neuroscience and Cognition" also at Utrecht University. She did her first internship (9 months) in the group of Prof. R.J. Pasterkamp at the Rudolf Magnus Institute of Neurosciences in Utrecht on a project entitled "The identification of MICAL-1 interacting proteins". In January 2009, Vanessa went to the lab of Prof G. Fishell at the New York University School of Medicine, USA for her second rotation (6 months). There she worked on a project to determine the molecular and cellular effects of conditional removal of ChAT activity on cortical regions. She wrote her Master thesis entitled "Neurogenesis and its association to epileptogenesis in temporal lobe epilepsy" under supervision of Dr. P. de Graan from the Rudolf Magnus Institute of Neurosciences. She obtained her Master's degree in July 2009.

In January 2010 Vanessa started working as a PhD student in the laboratory of Neuroimmunology and Developmental Origins of Disease (NIDOD) at University Medical Center Utrecht under supervision of Prof C.J. Heijnen, Prof. A. Kavelaars, Prof. F. van Bel and Dr. C.H. Nijboer. During the last 4 and half years she studied the potential to use mesenchymal stem cells to treat hypoxic-ischemic injury in the neonatal brain. The results are described in this thesis and have been published in international scientific journals and presented at international conferences.

From September 2014 on, Vanessa will start working as a postdoctoral researcher at the Stem Cell and Brain Research Institute, INSERM, U846 in Lyon, France under the supervision of Prof. O. Raineteau. She will be investigating the competence of neural stem cells in the subventricular zone of the mouse brain.

List of Abbreviations

ANOVA	Analysis of Variance
BRDU	[³ H]-thymidine or 5-bromo-2'-deoxy-uridine
CA	Cornu Ammonis
CRT	Cylinder Rearing Test
DAPI	4'6-diamidino-2-phenylindole
DCX	Doublecortin
DG	Dentate Gyrus
GFAP	Glial Fibrillary Acidic Protein
HE	Hematoxylin and Eosin
HI	Hypoxia-Ischemia
Iba-1	Ionized calcium binding adaptor molecule-1
MAP-2	Microtubule-associated protein-2
MBP	Myelin Based Protein
MRI	Magnetic Resonance Imaging
hMSC	human Mesenchymal Stem Cell
MSC	Mesenchymal Stem Cell
NeuN	Neuronal specific nuclear protein
NORT	Novel Object Recognition Test
NSC	Neural Stem Cells
OB	Olfactory Bulb
Olig2	Oligodendrocyte transcription factor 2
PBS	Phosphate Buffered Saline
PFA	Paraformaldehyde
RMS	Rostral Migratory Stream
SEM	Standard Error of the Mean
SGZ	Subgranular Zone
SVZ	Subventricular Zone